The Pennsylvania State University

The Graduate School

The Harold and Inge Marcus
Department of Industrial & Manufacturing Engineering

IMPROVED HEAT TREATMENT PROCESS CONTROL FOR FUEL EFFICIENCY AND CYCLE TIME REDUCTION

A Thesis in

Industrial Engineering and Operations Research

by

Thomas C.P. Karnezos

Submitted in Partial Fulfillment
of the Requirements
for the Degree of

Master of Science

May 2009

The thesis of Thomas C.P. Karnezos was reviewed and approved* by the following:

Robert C. Voigt
Professor of Industrial and Manufacturing Engineering
Thesis Advisor

Terry P. Harrison
Earl P. Strong Executive Education Professor of Business and
Professor of Supply Chain and Information Systems

Richard J. Koubek
Professor of Industrial and Manufacturing Engineering
Peter & Angela Dal Pezzo Department Head Chair

*Signatures are on file in the Graduate School

ABSTRACT

This thesis describes the development of an advanced heat treatment process control strategy for natural gas fired furnaces at Carpenter Technology, Corp. in Reading, PA. The primary goal of the project was to implement an improved annealing heat treatment 'on-heat' detection method capable of quantitatively determining when a load of metal within a furnace reaches its target temperature. Current practice techniques are subjective and inherently induce overly conservative heat treatment cycles. By more quantitative control of heat treatment cycles, the point in time when the load uniformly reached its target temperature could be determined with increased precision. This precision could facilitate shorter, less conservative heat treatment cycles with process time savings and energy savings.

Three different approaches for achieving quantitative on-heat determinism were surveyed including: heat transfer modeling, analysis of furnace gas consumption, and analysis of load surface temperature using an infrared sensor (OP-AID method). By comparison of these different approaches, the best control strategy capable of significant reductions in heat treatment cycle times was found to be the OP-AID method. Although the control strategy based on furnace gas consumption proved to be effective, its responsiveness was degraded by the amount of signal filtering it required. Also, since the OP-AID method reacted directly to the surface temperature of the load, it could better ensure product quality compared to the gas flow rate analysis that reacted indirectly to the furnace environment temperature.

Additionally, an analysis was conducted to study the balance between metallurgical constraints vs. cost constraints in the design of the OP-AID method. The aggressiveness associated with achieving time savings opposed the maximization of metallurgical specifications (load temperature uniformity), and this balance was quantified through a multi-criteria analysis. Through this analysis it was found that the parameters of the OP-AID method could provide heat treatment cost savings with sufficient product quality.

TABLE OF CONTENTS

LIST OF FIGURES

LIST OF TABLES

ACKNOWLEDGEMENTS

I would like to express my deep appreciation to Dr. Voigt for providing me a bridge from the field of mechanical engineering into industrial engineering, and for helping me greatly in my development as an engineer. Dr. Voigt has given me much direction throughout my degree, and his unwavering support has been invaluable.

Also I would like to thank Dr. Harrison for generously being a reader for my thesis, and for providing me guidance in the field of operations research as I was just beginning my degree.

At Carpenter Technology Corporation I would like to thank Jim Heilmann, Gary Dispensa, Kevin Grover, Rich Smith, and Mario Epler who instilled in me a passion for research, and helped guide me through the development of this project with their time, knowledge, and good humor. During my time at Carpenter, thanks to the support of these individuals, I grew in my ability to apply engineering concepts, and learned to temper these concepts with practicality.

Also at Carpenter, I would like to thank Dave Pachuilo and Matt Pennypacker for helping me with experimental trials, and the Carpenter Engineering Department for their assistance in gas meter installation. I would also like to express my appreciation for Frank Kaczmarczyk who was an original proponent of the gas flow analysis, and who helped me collect data in the mill.

Thank you also to my friends for helping me along the way, and for making my time here at Penn State so memorable.

Finally, I would like to thank my family for tirelessly being my greatest support net and for giving me strength and inspiration to pursue all my endeavors.

Chapter 1

Introduction

1.1 Project Overview

This thesis describes the development of an advanced heat treatment process control strategy for natural gas fired furnaces at Carpenter Technology, Corp. in Reading, PA. The primary goal of the project was to implement an automated control strategy capable of determining when a load of metal product within the furnace had reached its target temperature. Current practice techniques were subjective and inherently created long, overly conservative heat treatment cycles. By more quantitative control of the heat treatment cycle, the point in time at which the heat treatment load uniformly reached its target temperature could be determined with increased precision. This precision could allow shorter, less conservative cycles with process time savings, energy savings, and increased product consistency.

Three different approaches for achieving quantitative on-heat determinism were evaluated including: heat transfer modeling, measurement and analysis of furnace gas consumption, and direct analysis of load surface temperatures using an infrared sensor (OP-AID method). While only one of these strategies was recommended for implementation, all three will be discussed for completeness. Also by comparing the different approaches, the benefits of the preferred control strategy will become apparent.

Additionally, an analysis was conducted to study the balance between metallurgical constraints vs. cost constraints in the design of the control strategy that uses an infrared sensor to analyze the load surface temperature. As will be discussed, this particular control strategy allows the user to dictate the aggressiveness of the decision regarding load temperature determinism.

The aggressiveness associated with achieving time savings opposes certain metallurgical constraints and a multi-criterion analysis was used to analyze the boundaries between a conservative user approach and an aggressive user approach.

1.2 Project Motivations

The Annealing Department at Carpenter Technology Corporation has about 60 furnaces of different sizes and types that process a wide variety of different heat treatment "loads". The majority of these furnaces are fired with natural gas and operating costs are a significant concern as natural gas prices rise. Many factors within the heat treatment department contribute to the total energy consumption including process cycle times, load scheduling, and furnace efficiencies. The focus of this project was to decrease natural gas consumption by reducing process cycle times through improved process control. This reduction in annealing process cycle time was one step in Carpenter's initiative to reduce overall energy costs in their heat treatment departments. In addition to energy savings, tighter heat treatment process control and shorter heat treatment cycles could result in improved product quality and consistency, increased operational productivity, and reduction in greenhouse gas emissions.

Several elements of advanced heat treatment control were necessary to ensure the successful transition of the control strategy from R&D to the production floor. The methodology should be easily understandable for heat treatment operators, applicable to a wide range of furnace and load types, and result in significant cost savings. Another high priority goal was to eliminate direct furnace load instrumentation (thermocouples) through the use of robust non-contact temperature measurement sensors.

1.3 Heat Treatment Process Overview

1.3.1 Typical Heat Treatment Cycle

In general, heat treatment consists of heating to and holding a load of metal at a desired temperature (Chandler, 1995). Heating cycles drive temperature-sensitive transformations in the microstructure of the metal. Annealing heat treatments relieve cooling stresses induced by hot or cold working, and soften the metal for improved machinability and formability (Lankford, Samways, Craven, & McGannon, 1985).

The main focus of this project was to establish when the heat-up portion of the heat treating cycle was completed since delays in on-temperature determination correspond to the most wasteful and energy intensive part of the cycle. Figure 1-1 shows typical temperature versus time curves for the surface and center of a heat treatment load undergoing an annealing heating cycle. As can be seen, the load took approximately four hours to reach a uniform temperature at its surface and center. For the heat treatment shown in Figure 1-1, once the load being heat treated uniformly reached the furnace temperature set point, it was held at this target temperature (soaked) for a specified amount of time related to its alloy type. Thus, the overall heat treatment cycle could be viewed in two main portions, the control ramp and the control soak. The control ramp refers to the portion of the cycle required to uniformly heat the load to the target temperature. Once a furnace load has uniformly achieved the target temperature, the heat treatment cycle transitions to the control soak. The challenge was to accurately and repeatedly determine the precise time at which the heat treatment load was ‘at temperature.’

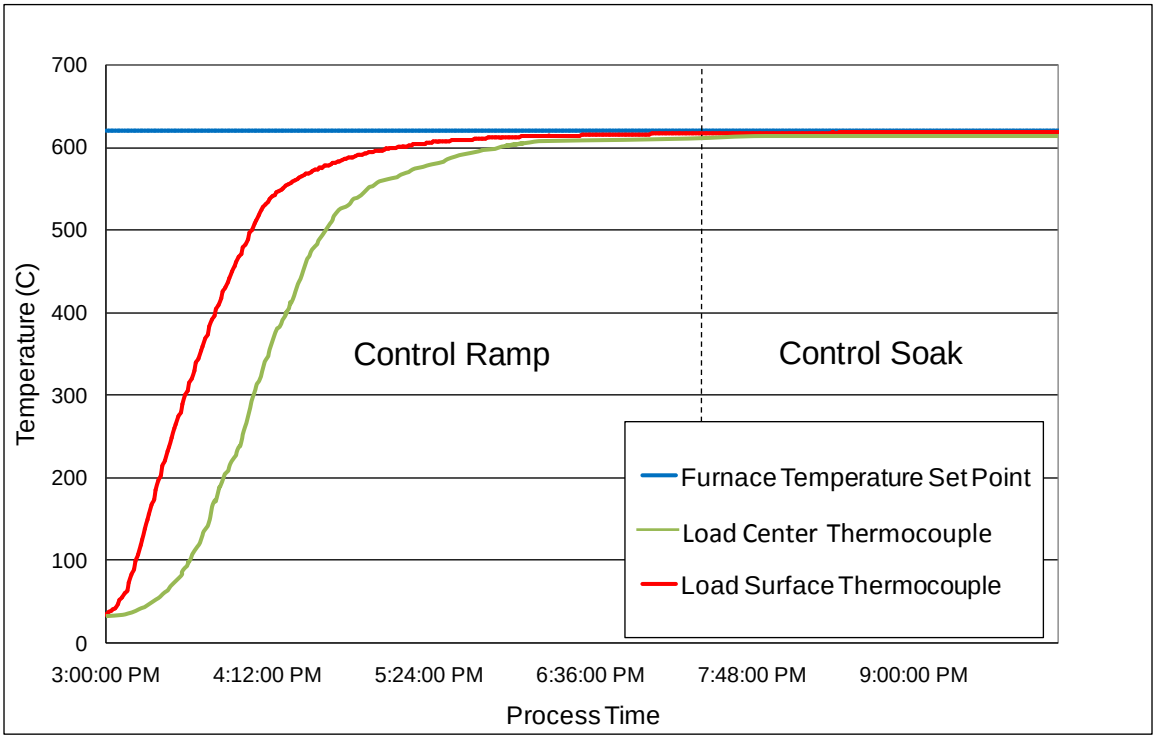

Figure 1-1: Typical load temperature vs. time profiles for an annealing heat treatment cycle

It should be noted that for most annealing heat treatments the metallurgical annealing reactions have been achieved early during the ramp-up time prior to establishment of steady state conditions (Deskevich, 2005). Thus the control soak period is often built into the heat treatment cycle as a safety buffer to insure that the entire load was uniformly heated to its required temperature. In contemporary practice this soak time far exceeds the necessary time requirements to cause the desired metallurgical reactions (Voigt, 2004). With a more accurate picture of the load temperature at the surface and center, the control ramp portion of the cycle could be more tightly controlled, and the safety buffer of the control soak could be reduced. While the primary goal of this project was to reduce the duration of the control ramp cycle, a logical next step would be to reduce the duration of the control soak.

1.3.2 Current Practice Techniques for Load Temperature Determinism in Annealing Heat Treatment Furnaces

Several different practices exist in industry for determining when an annealing heat treatment load has uniformly reached its target temperature. These methods include load thermocouples embedded in the actual furnace load (load thermocouples), visualizing the load surface for color match (temperature match) to the furnace, and relying on overly conservative rules of thumb. While the use of thermocouples gives quantitative feedback on the load temperature at specific locations, the color match method and application of rules of thumb can be fairly subjective and variable in terms of load temperature determination.

Load thermocouples are sometimes used to directly measure load temperature, and are one of the most common temperature measurement devices used in the heat treatment process for temperature sensing (Totten, 2007). While thermocouples provide valuable information, they are expensive to replace regularly, and require operator time for load instrumentation. Load thermocouples are typically used only when required by customer specifications. In less restricted cases, when direct load sensing is not specified, other load on-temperature estimates such as ‘the hour per inch rule’ and load color match methods are universally used.

The ‘hour per inch’ rule is another common industry practice for control of heat treating operations. It should be noted that application of this rule to determine heat treatment time varies between heat treaters (Deskevich, 2005). At certain steel mills, a form of this rule is used to initially estimate the duration of the control ramp portion of the cycle. Thus for the thickest part of the load, an hour per inch of thickness to the center point of the load is used to estimate when the load uniformly reaches temperature. As an example, when heat treating an 8 inch diameter cylindrical billet, the hour per inch rule dictates that four hours at the annealing temperature is required to allow the load to reach temperature. As will be shown, this rule is overly conservative and significant time savings are possible with advanced control strategies. Previous studies have

also indicated that this practice often results in holding loads at temperature for much longer than is required (Deskevich, 2005).

The third heat treating practice common in industry is the color-match method. This method requires the operator to visually assess the color of the load as compared to the furnace surroundings. Since all matter emits radiant energy as a consequence of its temperature, the visible spectrum of radiant energy emitted from metal can be used to judge its temperature in the annealing temperature range (DeWitt & Nutter, 1988). This method relies on the subjective judgment of the operator to match the color of the metal against the color of the surrounding furnace environment. Additionally, for furnaces that do not have sight ports into the interior, the furnace door must be opened to make this judgment which greatly affects energy usage. Figure 1-2 illustrates a load requiring an operator color match for on-heat determinism. In practice, once the color of the load is indistinguishable from the color of the environment, it is declared to be 'on-heat'.

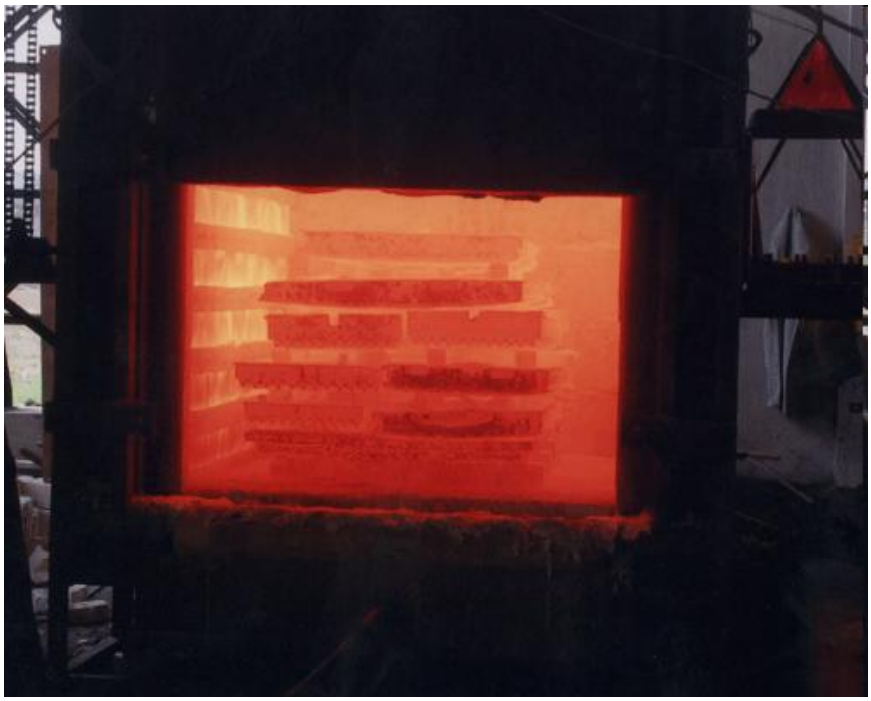

Figure 1-2: Furnace load temperature sensing using color match with the furnace environment. Source: www.bagree.com/facilities.htm

1.4 Summary of Heat Treatment Control Strategies

Three different types of control strategies were considered to more efficiently determine when the furnace load had uniformly reached its target temperature during annealing heat treatments. The implementation of these control strategies depends not only on theory but also on practicality in a production heat treatment environment. Both the underlying heat transfer mechanisms of the furnace system and the furnace load must be considered.

In this study, the first control strategy investigated involved heat transfer modeling to predict, in real time, the center temperature of a load based on a measured surface temperature using a non-contact infrared (IR) sensor. For this modeling technique to be successful it must use the rate of change of the load surface temperature to infer the furnace heat transfer coefficient. In this way, the need to empirically estimate the furnace heat transfer coefficient is eliminated. However at the same time, this method was very dependent on accurate knowledge of the load's thermal conductivity, density, specific heat and geometry. Since this control strategy based on heat transfer modeling was complex and would be difficult to implement, two other methods were developed that minimize the requirement of load specific inputs.

The second control strategy that was developed analyzed the rate at which gas fuel flows into the furnace to indicate when the furnace load uniformly reaches its target temperature. The basis for this method is that as long as the load is cooler than the furnace environment it draws heat from the furnace which requires a higher gas flow rate as compensation. When the load uniformly reaches its target temperature it ceases to draw heat from the furnace environment and the gas flow rate settles to a steady state gas flow rate. At steady state, a minimum constant rate of gas flow is required to maintain the furnace temperature against constant heat losses to the environment through the furnace walls and door.

The last control strategy investigated utilized an infrared sensor and measured the rate of change in the surface temperature of the furnace load to infer the load center temperature. The basis for this method is that the rate of change of the surface temperature of the load approaches zero as the load became uniformly heated throughout. This method achieved *On-heat Prediction through Aggressive Infrared Detection* and was given the acronym OP-AID. The implementation of this method would allow the operator to consistently determine when the center of a heat treatment load had reached its steady state temperature based on non-contact measurements of the rate of change of the load surface temperature over time.

Chapter 2

Literature Review

2.1 Introduction

Key aspects of heat treating and heat treatment process control strategies will be reviewed. In particular, control strategies that rely on heat transfer modeling as well as strategies that use gas flow meters and infrared sensors for load temperature sensing will be reviewed. This review is not intended to be fully comprehensive on all critical aspects of heat treatment, but identifies gaps in current heat treatment process control strategies and highlights the benefits of the work proposed in this study. The literature review proceeds as follows: first, different types of heat treatment will be briefly surveyed, and then sensor selection issues associated with heat treatment applications will be considered, followed by efforts in heat transfer modeling for load temperature determinism, as well as a brief discussion of other strategies for load temperature determinism.

2.2 Survey of Heat Treatment Procedures

In general, heat treatment consists of heating a load of metal to a uniform temperature and then controlling its cooling rate to achieve desired properties or conditions (Chandler, 1995). The term ‘heat treatment’ is an umbrella for a wide variety of different procedures that are each designed to differently influence the properties of the metal. The underlying material science of heat treatment occurs at the microscopic scale to influence the microstructure of the metal. For steel, the study of these microstructural changes under different heating procedures couples with

the study of the steel alloys on a chemical level to ultimately design a product with suitable properties for its intended application (Lankford, Samways, Craven, & McGannon, 1985). The balancing of alloying and heat treatment to achieve properties is critical to the success of steel components, as is the necessary heat treatment process control to develop consistent and desirable microstructures. The following discussion is intended to provide a quick outline of different heat treatment procedures to provide the background necessary to understand the key aspects of heat treatment process control.

Heat treating of steel can be widely classified into several types of procedures that produce different sets of properties for a given steel. The great benefit of these different heat treatment procedures is that, by allowing the metal properties to be manipulated and controlled, they drive the versatility of steel to suit many different applications (Lankford, Samways, Craven, & McGannon, 1985). For example, heat treating can be designed to remove processing stresses, refine grain structure, increase surface hardness, increase toughness, or alter the electric or magnetic properties of the metal (Chandler, 1995). Types of heat treating procedures that are briefly discussed include: annealing, normalizing, tempering, and stress relieving (Chandler, 1995). After this outline of heat treatment procedures, the different classifications of furnace equipment for heat treatment will be discussed.

Annealing is a common heat treatment that relieves part stresses resulting from cooling after hot or cold work to soften the metal for increased machinability and formability (Lankford, Samways, Craven, & McGannon, 1985). Annealing also helps to improve the dimensional stability of the part and can influence the magnetic or electrical properties of the steel. There are three types of annealing heat treatments commonly used: subcritical annealing, inter-critical annealing, and full annealing. While not discussed in detail, these different types of annealing procedures chiefly differ in their heat treatment temperature ranges and allowable cooling rates

from the heat treatment temperature. It should be noted that the required temperature and time for annealing can vary greatly from one type of steel to another. (Chandler, 1995)

Normalizing is another common steel heat treatment procedure designed to homogenize and refine the metal grain structure to create uniform properties in the product. While dependent on the steel composition, most normalization procedures occur around 1500°F-1700°F followed by cooling outside of the furnace. Normalization is often used on steel castings before the castings are hardened, or on cast steels before part working. (Chandler, 1995)

Tempering is another common heat treatment procedure that usually involves heating to, and soaking a part at 400°F to 1200°F for an hour or longer. Often high levels of residual stress can be induced within a part during operations such as quenching, and the result is a part that is hard and brittle. By relieving these stresses, tempering increases part ductility while sacrificing a degree of the hardness, which may be very desirable depending on the intended application of the steel. (Lankford, Samways, Craven, & McGannon, 1985)

Stress relieving, another type of heat treatment, is designed to remove stresses in the metal which may be introduced during hot or cold working. Stress relieving is a heat treatment procedure that typically heats the steel part up to approximately 1050-1150°F and then slowly cools it back to room temperature. Cooling after stress relieving is slow to ensure uniform cooling of the part and is necessary to avoid the introduction of added stresses within the part. (Chandler, 1995)

These different steel heat treatment procedures can be accomplished using a wide variety of heat treatment furnace types. Although individual furnace designs are not detailed here, the three main types of furnaces can be classified as batch furnaces, semi-continuous furnaces and continuous furnaces (Totten, 2007). A producer of steel products, such as Carpenter Technology, Corp. may have a mix of these different furnace types to suit a variety of heat treatment applications. In batch furnaces, products are placed in a box-type furnace, treated, and then

removed as a batch at the appropriate time. In continuous furnaces the parts move through different heated zones of a furnace along a conveyer system. The length of the furnace and the speed at which the steel product is conveyed through the furnace determines the heat treatment cycle time. In semi-continuous furnaces parts continuously move through the furnace in a stepwise manner (Totten, 2007). Figure 2-1 shows a small scale batch annealing furnace. This is the type of furnace in which the experimental studies for this project were conducted. Some common heat treatment procedures that can be performed in a batch annealing furnace include: normalizing, annealing, carburizing, and stress relieving (Chandler, 1995).

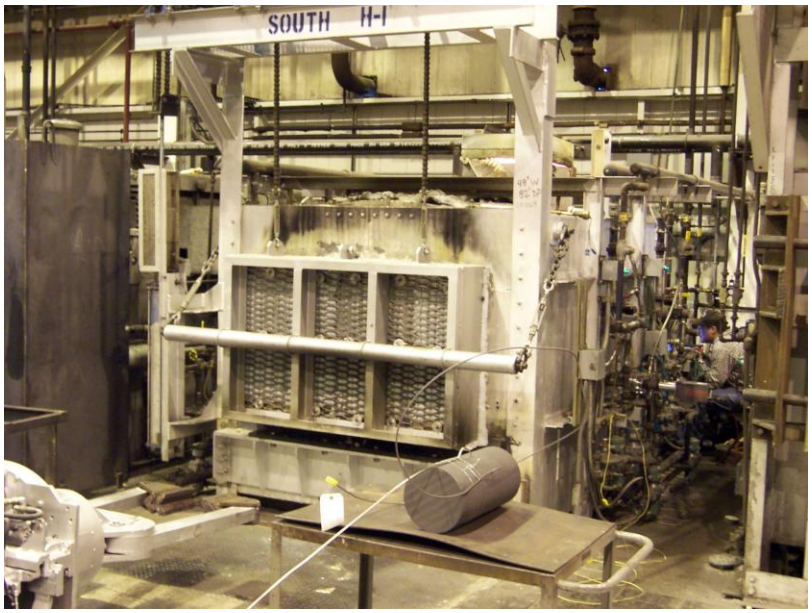

Figure 2-1: Small Scale Batch Furnace used in experimental trials (An instrumented 8 in. diameter cylindrical heat treatment sample is shown in front of the furnace on the cart).

2.3 Sensor Selection for Heat Treatment Process Control

To efficiently determine the actual load temperatures in heat treatment applications, load thermocouples are often used, and are indeed the most common load temperature measurement devices used in the heat treatment process (Totten, 2007). It was a goal of this project to eliminate the use of load thermocouples by exploring alternate non-contact temperature sensing

solutions. Control strategies were developed using an infrared sensor and a gas flow meter to interpret when the load had reached an 'on-heat' condition. Considerations for the selection of these sensors for non-contact control strategies are discussed below.

2.3.1 Infrared Sensor Selection Considerations for Heat Treatment Process Control

A number of non-contact, or non-invasive, temperature measurement systems are available including infrared thermometry, absorption and emission spectroscopy, and acoustic thermography (Childs, Greenwood, & Long, 2000). However, of these non-contact temperature measurement options, infrared sensors are the most suitable for heat treatment process control. Infrared sensors are commonly used in steel mills with applications in: hot rolling, continuous casting, galvanizing heat treatment, and continuous heat treatment (Peacock, 1999). Batch furnace heat treatment furnace applications present unique challenges for infrared sensors since the target of interest is surrounded by heated walls. The reflected energy from the hot furnace walls influences the infrared sensor measurement of the furnace load. This is a long-standing problem recognized in the steel industry (White & Saunders, 2008). Perhaps because of these challenges, many US steel mills rely on computer modeling to predict load temperatures inside reheat furnaces (Peacock, 1999). In this study, due to the unique way in which an infrared sensor was utilized, a robust load temperature-sensing control strategy for Carpenter's heat treatment application could be developed despite the previously mentioned challenges with infrared implementation.

While many considerations such as optical resolution and target sighting are important when selecting an infrared sensor, one primary consideration is variable target emissivity which influences the accuracy of the sensor measurement. Metal targets are subject to variable emissivity and reflectivity dependent on part type and temperature (Schneider, 2007). While this

inherently introduces emissivity related error, this error can be minimized by choosing the shortest suitable wavelength to improve accuracy (Schneider, 2007). Infrared sensors have been developed that measure radiant energy at a ratio of different wavelengths to cancel the effects of variable or unknown emissivity. These dual wavelength sensors however still tend to be influenced by background temperature levels that are hotter than the target temperature. This is a particularly relevant concern when considering the use of a dual wavelength sensor for a heat treatment furnace application (Barron, 1992). The appropriate infrared sensor system and operating wavelength for Carpenter's heat treatment furnace application was chosen through a comprehensive survey of commercially available infrared sensors in addition to multiple vendor trials in an actual furnace.

2.3.2 Gas Flow Meter Selection Considerations for Heat Treatment Process Control

In terms of gas flow meter selection, many considerations are necessary in heat treatment applications regarding the type of meter and its placement (Womack, 2008). Measuring gas flow into large scale furnaces is essential for direct feedback on gas consumption. Womack remarks that "as the costs of fuels and consumables (natural gas, hydrogen, oxygen, etc.) continue to rise, the ability to accurately measure the amount used in a process becomes significant in controlling costs and determining bottom line profits" (Womack, 2008). Some of the considerations necessary for the selection of a gas flow meter include: accuracy over a range of gas pressures, process temperatures, and turn-down ratios (Womack, 2008). The engineering department at Carpenter Technology Corporation was consulted with for the selection and installation of the gas flow meter in support of the annealing trials conducted in this study.

2.4 Heat Transfer Modeling for Heat Treatment Process Control

There is a wealth of heat transfer related research published on heat treatment furnace behavior and the use of modeling for heat treatment furnace control. This review is not intended to comprehensively discuss this entire body of literature as a whole. It is rather intended to demonstrate the breadth of heat transfer modeling previously performed and to identify gaps in the manipulation of well established heat transfer techniques as applied to heat treatment process control.

Complex models have been created to simulate heat conduction in heat treatment furnaces for varying furnace conditions. Work has been done to incorporate mathematical models of batch reheating furnaces with a parametric investigation of furnace characteristics in an effort to improve furnace efficiency through improved furnace design [(Chapman, Ramadhyani, & Viskanta, 1989), (Finlayson & Schofield, 1959)]. Heat transfer to the load in terms of radiation, convection and conduction inherent to a simulated furnace environment has also been modeled using numerical simulation [(Kang & Rong, 2006), (Jaluria, 1984)]. Some of these complex models can even account for detailed parameters such as the effect of thermodynamic phase transformations in the load (Tagliafico & Senarega, 2004). Furthermore, researchers have developed a three dimensional finite element mathematical model to calculate the non-stationary temperature field in rectangular blocks of steel subject to heat treatment (Lindholm & Leden, 1999). However, the use of such a model requires in-depth characterization of the furnace environment in addition to knowledge of the furnace load itself.

Simpler models have been developed in an attempt to reduce the number of input variables needed for effective furnace heat transfer modeling. To predict equilibration times and heating/cooling rates for varied load geometries, a virtual sphere method has been proposed for application to arbitrary geometries (Gao, Reid, Jahedi, & Li, 2000). While being easy to

implement, it requires prior knowledge of effective heat transfer coefficients which are assumed to be constant to simplify modeling. While this model is more adaptive to arbitrary load geometries, it is less adaptive to variable furnace conditions.

The integral boundary modeling approach used by Ingerslev & Henein is more adaptive to variable furnace conditions and temperature dependent properties, but also requires prior knowledge of the convective heat transfer coefficient which can be pre-determined from experimental measurements (Ingerslev & Henein, 1997). Other one-dimensional heat transfer models using balance and boundary equations have been generalized to numerically simulate heat transfer. However, these models also require prior definition of the heat transfer coefficient as an input (Barba & Lamberti, 2003).

The local convective heat transfer coefficient for a heat treatment process can be experimentally determined by numerical evaluation of transient surface temperature through the inverse heat conduction method (Oosthuizen & Naylor, 1999). The model developed in this thesis sidesteps direct calculation of this convective coefficient and generates a lumped heat transfer coefficient representative of the combined heat transfer due to radiation and convection. By monitoring the surface temperature of the load and also the furnace environment temperature, no prior knowledge of the heat transfer coefficient is needed to implement a heat treatment modeling control strategy.

2.5 Other Strategies for Heat Treatment Process Control

Compared to the amount of literature related to process control strategies developed from heat transfer modeling, there is considerably less literature similarly focused on the other two control strategies developed in this thesis. One heat treatment process control strategy developed in this thesis analyzes the rate of change in surface temperature of a steel billet, as measured by

an infrared sensor, to infer its internal temperature. Similar measurements of the rate of change of load temperature have been utilized in the aluminum industry to identify phase transformations in the material to aid in process control (Sparkman & Kearney, 1994).

A second proposed control strategy developed in this thesis analyzes the rate of change of the gas flow rate into the furnace to determine when the furnace load is uniformly heated. Steady state conditions arise in the gas flow rate when the load has equalized in temperature to the furnace environment and the furnace, no longer losing heat to the load, requires a lower constant gas flow to maintain its temperature relative constant losses to the environment. Using the gas flow to infer heat treatment load temperature equilibrium has been suggested in the past, however formal analysis of the effectiveness of these measurements for furnace control have not been reported (Peters, 2007).

2.6 Literature Review Summary

There are a wide range of steel heat treatment cycles including: annealing, normalizing, tempering, and stress relieving. The majority of these heat treatment applications require control of the load temperature to ensure property uniformity for all parts of the heat treated load. To attain quantitative measurement of the load temperature, load thermocouples are typically utilized in practice. In this project load thermocouples were eliminated, and control strategies using a non-contact infrared sensor and a gas flow meter were used to quantitatively determine the load temperature consistency. While difficulties in infrared sensor implementation for heat treatment furnace control has been reported, due to the unique way in which the infrared sensor was used in this project, these difficulties are expected to be overcome.

In this project three separate heat treatment process control strategies were developed and compared. One strategy developed utilizes the underlying heat transfer properties in the load to

predict a center temperature based on a measured surface temperature from an infrared sensor. A second strategy developed analyzes the gas flow rate into the furnace to indicate when a load has reached steady-state temperature. The third control strategy analyzes the rate of change of the surface temperature of the load, using an infrared sensor, to infer the center temperature of the load. Existing literature related to each of these heat treatment process control strategies was reviewed including heat transfer modeling of furnaces and furnace loads, as well as considerations for implementation of infrared sensors and gas flow meters for efficient load determinism.

Chapter 3

Methodology

In this chapter, the underlying methodology for each of the three heat treatment process control strategies for load temperature determination will be discussed. The first control strategy that will be discussed involves heat transfer modeling to predict, in real time, the center temperature of a load based on a measured surface temperature using a non-contact infrared sensor. The second control strategy to be discussed analyzes the rate at which gas flows into the furnace to indicate when the furnace load uniformly reaches its target temperature. Finally, the third control strategy to be discussed uses an infrared sensor to measure the rate of change of the surface temperature of the furnace load to infer the load center temperature.

3.1 Heat Transfer Modeling

A heat transfer modeling approach for load center temperature prediction was developed for cylindrical geometries. All nomenclature used in the following model development can be found in Appendix A. The basic heat transfer model was derived from the fundamental heat diffusion equation and is dependent on the following set of assumptions:

1) The furnace load is considered to be a cylinder infinite in length such that heat conduction occurs in the radial direction only. This assumption is valid for long cylindrical furnace loads where $L/r_o \geq 10$ (Incopera & DeWitt, 2002).
2) The thermal conductivity of the furnace load does not vary with temperature and is equal to the average thermal conductivity over the temperature range of the heating cycle. Also, there is no heat generation within the furnace load.

3) For all calculation time steps, an initial uniform temperature distribution is assumed in the cylinder that is equal to the average of the load surface and center temperatures. With each successive time step, as the load is heated, the average between the load surface temperature and the load center temperature more accurately approximates a uniform temperature distribution. The load surface temperature is measured via a non-contact infrared sensor, the furnace temperature is measured via the control thermocouple, and the load center temperature is carried forward from the prior computational time step.

Each iteration of the control algorithm begins a new solution to a one-dimensional heat transfer model with uniform initial temperature distribution and initial condition of time equal to zero. Thus, initially for each time-step, no characterization of the rate of radial heat conduction is necessary, and the Fourier number calculation (the ratio of the heat conduction rate to the thermal energy storage rate) is not required. Thus, the only transient term in the calculation drops out and takes with it material properties and dimensions.

The lumped heat transfer coefficient is assumed to be uniform over the surface of the cylinder. This assumption is necessary since the surface temperature of the cylinder is measured at a single point even though there may be some temperature variation within the load along the length of the load cylinder.

The heat diffusion equation in cylindrical coordinates can be expressed as (Incopera & DeWitt, 2002):

$$\frac{1}{r}\frac{\partial}{\partial r}\left(kr\frac{\partial T}{\partial r}\right)+\frac{1}{r^2}\frac{\partial}{\partial \phi}\left(k\frac{\partial T}{\partial \phi}\right)+\frac{\partial}{\partial z}\left(k\frac{\partial T}{\partial z}\right)+q=\rho c_p\frac{\partial T}{\partial t} \tag{1}$$

Simplifying Equation (1) by applying assumptions (1)-(2) yields:

$$\frac{1}{r}\frac{\partial}{\partial r}\left(kr\frac{\partial T}{\partial r}\right)=\rho c_p\frac{\partial T}{\partial t} \tag{2}$$

To solve Equation (2) for the temperature distribution, T(r, t), the following initial condition is necessary:

$$T(r,0) = T_i \tag{3}$$

Where by assumption (3):

$$T_i \cong \left(\frac{Ts_n + Tc_{n-1}}{2} \right) \tag{4}$$

In addition to this initial condition, the following boundary conditions are also needed:

$$\left. \frac{\partial T}{\partial r} \right|_{r=0} = 0 \tag{5}$$

$$-k \left. \frac{\partial T}{\partial r} \right|_{r=r_o} = h\left[T(r_o, t) - T_\infty \right] \tag{6}$$

The dimensionless temperature, radius, and time are respectively defined as (Incopera & DeWitt, 2002):

$$\theta^* = \frac{\theta}{\theta_i} = \frac{T - T_\infty}{T_i - T_\infty} \tag{7}$$

$$r^* = \frac{r}{r_o} \tag{8}$$

$$Fo = \frac{\alpha t}{L_c^{\,2}} \tag{9}$$

Where:

$$\alpha = \frac{k}{\rho c_p} \tag{10}$$

Furthermore, the characteristic length for an infinite cylinder can be expressed as:

$$L_c = \frac{V}{A_s} = \frac{r_0}{2} \tag{11}$$

Thus, the solution to Equation (2) for T(r, t) using the initial condition given by Equations (3) and (4), and the boundary conditions given by Equations (5) and (6) can be expressed in dimensionless form as (Incopera & DeWitt, 2002):

$$\theta^* = \sum_{n=1}^{\infty} C_n \exp(-\zeta_n{}^2 Fo) J_0(\zeta_n r^*) \tag{12}$$

Where:

$$C_n = \frac{2}{\zeta_n} \frac{J_1(\zeta_n)}{J_0{}^2(\zeta_n) + J_1{}^2(\zeta_n)} \tag{13}$$

$$Bi = \frac{hL_c}{k} = \zeta_n \frac{J_1(\zeta_n)}{J_0(\zeta_n)} \tag{14}$$

When Fo>0.2 the first term approximation to the infinite series is valid (Incopera & DeWitt, 2002), thus the time step is defined from Equation (9) such that:

$$\Delta t = 0.2 \left[\frac{L_c{}^2 \rho c}{k} \right] \tag{15}$$

Thus when evaluating Equation (12) over the time step given by Equation (15), the infinite summation in Equation (12) can be expressed as a first term approximation (Incopera & DeWitt, 2002):

$$\theta^* = C_1 \exp(-\zeta_1{}^2 Fo) J_0(\zeta_1 r^*) \tag{16}$$

By considering the definition of r* given in Equation (8), Equation (16) can be expressed for the surface and center of the cylindrical load as:

$$\theta_s^* = C_1 \exp(-\zeta_1{}^2 Fo) J_0(\zeta_1) \tag{17}$$

$$\theta_c^* = C_1 \exp(-\zeta_1^2 Fo) \tag{18}$$

Equation (7) further defines the dimensionless temperatures at the surface and center of the cylinder as given by Equation (19) and (20):

$$\theta_s^* = \frac{T_s - T_\infty}{T_i - T_\infty} \tag{19}$$

$$\theta_c^* = \frac{T_c - T_\infty}{T_i - T_\infty} \tag{20}$$

Using Equations (17-20), the ratio of the dimensionless surface temperature to dimensionless center temperature can then be expressed as:

$$\frac{\left(\frac{T_s - T_\infty}{T_i - T_\infty}\right)}{\left(\frac{T_c - T_\infty}{T_i - T_\infty}\right)} = \frac{C_1 \exp(-\zeta_1^2 Fo) J_0(\zeta_1)}{C_1 \exp(-\zeta_1^2 Fo)} \tag{21}$$

Where by simplification:

$$T_c = \frac{T_s - T_\infty}{J_0(\zeta_1)} + T_\infty \tag{22}$$

In order to solve for T_c, given T_s and T_∞, it is first necessary to solve for the value of ζ_1 for each time-step. This can be accomplished by manipulating and equating Equations (17) and (19) as follows. First, by recalling the definition of T_i given by Equation (4), Equation (19) can be expressed as:

$$\theta_s^* = \frac{T_s - T_\infty}{\left(\frac{T_s + T_c}{2}\right) - T_\infty} \tag{23}$$

Since T_s and T_∞ are measured and T_c is defined from the previous time-step, the value of θ_s^* is known for each time-step. Secondly, by assumption (4), the Fourier number in Equation (17) goes to zero, and Equation (17) can then be expressed simply as:

$$\theta_s^* = C_1 J_0(\zeta_1 r^*) \tag{24}$$

Finally, equating Equations (23) and (24) and substituting for the value of C_1, given by the first root of Equation (13), yields:

$$\theta_s^* = \left(\frac{2}{\zeta_1} \frac{J_0(\zeta_1) J_1(\zeta_1)}{J_0^{\,2}(\zeta_1) + J_1^{\,2}(\zeta_1)} \right) \tag{25}$$

Equation (25) can be solved for the value of ζ_1. This value of ζ_1 is then substituted back into Equation (22) and the center temperature during each time step can then be calculated. This process is repeated for each time step over the duration of the heat treatment cycle. An important implication of this result is that for each time step, given the value of ζ_1, an implied heat transfer coefficient can be expressed by rearranging Equation (14) as:

$$h = \frac{2k}{r} \zeta_1 \frac{J_1(\zeta_1)}{J_0(\zeta_1)} \tag{26}$$

It should be noted that this estimated value of h can possibly be also used to track furnace efficiency over time by control charting its value.

Figure 3-1 summarizes the inputs and outputs of the heat transfer modeling method. As can be seen, many of the inputs are load specific. This complexity would make the method very difficult to implement in a mill environment, as will be discussed in detail in Chapter 5.

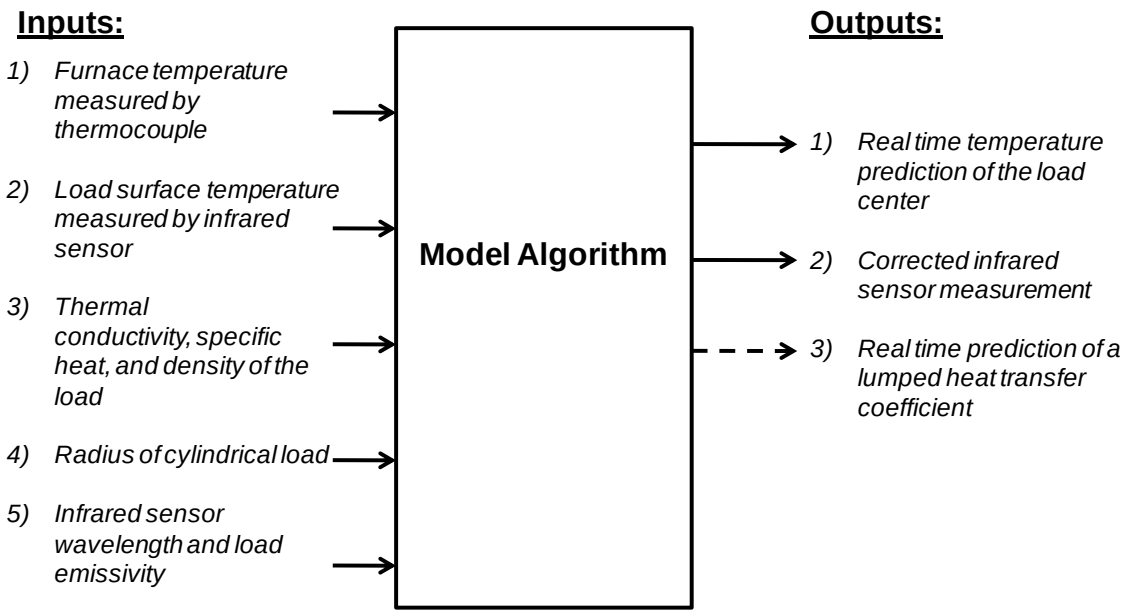

Figure 3-1: Heat Transfer Model - Input and Output Summary

3.2 Gas Flow Rate Analysis

The underlying hypothesis that drove the development of the gas flow rate analysis method for load temperature prediction was as follows: after addition of a cold load to a heated furnace, the gas flow rate into the furnace should reach a minimum steady state value when the load was uniformly heated throughout at its steady-state temperature. After the load was initially placed in the furnace, the load rapidly extracted heat from the furnace environment which required a higher gas flow rate to keep the furnace environment at its set-point temperature. Even after the load surface had reached the furnace temperature, the load continued to extract heat from the furnace environment until the center of the load reached the furnace temperature. When the load uniformly reached the furnace temperature, the gas flow rate settled to its steady state value since it was only necessary then to maintain the furnace temperature against constant losses to the external environment through the furnace exhaust, walls and door.

To study the viability of this hypothesis, and to explore the possibility of this control method, a gas flow meter was installed on the gas supply line to the R&D furnace used for fully instrumented heat treatment trials. The gas flow meter was selected in consultation with the Engineering Department at Carpenter Technology Corporation. The meter included a non-compensated, high frequency pulse transmitter that transmits a pulse for every 0.00625 cubic inches of gas flow. This allowed for very accurate capturing of the gas flow into the furnace. Furthermore, with this type of measurement resolution, incremental changes in the gas flow rate could be identified. The flow meter counter generated a cumulative sum of the pulses. To determine the rate of gas flow from this output, it was necessary to take the derivative of the cumulative pulse count with respect to time. This will be referred to as the first derivative of the gas flow which yields the gas flow rate.

Steady state conditions could be characterized by the point in time when the gas flow rate drops to and maintains a constant value. The first derivative of the gas meter signal gives the flow rate vs. time which was furnace specific. Each furnace may require a different amount of gas flow to maintain environment temperature at steady state depending on the size of the furnace, and the types of furnace losses related to the furnace's insulation type and door seals. However, the second derivative of the gas flow signal is independent of the furnace type since at steady state, for any furnace and load type, the rate of change of the gas flow rate will essentially be zero. Thus, to generally identify the steady state point, the second derivative was used. When the second derivative goes to zero, the rate of change in gas flow rate is zero, and the gas flow rate is constant with respect to time. The gas flow rate will be expressed in terms of cubic feet per hour, and the subsequent derivative of the gas flow rate will be expressed in cubic feet per hour squared.

The basic procedure for evaluating this control method was to instrument a furnace load with center and surface thermocouples, and then to monitor the gas flow rate as it related to the

load temperature at a constant furnace set point temperature. The actual load temperature responses were then compared to the target furnace temperature values at the point in time when the gas flow reached its steady state. Load thermocouples provided a direct measurement for how accurately the steady state gas flow analysis identified when the load uniformly reached the target temperature. More specifically, the following metrics were used to describe the conditions related to when the gas flow rate analysis declared a load 'on-heat:'

1. The surface temperature of the load as measured by the load surface thermocouple.
2. The center temperature of the load as measured by the center load thermocouple.
3. The time savings of the gas flow rate analysis compared to the hour per inch rule (current practice technique).

To study the robustness of this control method, trials were conducted for varying load geometries. All trials were conducted in the R&D facility at Carpenter Technology, Corp. in a small scale batch furnace (approximate furnace volume = 311,000 cubic inches). The following geometries are analyzed:

1. An 8 in. diameter cylinder with approximate volume of 1,700 cubic inches (Figure 3-2a)
2. A 49.25 in. x 7.88 in. x 3 in. rectangle with approximate volume of 1,165 cubic inches (Figure 3-2b)
3. A 3 in. diameter bundle of 0.3125 in. diameter rods with approximate volume of 375 cubic inches (Figure 3-2c)

a b c

Figure 3-2: Trial Load Geometries

Identification of when the gas flow rate is indeed at steady state is a computational challenge. The first issue encountered when evaluating this method was the large amount of noise in the gas flow rate first derivative calculation. A large portion of this signal noise was inherent to taking the derivative of a non-smooth signal such as that of the gas flow meter. The gas flow measurement was subject to fluctuations in flow rate due to the controller design, fluctuations in gas supply pressures, and other types of interferences that created noise in the output signal. This noise created a non-smooth signal that makes its derivative very messy. To adequately interpret the derivative of the signal, significant filtering was necessary.

Obtaining the necessary rate of change in the gas flow rate signal required two derivatives: the first derivative on the cumulative pulses per time to get the gas flow rate, and the second derivative on this gas flow rate to get the change in gas flow rate. Therefore, filtering was necessary prior to taking each derivative. A moving average filter proved to be adequate in filtering the signal prior to each derivative to yield interpretable results. Temperature and gas flow data points were collected every 30 seconds for the duration of each trial. Moving averages with various window lengths were experimented with ranging from 2 minute windows (4 data points) to 10 minute windows (20 data points). It was found that a 10 minute window was necessary so that each derivative could truly accentuate the signal change relative to the amount of signal noise. The length of the moving average window is one of the main drawbacks to this method. Since this moving average requires 10 minutes of data collection to generate the first filtered data point, there is a 10 minute time delay between the filtered signal and the actual signal. In the case of the gas flow rate analysis, since two 10 minute filters were required for each derivative, there is a 20 minute delay associated with any control decision based on the second derivative signal analysis.

While the length of the moving average time window may seem very detrimental to the implementation of the control method, there is a good way to compensate for this time delay

associated with the gas flow signal filtering. Most heat treatment cycles require a period of soak time after the initial ramp period when the load is brought to temperature. This soak time can be used as a buffer that can absorb the delay in the 'on-heat' prediction of the load without extending overall heat treatment time. In other words, when the load is declared 'on-heat' by the gas flow rate derivative analysis, due to the 20 minute filtering delay associated with this detection point, the load has already been soaking for 20 minutes. The control soak can then be shortened by 20 minutes and effectively the filtering delay has been fully absorbed.

Once the signal has been filtered adequately to yield interpretable results in the presence of signal noise, the next issue is how to determine the steady state point ('on-heat' time) based on the signal. This was accomplished with a classic three-sigma control chart approach (Montgomery, 2001). The control charting criteria can be used to identify when the change in gas flow rate oscillates within an upper and lower limit for a set amount of time indicative of steady state behavior. A two minute window was used to ensure that the signal stayed between the upper and lower control limit. This arbitrary two minute window designated for the limit check worked well for all cases tested. To calculate the upper and lower control limits, initial data was collected under conditions of steady state gas flow behavior. A necessary assumption for control chart construction is that the signal at steady state is normally distributed (Montgomery, 2001). This was checked using a probability plot in MINITAB. This plot is shown in Figure 3-3. The null hypothesis was that the data was normally distributed, while the alternate hypothesis was that the data was not normally distributed. This was tested with a level of significance of alpha equal to 0.05. As is shown in the probability plot, the p-value of the Anderson-Darling test is 0.135. Since the p-value is greater than alpha, one can fail to reject the null hypothesis and conclude that there is no statistically significant evidence to reject the assumption of normality in the data.

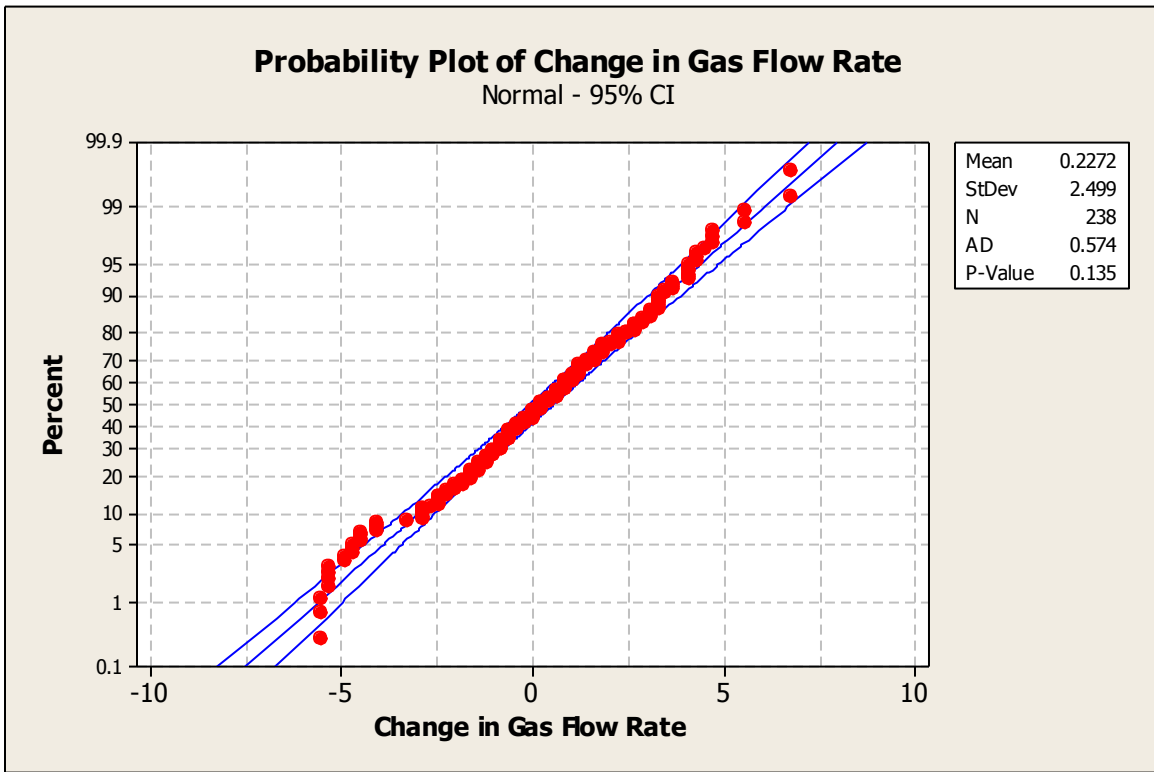

Figure 3-3: Probability plot and Anderson-Darling statistic for test of normally distributed data for steady state gas flow.

The next step to determining the upper and lower control limits of the three-sigma control chart was to take the mean and standard deviation of the data, as is shown in the Figure 3-3. The upper and lower control limits were calculated at three standard deviations above and below the mean, respectively. As will be demonstrated, the control chart approach proves to be very effective at reliably identifying when the gas flow rate attains steady state behavior.

3.3 Infrared Signal Derivative Analysis

A similar control strategy was also developed to analyze the rate of change of the surface temperature of the load to infer when the center of the load has reached the target temperature. The surface temperature of the load was directly measured via an infrared sensor. Since the

measurement of interest was the rate of change of the load surface temperature, the absolute accuracy of the infrared sensor measurement was less critical. The relative measure of the rate of change in load surface temperature was far less affected by variables such as load emissivity and furnace wall reflectivity, and therefore was a very robust measurement system for load 'on-heat' detection. This robustness of the signal derivative measurement established a robust method of control.

The control strategy has been given the acronym OP-AID for *On-heat Prediction through Aggressive Infrared Detection*. While this acronym will help in the referencing of this control method, it has the added benefit of promoting furnace operator acceptance during implementation. The acronym OP-AID suggests that it is an *operator aid* that helps the operator perform his/her job more easily.

The underlying theory for the OP-AID method was that when the surface temperature of the load was constant at its target temperature, then the center of the load was also constant and at its target temperature. At this point in time, the rate of change of the non-contact surface temperature signal will approach zero. This theory can be proved mathematically as follows:

Beginning with the Equation (22) for cylindrical geometries:

$$T_c = \frac{T_s - T_\infty}{J_0(\zeta_1)} + T_\infty \tag{22}$$

Rearranging terms:

$$T_s = J_0(\zeta_1)T_c - J_0(\zeta_1)T_\infty + T_\infty \tag{27}$$

Taking the derivative of temperature with respect to time:

$$\frac{dT_s}{dt} = J_0(\zeta_1)\frac{dT_c}{dt} - J_0(\zeta_1)\frac{dT_\infty}{dt} + \frac{dT_\infty}{dt} \tag{28}$$

Since the furnace temperature is constant:

$$\frac{dT_\infty}{dt} = 0 \tag{29}$$

Thus substituting Equation (29) into Equation (28) yields:

$$\frac{dT_s}{dt} = J_0(\zeta_1)\frac{dT_c}{dt} \tag{30}$$

Where:

$$J_0(\zeta_1) \neq 0 \text{ and } J_0(\zeta_1) \neq \infty \tag{31}$$

Thus when:

$$\frac{dT_s}{dt} \to 0 \text{ then } \frac{dT_c}{dt} \to 0 \tag{32}$$

In other words, when the surface temperature of the load is constant at its target temperature, then it can be expected that the center temperature of the load is also constant. Equation (22) also applies to cylindrical bundles, and the proof can easily be extended to cylindrical bundles of rods.

The conditions in Equation (31) are necessary since zero times infinity may or may not equal zero, and furthermore the conclusion in Equation 32 will only hold if $J_0(\zeta_1)$ never equals zero. For the exact solution to the transient, one-dimensional form of the heat equation, the discrete values of ζ_n are given by the positive roots of Equation (14) (Incopera & DeWitt, 2002). It follows that $J_0(\zeta_n)$ can never equal zero or infinity, for any *n*, otherwise ζ_n would be undefined.

$$Bi = \frac{hL_c}{k} = \zeta_n \frac{J_1(\zeta_n)}{J_0(\zeta_n)} \tag{14}$$

The analogous equation to Equation (22) for rectangular geometries is given by Equation (33).

$$T_c = \frac{T_s - T_\infty}{\cos(\zeta_1)} + T_\infty \tag{33}$$

Therefore, it can be similarly proved that when the surface temperature of the rectangular load is constant and at target, that the center temperature is also constant and at target.

The OP-AID method was experimentally evaluated for four trials of varying geometries. All trials were conducted in the R&D facility at Carpenter Technology, Corp. in a small scale gas fired batch furnace (approximate furnace volume = 311,000 cubic inches). The different load geometries tested include:

1. An 8 in. diameter cylinder with approximate volume of 1,700 cubic inches (Figure 3-2a)
2. A 49.25 in. x 7.88 in. x 3 in. rectangle with approximate volume of 1,165 cubic inches (Figure 3-2b)
3. A 3 in. diameter bundle of 0.3125 in. diameter rods with approximate volume of 375 cubic inches (Figure 3-2c)

In each trial, the load was also fully instrumented with load thermocouples so that the center temperature of the load could be monitored throughout the heat treatment trials. The effectiveness of 'on-heat' detection by the OP-AID method was judged by the following metrics:

1. The surface temperature of the load as measured by a load surface thermocouple.
2. The center temperature of the load as measured by the center load thermocouple.
3. The time savings of the OP-AID method compared to the hour per inch rule (current practice technique).

As was mentioned previously, the derivative of the collected signal was inherently noisy, and required filtering for the signal to be interpreted easily. To filter the derivative signal of the surface temperature measurement, a moving average filter was applied. In the case of the OP-AID method, the infrared sensor supplied a much cleaner signal than the gas flow meter, so a shorter moving average of five minutes (10 data points) could be used to develop the derivative

signal for ‘on-heat’ detection. Also it should be noted that a two minute moving average (4 data points) was used on the original signal prior to taking its derivative to reduce noise in the derivative signal. Thus for the OP-AID method there was a total time delay due to filtering of seven minutes. Through experimentation it was found that each of the two and five minute moving average filters represented the smallest averaging windows that could adequately filter the signal to reflect the change of the infrared signal relative to the signal noise.

To identify when the derivative of the infrared signal was constant at zero, a similar type of control charting approach used previously for the gas flow analysis was employed with a few key differences. The main difference was driven by the lack of normality in the infrared derivative signal at steady state, as shown in Figure 3-4. The null hypothesis for the normality test was that the data was normally distributed, while the alternate hypothesis was that the data was not normally distributed. This was tested with a level of significance of alpha equal to 0.1. As is shown in the probability plot, the p-value of the Anderson-Darling test is <0.005. Since the p-value is less than alpha, one would reject the null hypothesis and therefore conclude that the data was not normally distributed.

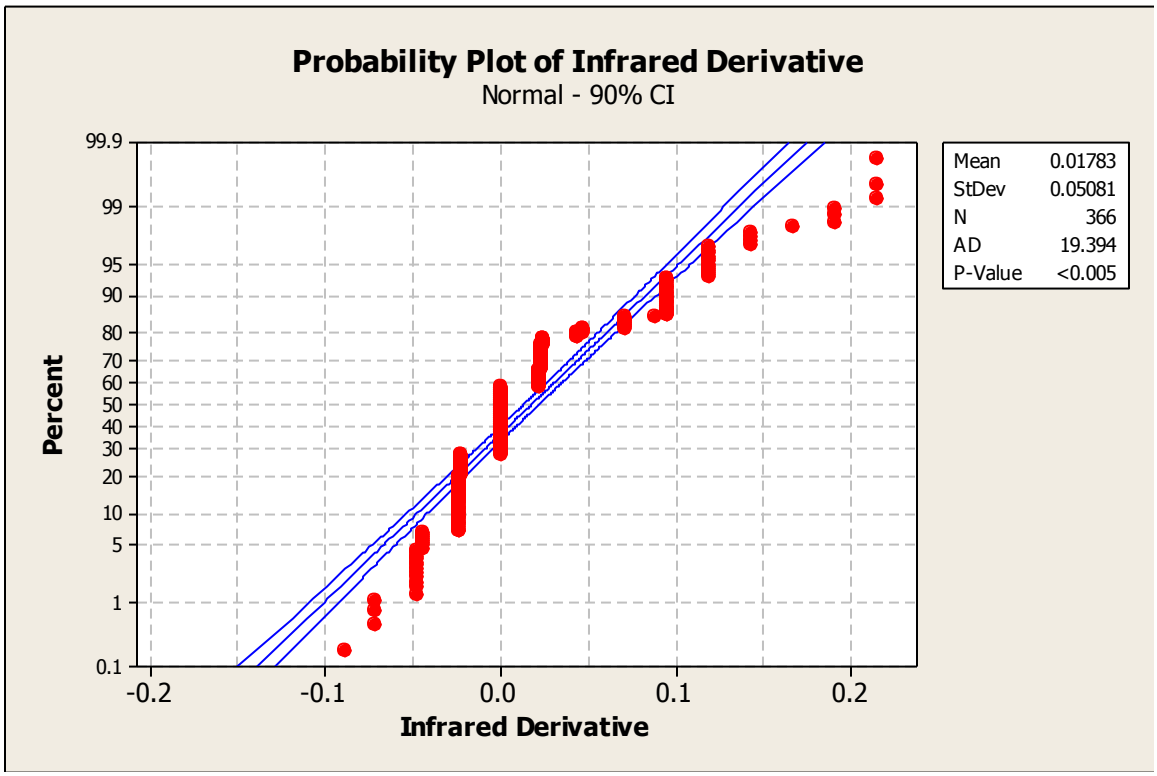

Figure 3-4: Probability plot and Anderson-Darling statistic for test of normally distributed data for steady state load surface temperature.

The control limits for the OP-AID method can be selected in a more direct and intuitive fashion by the user based on acceptable load temperature deviations. This has the key benefit of allowing the user to be particularly conservative or aggressive in setting the control limits which in turn establish conservative or aggressive 'on-heat' times for the furnace load being heated. The upper and lower control limits represent the maximum allowable change of surface temperature vs. time associated with 'on-heat' determination. By manipulating the upper and lower bounds, the user could be as conservative or aggressive with heat treatment time savings as would be tolerable from a metallurgical standpoint.

This approach worked particularly well due to the exponential nature of the temperature vs. time profile of the load surface. As the load approached its target temperature, an incremental increase in load temperature was achieved for an exponential increase in time. This phenomenon

was countered by the OP-AID control method because it declared the load at temperature as soon as an incremental decrease in the rate of change of the load temperature was detected.

For the general implementation of the method to be successful, a single specification of upper and lower control limits was sought that could be applicable to a wide range of load geometries. These control limits were set at 0.5, -0.5 °F/min for the upper and lower limit, respectively. This choice implied that the load was 'on-heat' when the surface temperature was changing at less than one degree every two minutes.

While arbitrary in choice, an in-depth analysis will show that 0.5 degrees/min was indeed a good control limit choice, and will work well for a variety of load geometries. The implications of this control limit choice will be put into perspective across a number of different trials through the analysis of the trade-offs associated with different limit specifications, in terms of cost and quality. This analysis was conducted using a multi-criteria selection process that balanced the metallurgical constraints with varying levels of aggressiveness in achieving cost savings, and is detailed in the following section.

3.4 OP-AID Limit Choice Multi-Criteria Analysis

The OP-AID Limit Choice Multi-Criteria Analysis allowed for selective tuning of the control limits to choose the desired level of aggressiveness in 'on-heat' determinism from a cost savings perspective. However, in seeking to lower costs by aggressive 'on-heat' determinism, the trade-off between cost and quality associated with the control limit choice should be investigated. Figure 3-5 shows the percent surface and center temperatures of target vs. time for an 8 inch cylinder placed in a 2000°F furnace. The percent surface temperature and percent center temperature of target both incrementally increased with an exponential increase in time as the load approached its set-point temperature (Figure 3-5). The exponential nature of the heating

curves favored early ‘on-heat’ determination because a small amount of load heating was lost for a large savings in overall cycle time. The nature of this trade-off presented conflicting objectives between metallurgical constraints that favored small temperature deviations (longer heating times) versus cost constraints that favored shorter heating times.

Selection of control limits for the OP-AID method established when the load was determined ‘on-heat’ and therefore the control limit selection could be viewed as directly influencing the trade-off balance between cost and quality. The control limits denoted the minimum rate of change in the surface temperature of the load necessary to indicate that the load was ‘on-heat’. Wide control limits favored early on-heat determinism, while narrow control limits favored longer heating times and slightly higher load center temperatures. From a cost savings perspective, an aggressive user would choose wide control limits and would accept a somewhat larger load surface to center temperature differential to represent when the load has more or less uniformly attained its target temperature. On the other hand, from a metallurgical perspective, a conservative user would choose narrow limits to ensure the rate of change in the surface of the load was so minimal that he/she could be certain that the center of the load was very close to the target temperature. A multi-criterion selection problem was utilized to investigate the balance of these opposing constraints in the selection of the control limits for the OP-AID method.

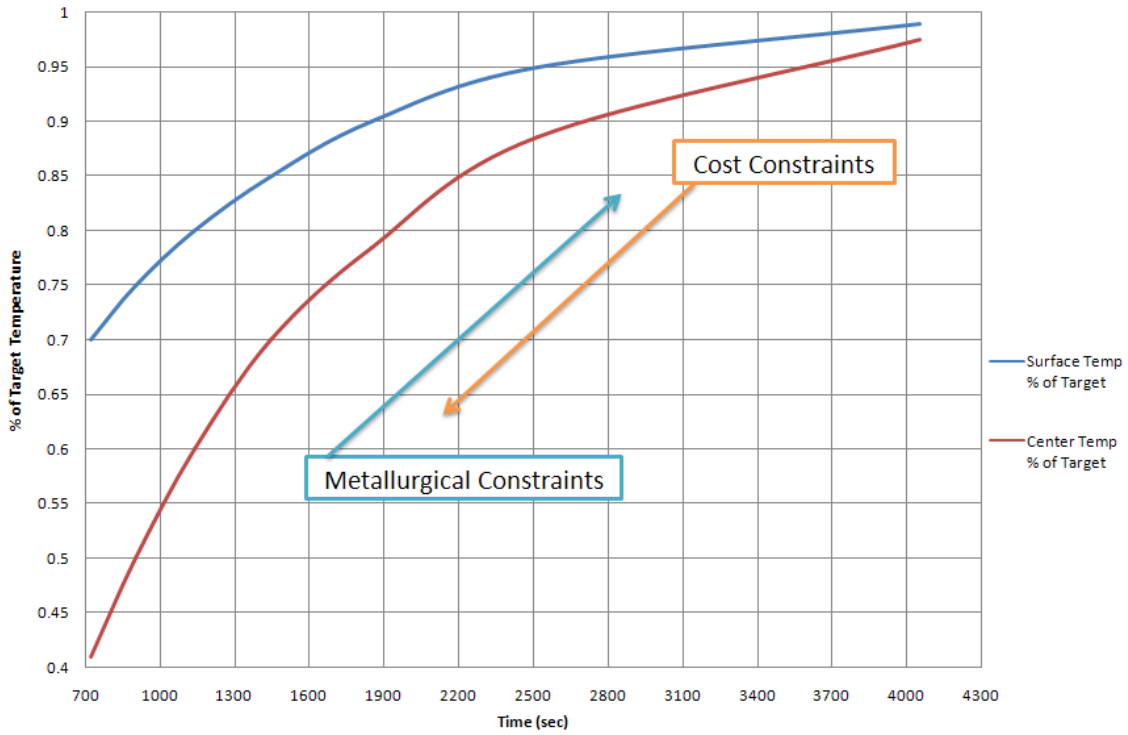

Figure 3-5: Percent surface and center temperatures of target vs. time for an 8 inch cylinder placed in a 2000F furnace. Also indicated are the direction the metallurgical and cost constraints act with respect to time.

Multi-criterion selection is a basic method that quantitatively ranks different alternatives that are each characterized by several criteria. The multi-criteria methodology used in this study, including the rating method and scaling techniques, can be referenced in Masud & Ravindran, 2008. In this application, the varying alternatives corresponded to specified levels of the rate of change of temperature control limits that ranged from narrow limits to wide limits. Since the control limits specified were intended to apply to a wide range of scenarios, differing limit alternatives were compared across four trials. Characteristic of a multi-criterion problem, each control limit alternative was characterized by more than one criterion. For each of the four trials, the following two criteria were simultaneously considered for each alternative:

1. The center temperature of the load, measured by a load thermocouple, that corresponded to the timing of the 'on-heat' decision due to a given control limit specification in the OP-AID method.
2. The time at which the load was declared 'on-heat' due to a given control limit specification in the OP-AID method.

Thus, each alternative was characterized by eight criteria (two criteria for each of four trials). The surface temperature was not directly formulated into the multi-criteria analysis; however, the surface temperature does impose a strict constraint. It was specified by Carpenter Technology, Corp. that the surface temperature of the load should be within ±18°F of the target temperature. This constraint was easily enforced since the infrared sensor did provide a relatively accurate measurement of load surface temperature as the load approaches the furnace temperature. The tradeoff associated with cost and quality was then examined within these tolerable limits of the load surface temperature.

Since the multi-criteria analysis consisted of discrete alternatives and deterministic criteria, a rating method (Masud & Ravindran, 2008) was used to study the implications of different control limits from aggressive to conservative limit choices. The rating method allowed for the manipulation in emphasis between minimizing costs (aggressive) relative to maximizing quality (conservative). Based on this method, three different control limit specifications for the OP-AID method were given that corresponded to a conservative, a moderate, and an aggressive approach to cost savings. A generalized model of the rating method as it applies to this application is presented as follows:

Let i and j denote variable indices where:

i = number of alternatives (i = 1, 2, …, 22)

j = number of criteria (j = 1, 2, …, 8)

Thus the alternatives can be denoted by a_i where:

a_i = upper and lower control limit specification for alternative i (i = 1, 2, …, 22)

Furthermore the eight criteria for each alternative i could be expressed as:

f_{ij} = criterion j for alternative i (i = 1, 2, …, 22)

The weighted score for each alternative was used for ranking purposes and was denoted:

s_i = weighted score for each alternative i (i = 1, 2, …, 22)

The weights involved in calculating the score for each alternative were based on the rating of importance the user specifies for each criterion. Using this rating method (Masud & Ravindran, 2008), the two criteria for each alternative were rated on a scale from 0 to 10, where 0 puts no importance on the criteria and 10 puts high importance on the criteria. Minimizing the amount of heating time until the load was determined 'on-heat' was a criterion related to cost savings and was ranked from 0-10 in degree of importance. Maximizing the center temperature of the load through longer heating times was related to quality and was also ranked on this scale in degree of importance. It is clear that these two criteria oppose each other in a balance between cost and quality.

Three different ratings on the importance of minimizing cost relative to quality were studied: a conservative rating, a moderate rating, and an aggressive rating. These ratings were then used to propose conservative, moderate and aggressive control limit specifications for the OP-AID method. It should be noted that, due to the exponential nature of the heating curve, low ratings on the importance of minimizing the 'on-heat' time have a significant impact on the balance of cost to quality. For the conservative approach, the importance of maximizing the center temperature for each trial was given a 10, while heat treatment time minimization criteria were ignored and rated at 0. For the moderate rating, the importance of maximizing the center temperature was maintained at 10, but a rating of 1 was given to the importance of minimizing the 'on-heat' time. Finally for the aggressive approach, an importance rating of 10 was given to maximizing the center temperature, however the importance of minimizing the time until a load

was ‘on-heat’ was rated a 2. Again, although the importance ratings assigned to minimizing the ‘on heat’ time seems low, because of the exponential behavior of the heating curves, these low ratings had a significant impact.

Let r_j = rating value assigned to criterion j (j=1, …, 8). Then, the weights were calculated based on the ratings of each criterion as follows:

$$w_j = \frac{r_j}{\sum_{j=1}^{8} r_j} \qquad \text{for } j=1, 2, \ldots 8 \tag{34}$$

The weights calculated in Equation (34) were then utilized in the weighted sum of the criteria to determine the score for each alternative. The weighted score for each alternative was calculated by Equation (35).

$$s_i = \sum_{j=1}^{8} w_j \, f_{ij} \qquad \text{for } i = 1, 2, \ldots, 22 \tag{35}$$

Once a score was calculated for each alternative, the alternatives were ranked based on scores from highest to lowest. For this application of the rating method however, the highest score represented the control limits that best satisfied the user’s specifications across all trials tested.

The generalized terms defined above were organized below in Table 3-1 to aid in visualization of the problem set-up. The experimentally collected data for the differing trials were used to populate this generalized table.

Table 3-1: Multi-criterion Selection Problem Set-up

		Criteria		
	a_i	f_{ij}		S_i
Alternatives	a_1	f_{11} . . .	f_{18}	s_1
	a_2	f_{21} . . .	f_{28}	s_2
	-	-	-	-
	-	-	-	-
	-	-	-	-
	a_{22}	f_{221} . . .	f_{228}	s_{22}
Max	f_{ij}	v_1 * . . .	v_8 *	

When implementing the multi-criteria rating method, it was important that the original criteria values for each alternative were first scaled. If the original values were not scaled, the values of larger magnitude would dominate the weighted sum across the criteria for each alternative. Prior to any calculations, the criteria values were first scaled using the ideal value method (Masud & Ravindran, 2008). The ideal value method was a simple yet effective method to scale all criteria values between zero and one. This was accomplished as follows:

First, let g_{ij} = scaled value of f_{ij}. Then the ideal values for each criterion were denoted as follows:

For quality maximization criterion 'j':

$$H_j = max(f_{ij}) \qquad \text{for } i = 1, 2, \ldots, 22 \tag{36}$$

For time minimization criterion 'j':

$$L_j = min(f_{ij}) \qquad \text{for } i = 1, 2, \ldots, 22 \tag{37}$$

It should be noted that the ideal solution is unattainable for any alternative since it represented achieving the highest load temperature in the smallest time span for each trial.

To continue with the scaling of the criteria values, for criterion 'j' that required maximization:

$$g_{ij} = \frac{f_{ij}}{H_j} \qquad \text{for } i = 1, 2, \ldots, 22 \tag{38}$$

And for criterion that required minimization:

$$g_{ij} = \frac{L_j}{f_{ij}} \qquad \text{for } i = 1, 2, \ldots, 22 \tag{39}$$

Once Equations (38) and (39) were applied to the original criteria values, all criteria objectives became maximization objectives. The weighted score for each alternative using the scaled criteria values was then calculated using Equation (35) with g_{ij} replacing f_{ij}.

Chapter 4

Results

In this chapter, the results for the trials conducted with each heat treatment control strategy will be discussed. Also, results will be presented for the multi-criteria analysis of cost vs. quality tradeoffs associated with different levels of aggressiveness in the definition of the OP-AID control limits. The chapter will proceed as follows: first, the results and validation of the heat transfer model will be presented, and then the results of the gas flow rate analysis will be presented, followed by the results of the OP-AID method. Finally, the results of the multi-criteria analysis of varying OP-AID control limits will be discussed.

4.1 Heat Transfer Modeling

For the heat transfer modeling portion of the project SI units were used, although conversions are given throughout. To determine model accuracy for each of the heat treatment scenarios presented, the calculated load center temperature can be compared to the measured load center temperature values as follows: First, the root mean square error (RMSE) was calculated using Equation (40):

$$RMSE = \sqrt{\frac{1}{n}\sum_{i=1}^{n}(Tc_{measured,i} - Tc_{calculated,i})^2} \tag{40}$$

The coefficient of variation using the RMSE was then calculated by Equation (41) and expressed as a percentage.

$$c_{v,RMSE} = \frac{RMSE}{\frac{1}{n}\sum_{i=1}^{n} Tc_{measured,i}} \quad (41)$$

The coefficient of variation expressed as RMSE was relatively low for each model validation method with coefficients of variation of less than 2% (Table 4-1). Thus the model was able to predict the center temperature in all cases with very good accuracy. It should be noted that for the third validation method utilizing the infrared sensor, the coefficient of variation using the RMSE was calculated only for time greater than 2000 seconds where the load surface temperature was greater than 315°C (600 °F) as this was the low end of the infrared sensor's measurable temperature range.

Table 4-1: RMSE and coefficient of variation values for each model validation method.

	Description of Method	RMSE (°C)	Coefficient of Variation
Method 1	Center Temperature modeled from surface temperatures generated by DEFORM-2D (17 in. diameter trial)	2	0.22%
Method 2	Center Temperature modeled from experimentally measured surface temperatures (thermocouple)	5	1.06%
Method 3	Center Temperature modeled form experimentally measured surface temperatures (corrected infrared sensor)	8	1.72%

4.1.1 Model Validation

Three methods were used to validate the effectiveness of the model to generate an accurate furnace load center temperature from load surface temperature:

1) Comparison with FEM simulated data using DEFORM^{TM}-2D[1]
2) Experimental data collected by load thermocouples
3) Experimental data collected by infrared sensor measurements

DEFORM^{TM}-2D simulations were run to test a variety of situations in which experimental validation would be difficult in terms of furnace time reservation and load thermocouple instrumentation. In the following case presented, DEFORM^{TM}-2D was used to simulate the heating of a 43 cm (17 in.) diameter cylinder of metal with a uniform starting temperature of 426°C (800°F). The model algorithm was then executed using the input of the simulated surface temperature, shown in Figure 4-1, to predict the center temperature and was compared to the modeled center temperature. The model was able to closely approximate the center temperature of the load generated by DEFORM^{TM}-2D to within one degree Celsius (Figure 4-1).

[1] DEFORM^{TM}-2D is a registered trademark of Scientific Forming Technologies Corporation

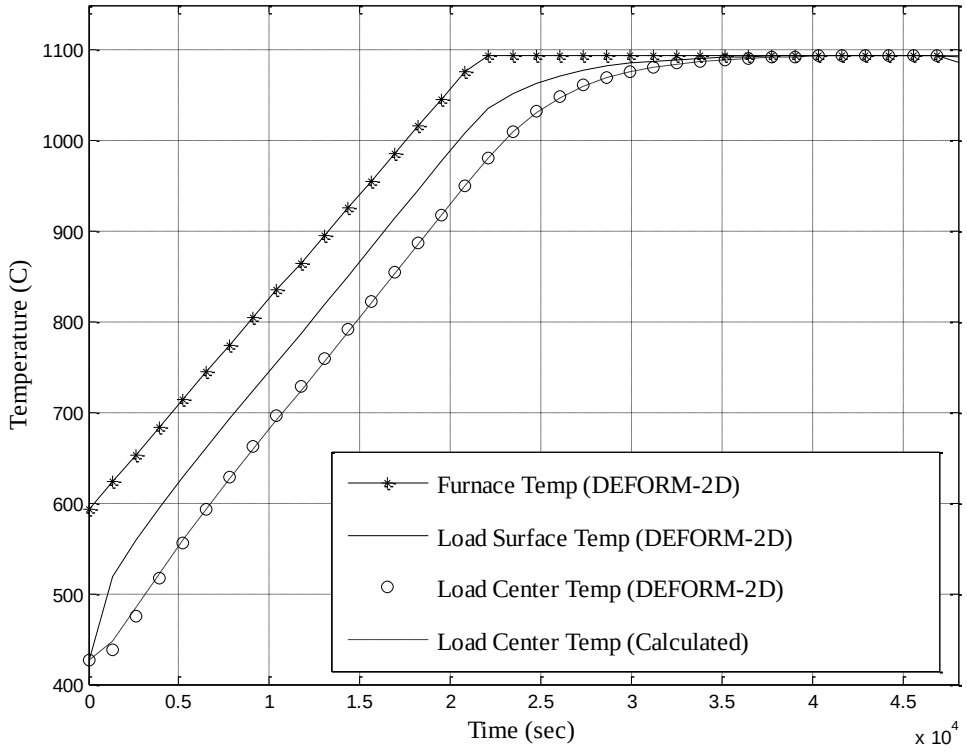

Figure 4-1: Temperature vs. time for 43 cm (17 in.) diameter cylinder with comparison to DEFORMTM-2D.

For the second validation method, a 20 cm (8 in.) diameter cylinder of metal was instrumented with load thermocouples at its surface and center. The cylinder, initially at room temperature was placed in a furnace at a constant 649°C (1200°F). The model algorithm used the input of the load surface thermocouple temperature measurement to predict the load center temperature. The model results were compared to the actual center temperatures in Figure 4-2. It can be seen that the model estimated center temperatures of the load were in close agreement to the experimentally measured center temperatures of the load. At 12,400 seconds into the heat treatment trial, the modeled center temperature (with the surface thermocouple temperature measurement as a model input) was less than 4°C different than the load center temperature measured by the center thermocouple.

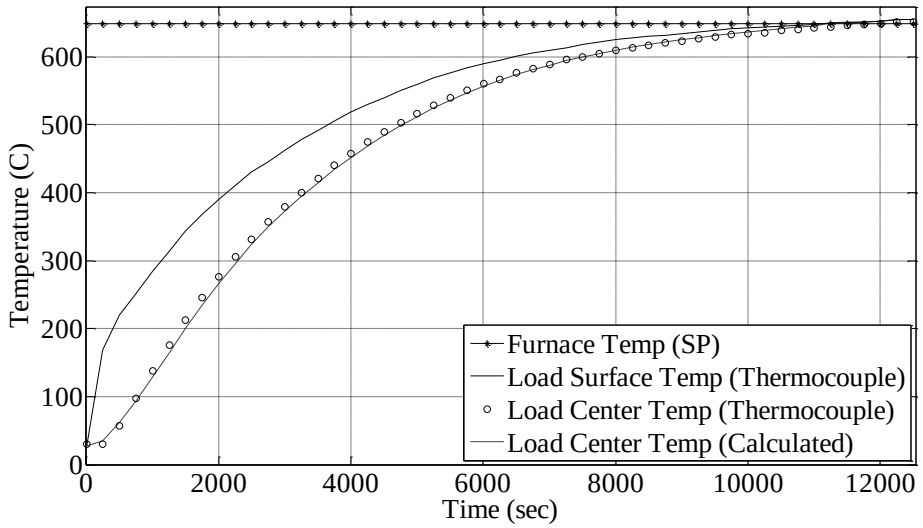

Figure 4-2: Temperature vs. time for 20 cm (8 in.) diameter cylinder with comparison to experimental data. The center temperature is predicted from the surface temperature of the load as measured by a load thermocouple.

Figure 4-3 shows the result of the lumped heat transfer coefficient calculation estimated by the model. The overall shape of this curve was similar to the heat transfer coefficient vs. ingot skin temperature curve previously calculated by Finlayson and Schofield (Finlayson & Schofield, 1959). As noted by Finlayson and Schofield, the "heat transfer coefficient rises at an increasing rate because of the increasing effect of radiation from the furnace walls." Further experimental data was needed to truly validate the lumped heat transfer coefficient values shown in Figure 4-3. It should be noted that changes in the calculated heat transfer coefficient value could conceivably be used to evaluate furnace efficiency variations over time.

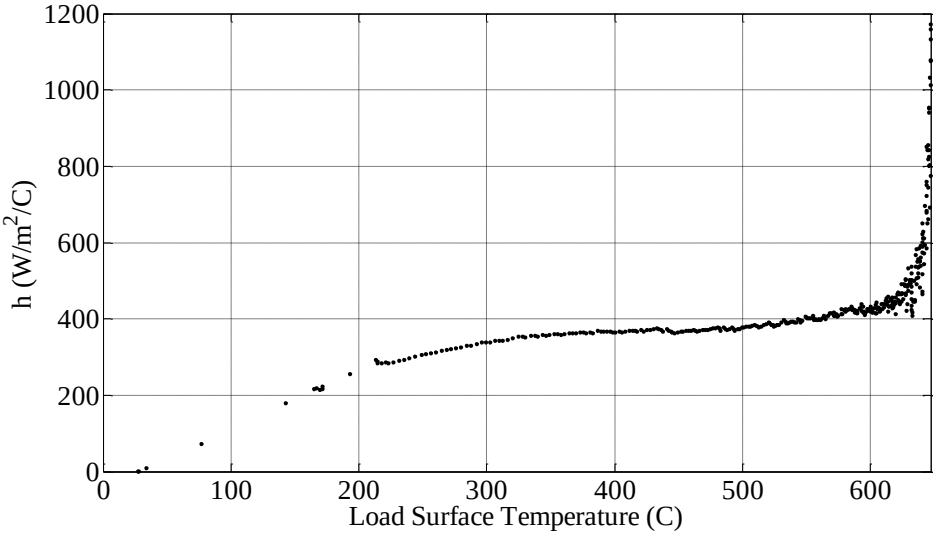

Figure 4-3: Lumped heat transfer coefficient vs. load surface temperature calculated for 20 cm (8 in.) diameter cylinder from experimental data.

Before presenting the third validation method, it is necessary to discuss infrared sensor reflectivity corrections needed to achieve accurate load surface temperature measurements for model implementation. When the load surface temperature was significantly cooler than the furnace environment temperature, the infrared sensor readings were artificially high due to furnace wall reflections. The model incorporated a reflectivity correction factor to compensate for the furnace background effects. The furnace interior can be approximated as a blackbody (White & Saunders, 2008), and since a blackbody is a diffuse emitter, the spectral intensity of radiation is independent of direction (Incopera & DeWitt, 2002).

Building on this concept, the following reflection correction is presented by White and Saunders (White & Saunders, 2008):

$$S(T_s, T_w, \varepsilon) = \int_0^\infty \varepsilon(\lambda) R(\lambda) L_b(\lambda, T_s) d\lambda + \int_0^\infty [1 - \varepsilon(\lambda)] R(\lambda) L_b(\lambda, T_w) d\lambda \qquad (42)$$

Assuming a constant spectral emissivity (ε) at the specified wavelength (λ) of the infrared sensor, the measured spectral emissive power, $S(T_s, T_w, \varepsilon)$ can be further expressed in terms of

the radiant load temperature (given by the uncorrected infrared sensor measurement), T_m, by Equation (43) and (44):

$$S_b(T_m) = \varepsilon S_b(T_s) + (1-\varepsilon) S_b(T_w) \tag{43}$$

$$\text{Where: } S_b(T) = \int_0^\infty R(\lambda) L_b(\lambda, T) d\lambda \tag{44}$$

Solving Equation (43) for $S_b(T_s)$, and converting to temperature, yields a corrected infrared sensor temperature measurement which was compared to the uncorrected signal in Figure 4-4. As shown in Figure 4-4, the reflection corrections applied to the infrared sensor are effective throughout the sensor's operating temperature range of 316-1137°C (600-2500°F).

The center prediction algorithm was then executed using the corrected infrared sensor temperature measurement as an input. Figure 4-4 shows that initially the corrected infrared sensor measurement was not in good agreement with the load surface thermocouple measurement. However, as the corrected infrared measurement began to more closely follow the surface thermocouple measurement, the center temperature prediction tended to more closely agree with the center thermocouple measurement. This was due largely to the way the model defined, at the beginning of each time-step, an initial temperature distribution equal to the average of the measured load surface temperature and the previously calculated center temperature. At 12,400 seconds into the heat treatment trial, the modeled center temperature (with the infrared sensor measurement of the load surface temperature as a model input) was less than 2°C different than the load center temperature measured by the center thermocouple.

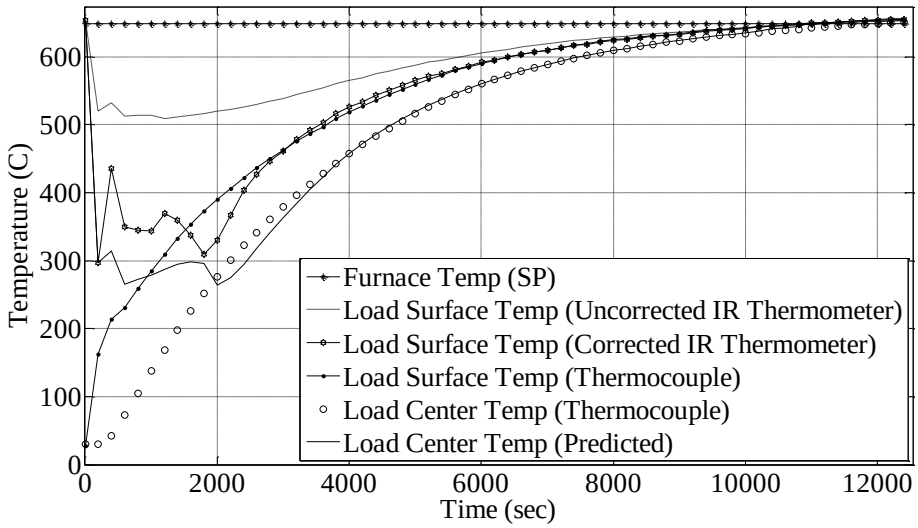

Figure 4-4: Temperature vs. time for 20 cm (8 in.) diameter cylinder with comparison to experimental data. The center temperature is predicted from the corrected IR sensor measurement of the load surface temperature.

4.2 Gas Flow Rate Analysis

In this section, four different trials were conducted to analyze the effectiveness of the gas flow rate analysis method, and the results will be presented. After individual discussion of each trial, the key results will be summarized. The trials will be referred to by the abbreviations given in Table 4-2, and will be presented in the order listed.

Table 4-2: Gas Flow Rate Analysis Trial Description Abbreviations

Trial Abbreviation	Trial Description
GF1	49.25 in x 7.88 in. x 3 in. rectangle placed in a 1600°F furnace. (Trial 1)
GF2	49.25 in. x 7.88 in. x 3 in. rectangle placed in a 1600°F furnace. (Trial 2)
GF3	An 8 in. diameter cylinder placed in a 2000°F furnace
GF4	A 3 in. diameter bundle of 0.3125 in. diameter rods placed in a 1600°F furnace

This analysis compared load temperatures to the change in the gas flow rate. In this section, for comparison sake, the time delays associated with the moving average filters applied for the gas flow rate and the change in gas flow rate were assumed to be absorbed in the control soak period. Furthermore, it was assumed that the window of time designated for the limit check was also absorbed in the control soak period. All results presented in this section were based on these assumptions. In the following trials, an 'on-heat' detection point will be depicted that was consistent with these assumptions. For reference, an additional 'on-heat' detection point will be depicted that corresponds to a relaxation of these assumptions. This delayed 'on-heat' detection point will be further discussed in Chapter 5 while comparing the different control methods.

Also, the thermocouple measurements in the following trials were adjusted for calibration errors that could be quantified when the load was at the steady state temperature. Thus to accomplish uniformity, the thermocouple measurements were adjusted by their difference from the furnace thermocouple measurement at steady state. This type of correction assumes the furnace thermocouple reading was accurate.

4.2.1 Trial GF1

The first trial involves placing a 49.25 in. x 7.88 in. x 3 in. rectangle in a 1600°F furnace and studying the gas flow rate as the load came up to temperature. Figure 4-5 displays the furnace and load thermocouple measurements vs. time. For the rectangular geometry, there was not a significant lag between the center temperature and the surface temperature.

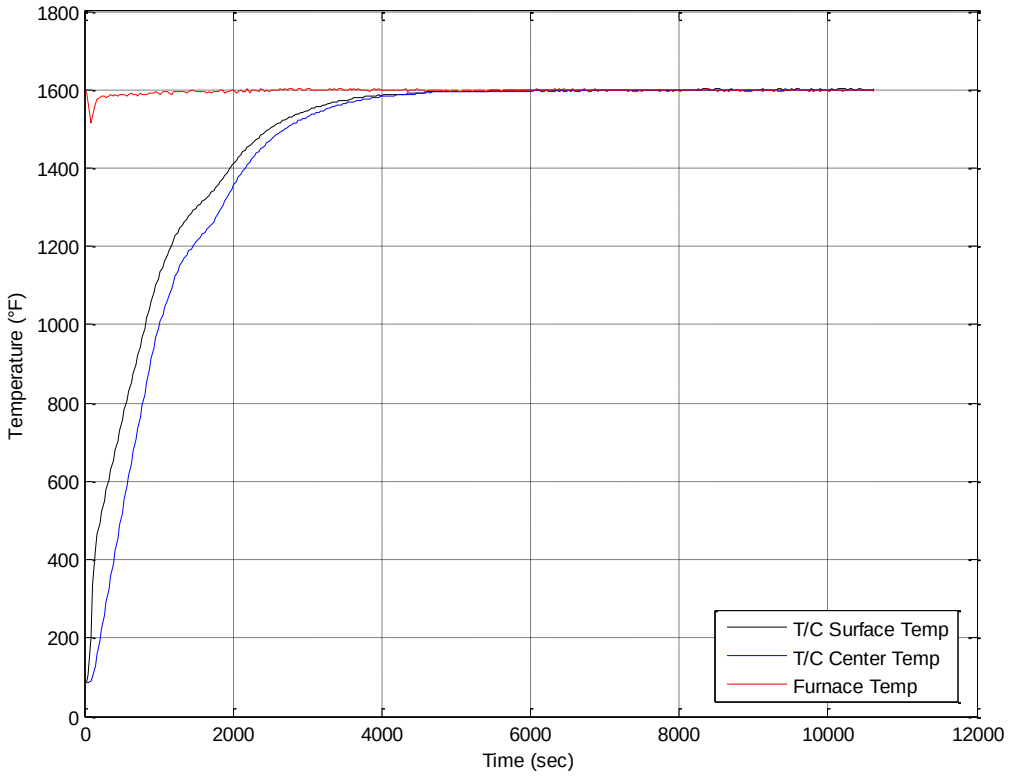

Figure 4-5: Surface and Center Temperature vs. Time (via Load Thermocouples) – Trial GF1

The corresponding gas flow rate for this trial is shown in Figure 4-6. As can be seen, the initial gas flow rate was very high in response to adding the cold load to the furnace environment. As the load increased in temperature, the gas flow rate decreased until it maintained a steady flow rate vs. time corresponding to the load uniformly reaching its target temperature.

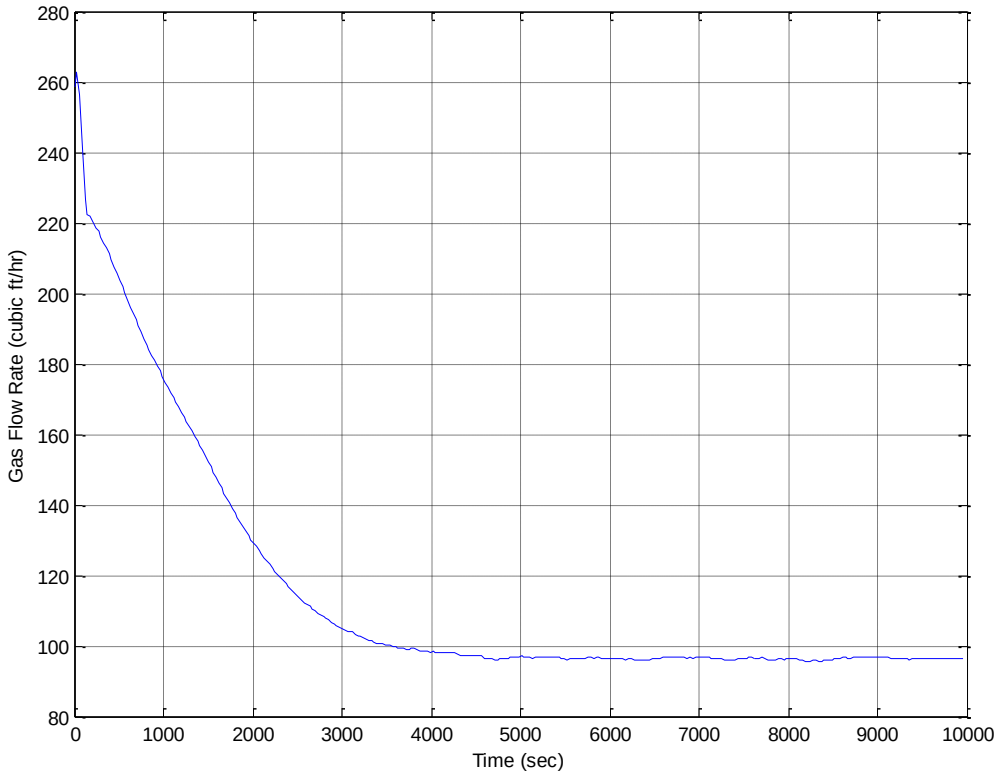

Figure 4-6: Furnace Gas Flow Rate - Trial GF1

The control chart for the derivative of the gas flow rate is shown in Figure 4-7. The magenta lines represented the upper and lower control limits that were statistically determined as three standard deviations above and below the mean of the steady state gas meter behavior. As can be seen, the signal was maintained between the upper and lower control limit from 4,260 seconds into the process and onwards. This point in time represented when the gas flow rate analysis determined the load to be 'on-heat' (under the assumption that the filtering delay was absorbed in the soak period).

Using the conventional hour per inch rule, the load would have been determined to be 'on-heat' at: 1.5 inches * 3600 seconds/inch = 5,400 seconds. Thus the gas flow rate analysis in this trial provided a heat treatment time savings over the hour/inch rule of 1,140 seconds (19

minutes). This represented a 21% efficiency improvement over the current practice technique for load temperature determinism. It should also be noted that when the gas flow rate analysis determined the load to be on heat, the surface thermocouple measured 1589°F which was 11°F below the target temperature (1600°F). The center temperature of the load at this point in time was 1587°F which was 13°F below the target temperature (1600°F). The signal filtering progression used to obtain the signal shown in Figure 4-7 is detailed in Appendix B.

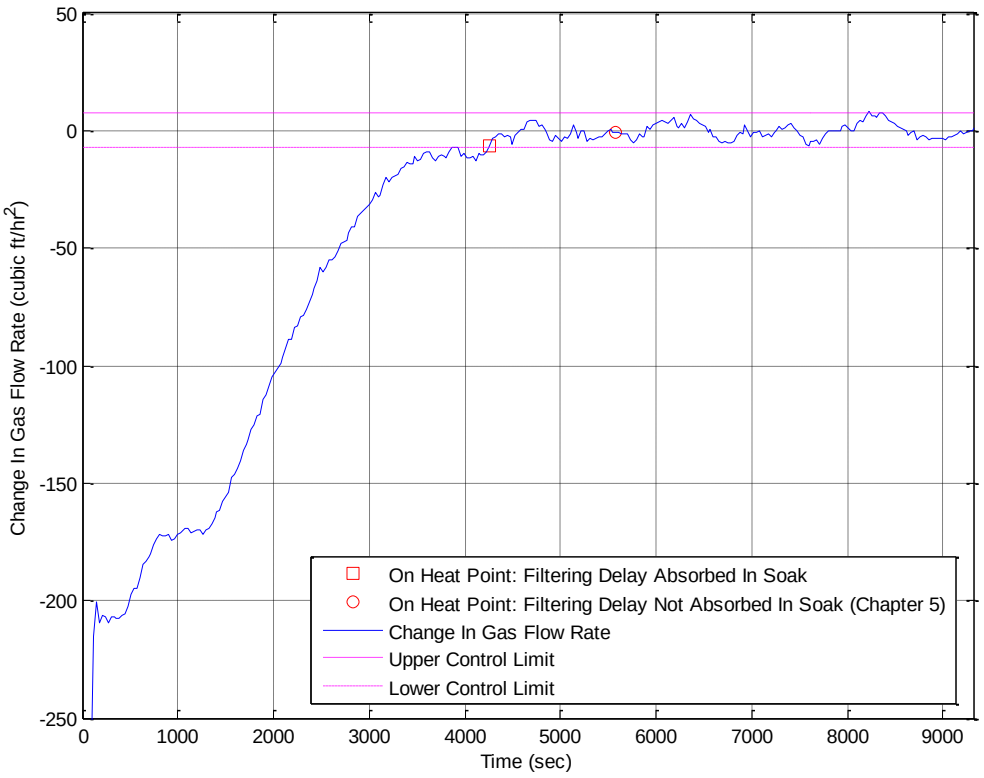

Figure 4-7: Change in Furnace Gas Flow Rate - Trial GF1

4.2.2 Trial GF2

A second trial of the rectangular geometry under identical conditions to the first trial was conducted to evaluate the reproducibility of the gas flow rate analysis method. More trials should

be conducted to further examine the consistency of the method. This type of extensive testing could not be conducted due to furnace scheduling constraints. The furnace thermocouple, and load thermocouple measurements vs. time are shown in Figure 4-8.

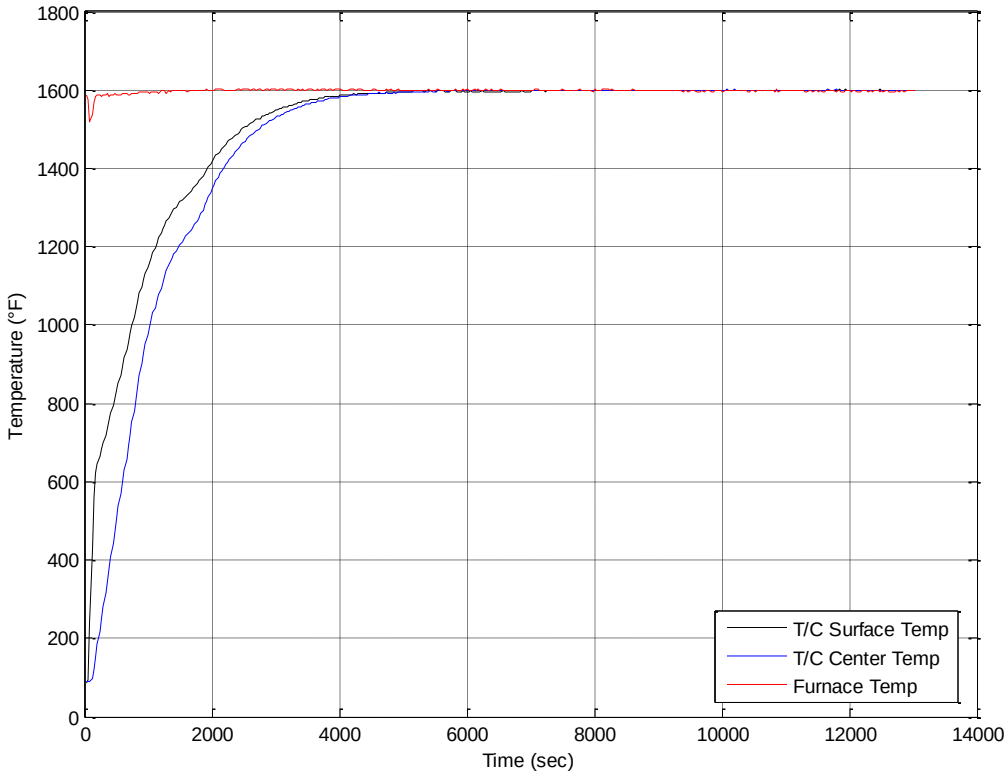

Figure 4-8: Surface and Center Temperature vs. Time (via Load Thermocouples) – Trial GF2

Figure 4-9 displays the gas flow rate vs. time for the second rectangular geometry trial. The behavior of this signal was identical to that of the first trial, as expected. The gas flow rate for both trials drops from about 260 cu. ft gas/hr to around 90 cu. ft gas/hr in about 4,000 seconds.

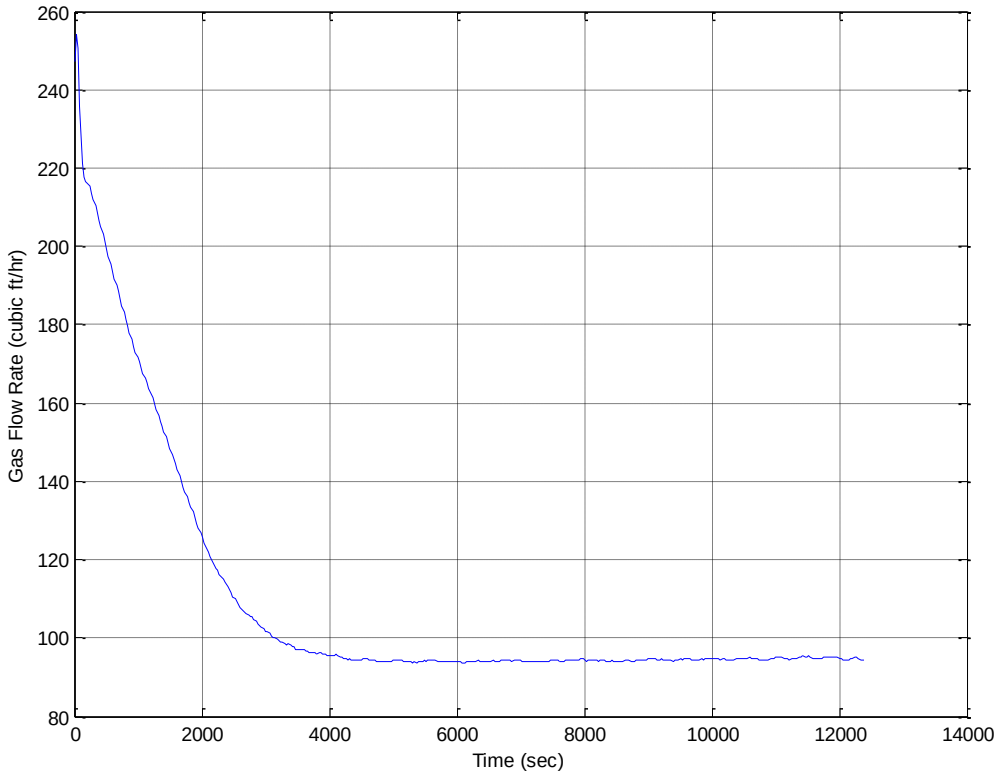

Figure 4-9: Furnace Gas Flow Rate – Trial GF2

Figure 4-10 displays the control chart for the derivative of the gas flow rate. As can be seen, the signal was maintained between the upper and lower control limit from 3,900 seconds into the process onwards. This is only a 6 minute difference compared to the previous trial, which is an indication that this control method is very consistent. However, further trials are necessary to confirm this with a variety of different furnaces and loads.

The determination of the 'on-heat' time of the load in this trial provided a time savings over the hour/inch rule of 1,500 seconds (25 minutes). This represented a 27.8% improvement over the current practice. It should also be noted that, at the point in time at which the gas flow rate analysis determined the load to be on heat, the surface thermocouple measured 1584°F which

was 16°F below the target temperature (1600°F). The center temperature of the load at this point in time was 1580°F which was 20°F below the target temperature (1600°F).

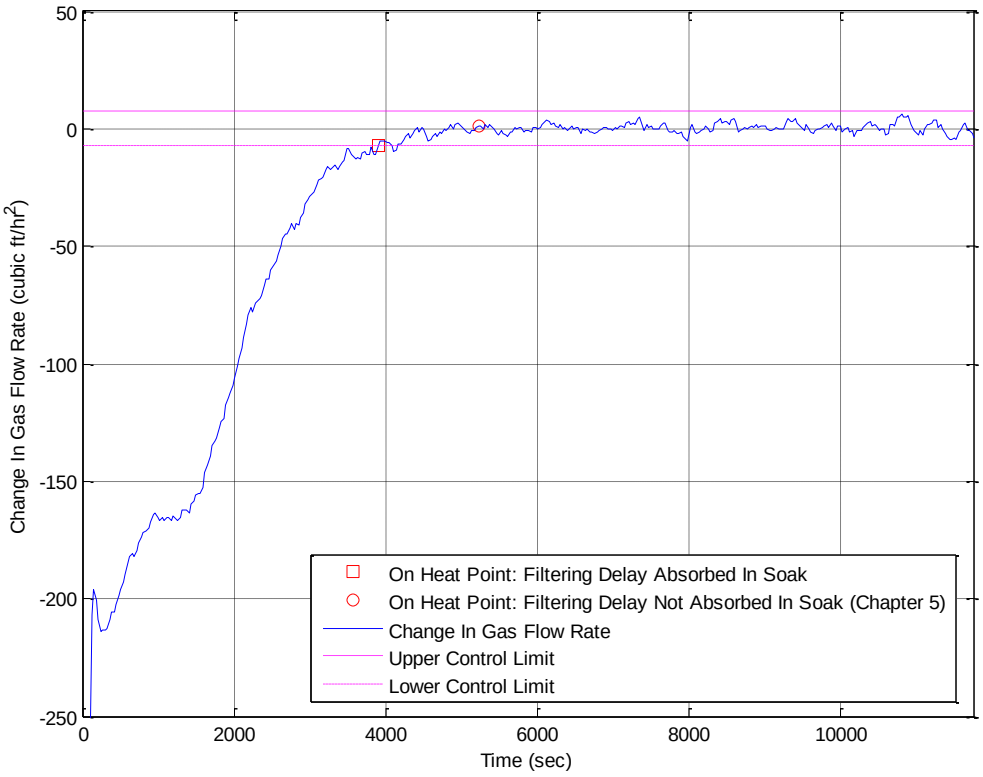

Figure 4-10: Change in Furnace Gas Flow Rate – Trial GF2

4.2.3 Trial GF3

The next heat treatment load geometry to be tested was a solid 8 in. cylinder, which was placed in a furnace at 2000°F. Figure 4-11 gives the furnace and load thermocouple measurements vs. time for this trial. It can be seen that for this large diameter cylindrical geometry, the center temperature of the load lagged behind the surface temperature more

significantly than what was observed for the case of the thin rectangular geometry used in Trials GF1 and GF2.

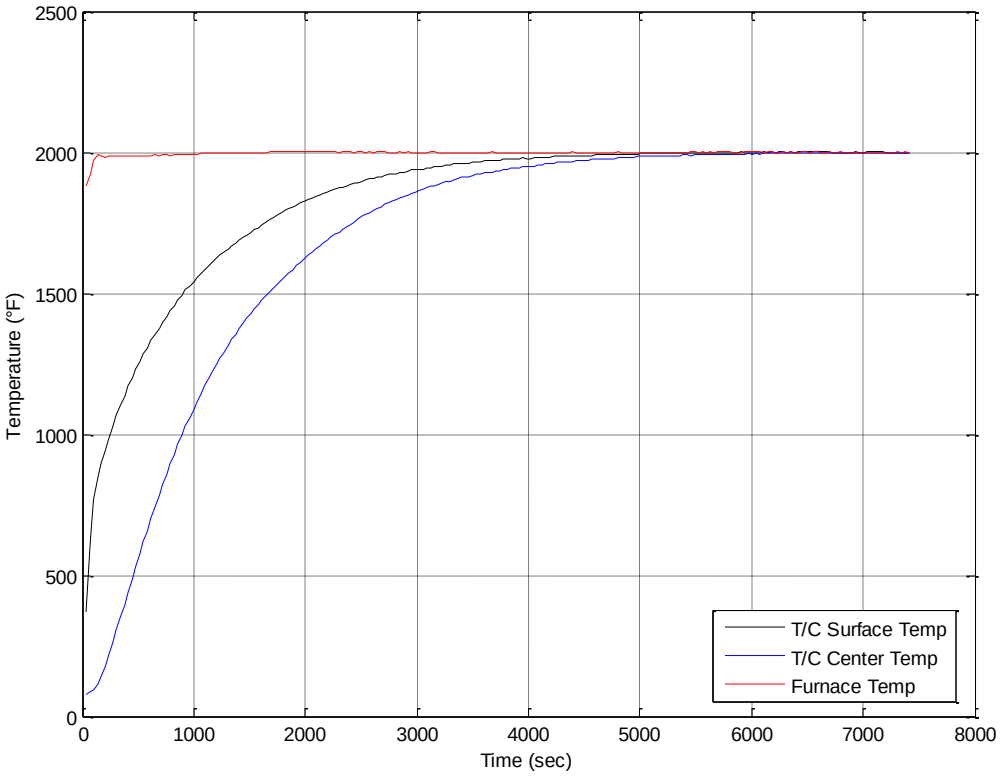

Figure 4-11: Surface and Center Temperature vs. Time (via Load Thermocouples) – Trial GF3

Figure 4-12 shows the gas flow rate vs. time for the 8 in. cylinder. As can be seen in the figure, the behavior of the gas flow rate signal was similar to the signal behavior observed in previous trials. The gas flow rate ramped up when the load was first placed in the furnace at time zero and then slowly decreased, with respect to time, as the load uniformly reached the target temperature.

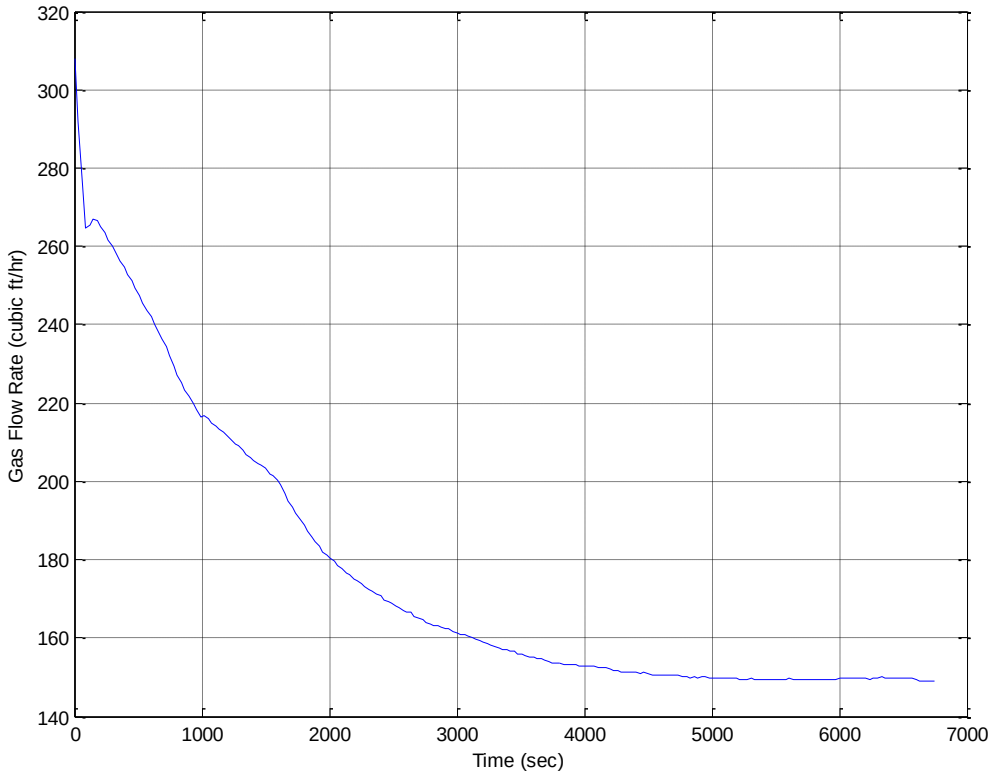

Figure 4-12: Furnace Gas Flow Rate – Trial GF3

Figure 4-13 displays the derivative of the gas flow rate for the 8 in. diameter cylinder. As can be seen, the signal was maintained between the upper and lower control limit from 4,410 seconds into the process onwards. At this point in time, the gas flow rate analysis indicated that the load had uniformly reached its target temperature (under the assumption that filtering delays were absorbed in the control soak). Using the conventional hour per inch rule, the load would have been determined to be 'on-heat' at: 4 inches * 3,600 seconds/inch = 14,400 seconds. Therefore the gas flow rate analysis for the cylindrical geometry in this trial provided a time savings over the conventional hour/inch rule of 9,990 seconds (166.5 minutes). This represented a 69.4% improvement over the current practice. It should also be noted that at the point in time at which the gas flow rate analysis determined the load to be on heat, the surface thermocouple

measured 1996°F which was 4°F below the target temperature (2000°F). The center temperature of the load at this point in time was 1984°F which was 16°F below the target temperature (2000°F).

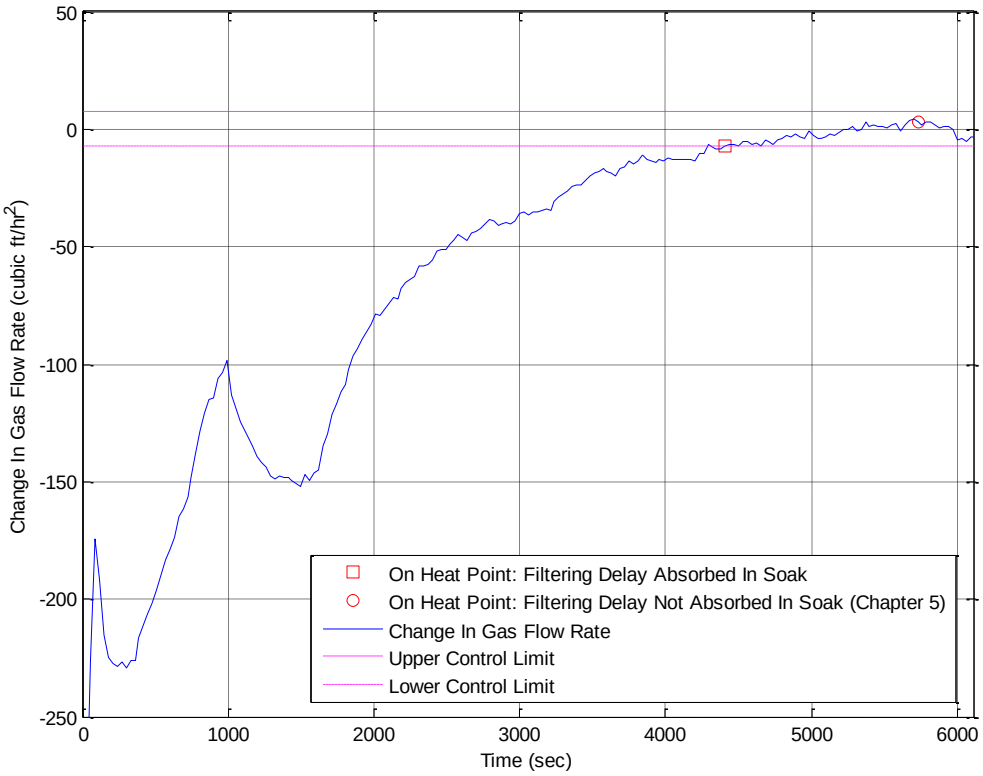

Figure 4-13: Change in Furnace Gas Flow Rate – Trial GF3

4.2.4 Trial GF4

Once the time savings potential for the gas flow rate analysis had been proven for the solid geometries, the next step was to analyze the effectiveness of the control method for a cylindrical bundle of small diameter rods which are commonly annealed at Carpenter Technology, Corp. To this end, a trial was conducted with a 3 in. diameter bundle of 0.3125 in.

diameter rods placed in a 1600°F furnace. Figure 4-14 shows the furnace and load thermocouple measurements vs. time for the trial.

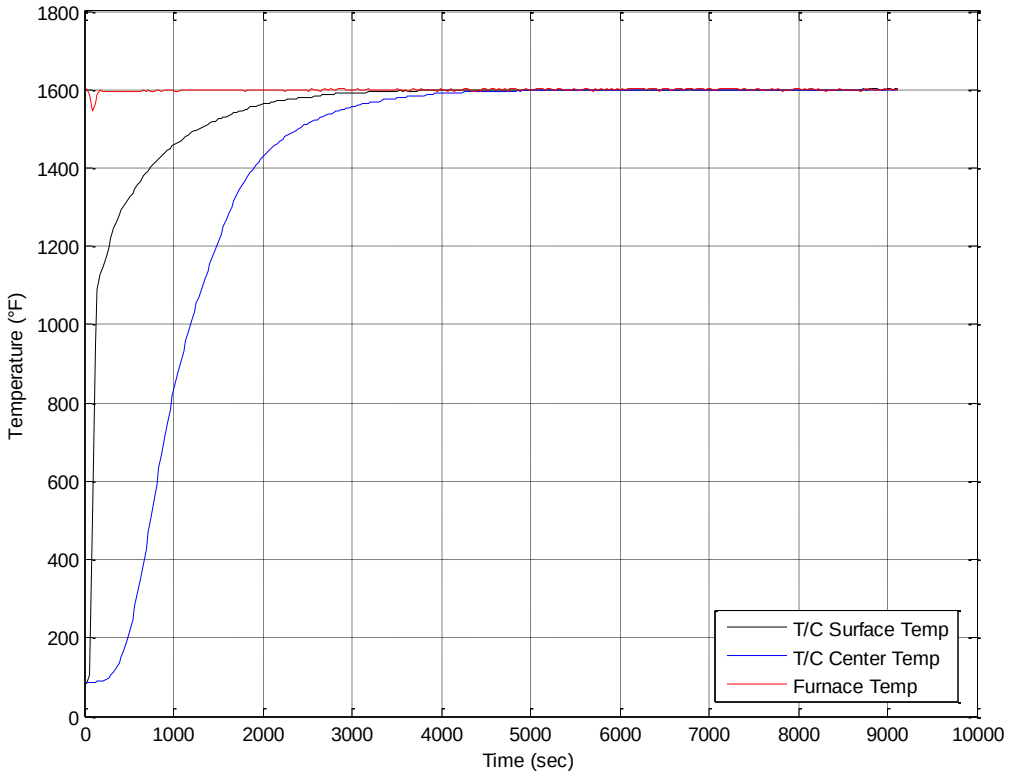

Figure 4-14: Surface and Center Temperature vs. Time (via Load Thermocouples) – GF4

The graph of gas flow rate vs. time for this trial is shown in Figure 4-15. The less pronounced change in gas flow indicated in this graph was due to the smaller size of the load compared to the previous trials. However, even for this small load, it should be noted that the gas flow into the furnace environment was still significantly influenced by the addition of the load.

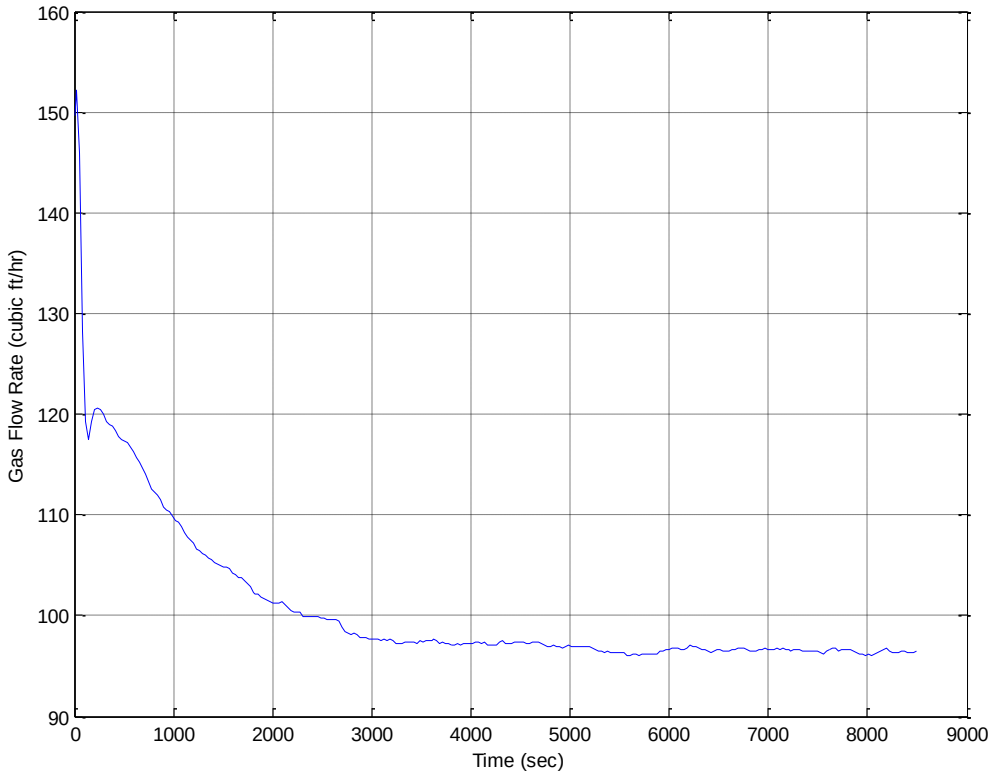

Figure 4-15: Furnace Gas Flow Rate – GF4

The change in furnace gas flow vs. time for the 0.3125 in. rod bundle is indicated in Figure 4-16. As can be seen, the signal was maintained between the upper and lower control limit from 2,730 seconds into the process onwards. At this point in time, the gas flow rate analysis indicated that the load had uniformly reached its target temperature. Using the hour per inch rule, the load would have been determined to be 'on-heat' at: 1.5 inches * 3,600 seconds/inch = 5,400 seconds. Therefore the gas flow rate analysis for the 0.3125 in. bundle provided a time savings over the hour/inch rule of 2,670 seconds (44.5 minutes). This represented a 49.4% improvement over the current practice. It should also be noted that at the point in time at which the gas flow rate analysis determined the load to be on heat, the surface thermocouple measured 1588°F which was 12°F below the target temperature (1600°F). The

center temperature of the load at this point in time was 1539°F which was 61°F below the target temperature (1600°F).

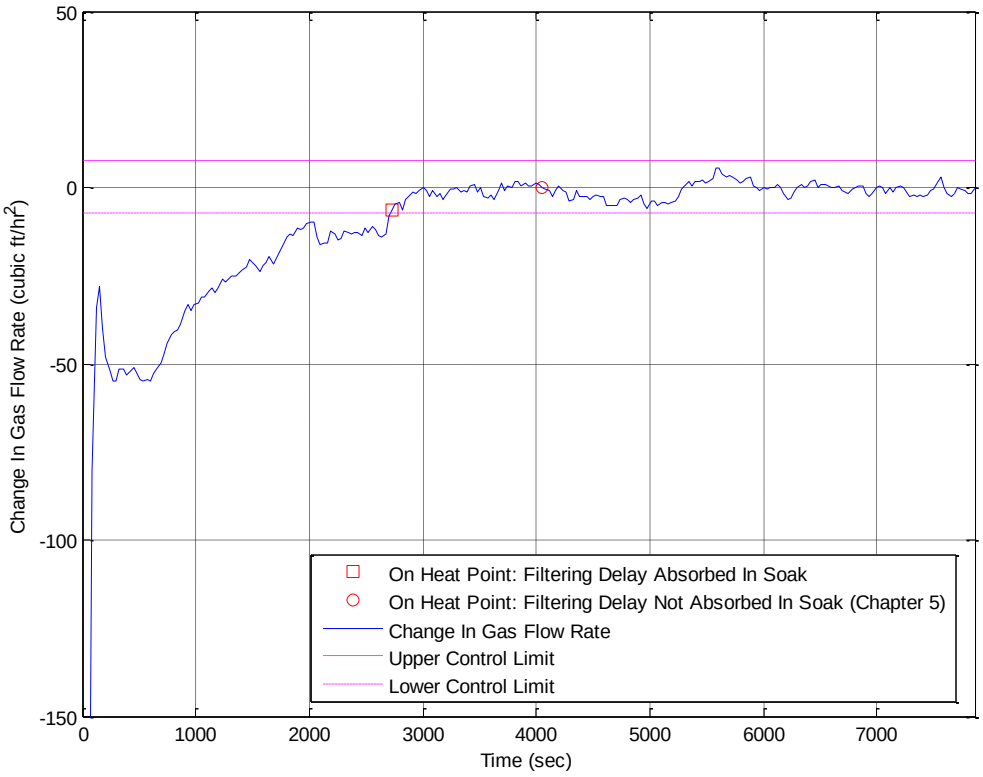

Figure 4-16: Change in Furnace Gas Flow Rate – GF4

4.2.5 Summary of Trials

Table 4-3 displays a summary of the previously discussed gas flow analysis trials. The time savings results displayed in this table assumed that the filtering time necessary to interpret the derivative of the gas flow rate was absorbed in the control soak portion of the heat treatment cycle. Additionally, it was assumed that the window of time used to verify that the signal was within its upper and lower limits was also absorbed in the control soak period. Chapter 5 will discuss the implications of dropping these assumptions.

As can be seen in Table 4-3, the gas flow rate analysis provided significant time savings for each trial. It should be noted that the 8 in. diameter cylinder was placed in a 2000°F furnace, while the other trials were conducted in a 1600°F furnace. It is possible that the larger time savings for the 8 in. diameter cylinder could partly be attributed to its faster rate of heating. However, that the hr/inch rule is not adjusted for differing furnace temperatures.

Also, the results show that the surface temperature in all trials at the 'on-heat' time was within the maximum tolerance of 18°F. The difference between the center temperature and the target at the 'on-heat' time was below 20°F for all trials except for the rod bundle trial which had a center temperature difference of 61°F. This may be considered too low to satisfy metallurgical specifications. Further trials should be conducted to evaluate the gas flow rate analysis for bundles of rods of varying diameters. Unfortunately, due to project time restrictions, this was not possible.

Table 4-3: Gas Flow Analysis Summary of Results

Trial Description	"On-Heat" Time (sec)	Time Savings over hr/inch rule (min)	Surface Temperature (°F)	Temperature Difference Between Surface and Target (°F)	Center Temperature (°F)	Temperature Difference Between Center and Target (°F)
GF1 - Rectagle Trial 1	4260	19	1589	11	1587	13
GF2 - Rectangle Trial 2 (replicate of GF1)	3900	25	1584	16	1580	20
GF3 - 8 in. Cylinder	4410	167	1996	4	1984	16
GF4 - 0.3125 in. Rod Bundle	2730	45	1588	12	1539	61

4.3 Infrared Signal Derivative Analysis

In this section the four different trials conducted to analyze the OP-AID method will be summarized, and the results will be presented. After individual discussion of each trial, the key results will be summarized. The trials will be referred to by the abbreviations given in Table 4-4, and will be presented in the order listed. It should be noted that these trial conditions were identical to the previously discussed gas flow rate analysis trials.

Table 4-4: OP-AID Method Trial Description Abbreviations

Trial Abbreviation	Trial Description
OP-AID 1	49.25 in. x 7.88 in. x 3 in. rectangle on its side at 1600°F with 2.2um sensor at 0.925 emissivity (Trial 1)
OP-AID 2	49.25 in. x 7.88 in. x 3 in. rectangle on its side at 1600°F with 2.2um sensor at 0.925 emissivity (Trial 2)
OP-AID 3	8 in. cylinder at 2000°F with 2.2um sensor at 0.95 emissivity
OP-AID 4	0.3125 in. rod bundle (D=3 in.) at 1600°F with 1.65um sensor at 0.9 emissivity

This analysis compared load temperatures to the rate of change of the load surface temperature. Similar to the gas flow analysis, the time delays associated with the moving average filters applied for the surface temperature derivative were assumed to be absorbed in the control soak period. Furthermore, it was assumed that the window of time designated for the limit check was also absorbed in the control soak period. All results presented in this section were based on these assumptions. In the following graphs, an ‘on-heat’ detection point will be depicted that is consistent with these assumptions. For reference, an additional ‘on-heat’ detection point will be depicted that corresponds to a relaxation of these assumptions. This delayed ‘on-heat’ detection point will be further discussed in Chapter 5 while comparing the different control methods.

Also, the thermocouple measurements in all of the following trial results have been adjusted for calibration errors that could be quantified when the load was at steady state temperature. Thus to provide uniformity to the results, the thermocouple measurements have been adjusted by their difference from the furnace thermocouple measurement at steady state. This type of correction assumes the furnace thermocouple reading was accurate. The infrared signal has not been correspondingly adjusted, so some of the high readings of the infrared sensor at steady state load temperature may be attributed to IR sensor calibration error. It should be noted that these errors have no impact on the control strategy developed.

4.3.1 Trial OP-AID 1

The first trial in which the OP-AID method was tested involved heating a rectangular billet of dimension 49.25 in. x7.88 in. x 3 in. to 1600°F. Figure 4-17 displays the thermocouple and infrared sensor measurement for the rectangular geometry for its first trial. The rectangle was laid on its narrow side for the trial. As can be seen in Figure 4-17, due to the thin width of the rectangular billet, the center of the load does not significantly lag behind the surface temperature of the load.

The infrared temperature signal is shown in Figure 4-17 in light blue and was consistently slightly above the surface thermocouple measurement. The probable explanation for this discrepancy is that the surface thermocouple in the rectangular billet was embedded slightly below the surface, which could account for its lag in temperature measurement as compared to the infrared sensor surface temperature measurement. Also as expected, in the early stages of the heating process, the infrared measurement was artificially high due to the background radiation effects from the furnace environment that reflect more energy than that generated by the load.

However, as the surface of the load approaches the furnace temperature, the infrared sensor becomes more and more accurate. This was characteristic of all the trials conducted.

It should be noted that despite the discrepancy between the surface thermocouple and the infrared sensor measurement, the OP-AID method provided good results. This was due largely to the fact that the OP-AID method relies on the relative measure of the 'rate of change of the infrared sensor measurement' rather than on its absolute accuracy. Therefore, the previously mentioned inaccuracies have virtually no effect on the method's ability to accurately predict when the load reaches its target temperature.

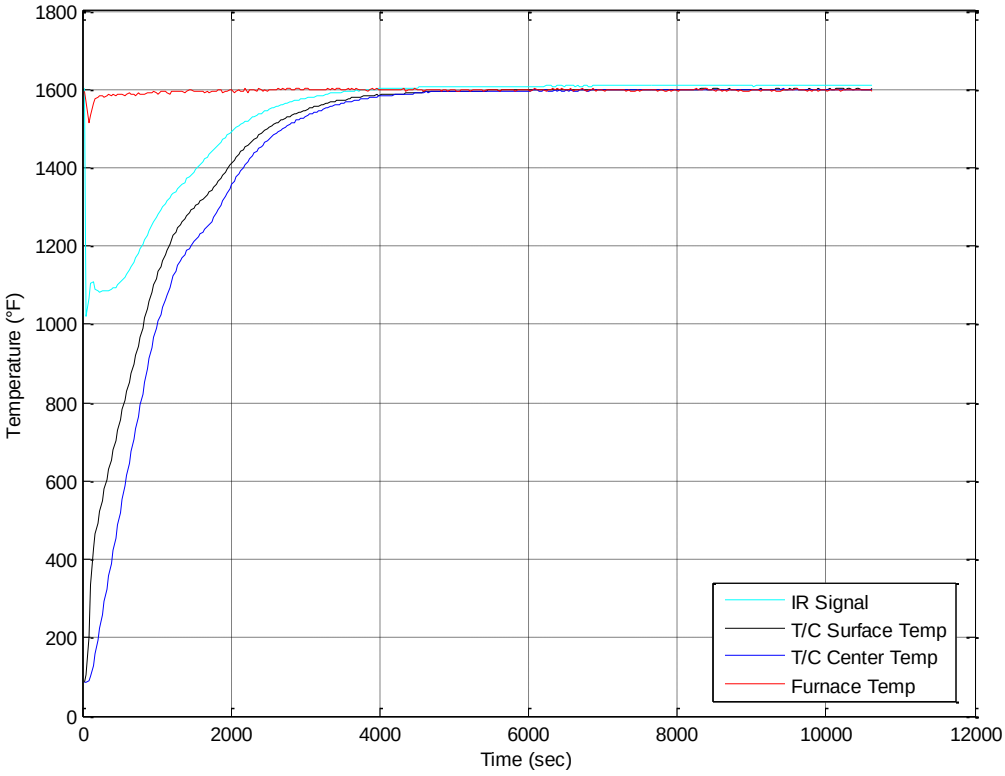

Figure 4-17: Thermocouple Data: Trial OP-AID 1

The infrared signal derivative of the rectangle surface temperature is shown in Figure 4-18. The signal was maintained between the upper and lower control limit from 3,960 seconds

into the process onwards. This point in time represents when the OP-AID method would determine the load to be ‘on-heat’ (under the assumption that the filtering delays are absorbed in the soak period). Using the conventional hour per inch rule, the load would have been determined to be ‘on-heat’ at: 1.5 inches * 3600 seconds/inch = 5,400 seconds. Thus the OP-AID method provided a time savings over the hour/inch rule in this trial of 1,440 seconds (24 minutes). This represented a 26.7% improvement over the current practice. It should also be noted that at the point in time at which the OP-AID method determined the load to be on heat, the surface thermocouple measured 1587°F which was 13°F below the target temperature (1600°F). The center temperature of the load at this point in time was 1580°F which was 20°F below the target temperature (1600°F). The signal filtering progression used to obtain the signal shown in Figure 4-18 is detailed in Appendix C.

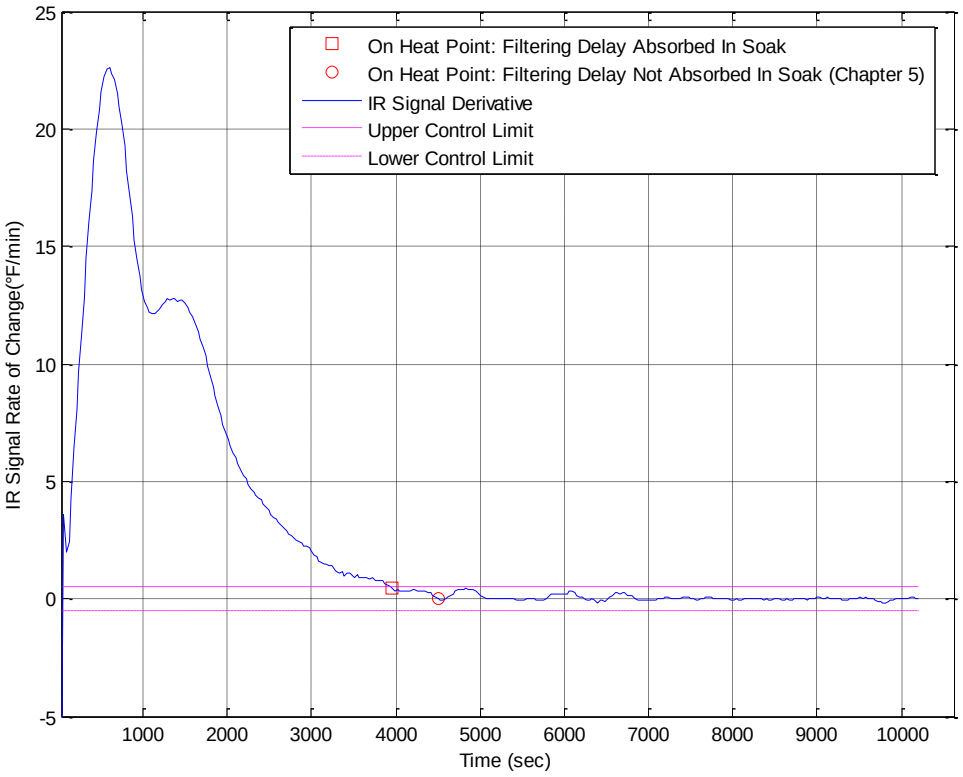

Figure 4-18: Infrared Signal Derivative Control Chart: Trial OP-AID 1

4.3.2 Trial OP-AID 2

Figure 4-19 displays the thermocouple and infrared sensor measurement versus time for a second trial conducted with the rectangular geometry. A second trial was run under the exact same conditions as the first trial, but the surface thermocouple was exchanged with a new thermocouple to check if its discrepancy with the infrared sensor could be attributed to the thermocouple. The results of this second trial were identical to the first, which suggests that these discrepancies were caused by the thermocouple placement rather than thermocouple error.

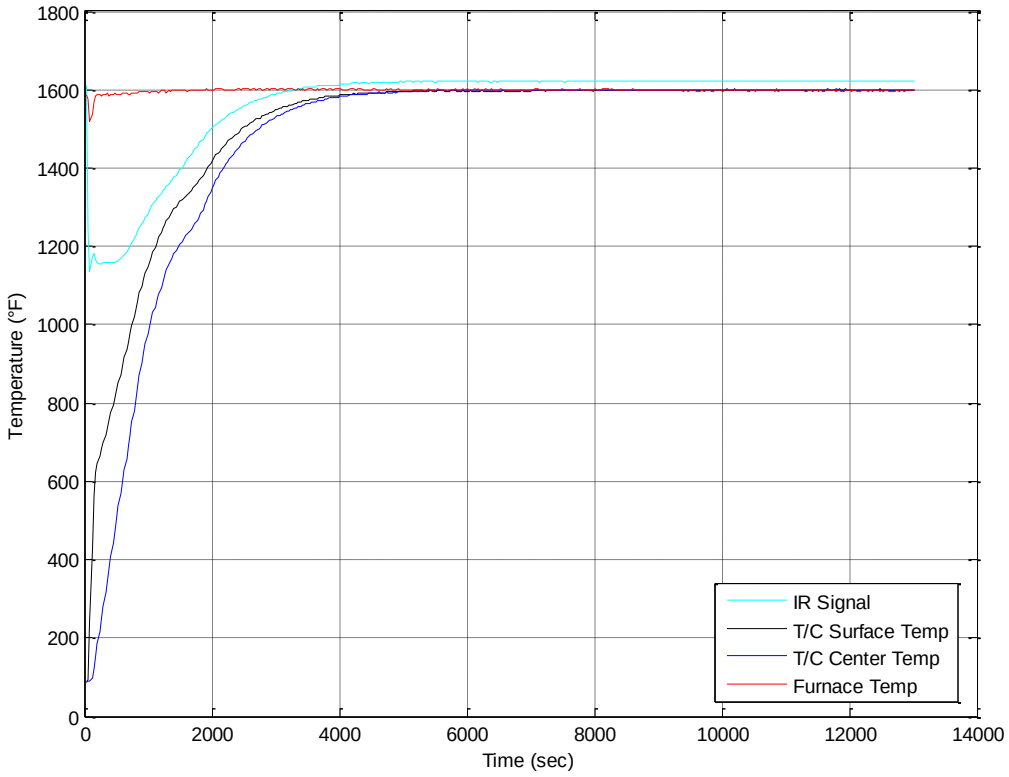

Figure 4-19: Infrared Signal Derivative Control Chart: Trial OP-AID 2

The derivative of the infrared sensor measurement for the second trial is shown in Figure 4-20. The signal was maintained between the upper and lower control limit from 3,990 seconds into the process onwards. This point in time corresponds to 'on-heat' detection by the OP-AID method assuming signal filtering time was absorbed in the control soak. It should be noted that this was only a 30 second difference from the first trial which indicates a high degree of consistency in the OP-AID method. Again, using the hour per inch rule the load would have been determined to be 'on-heat' at: 1.5 inches * 3600 seconds/inch = 5,400 seconds. Thus the OP-AID method provided a time savings over the hour/inch rule of 1,410 seconds (23.5 minutes) which was a 26.1% improvement over the current practice. It should also be noted that at the point in time at which the OP-AID method determines the load to be on heat, the surface thermocouple

measured 1584°F which was 16°F below the target temperature (1600°F). The center temperature of the load at this point in time was 1580°F which was 20°F below the target temperature (1600°F).

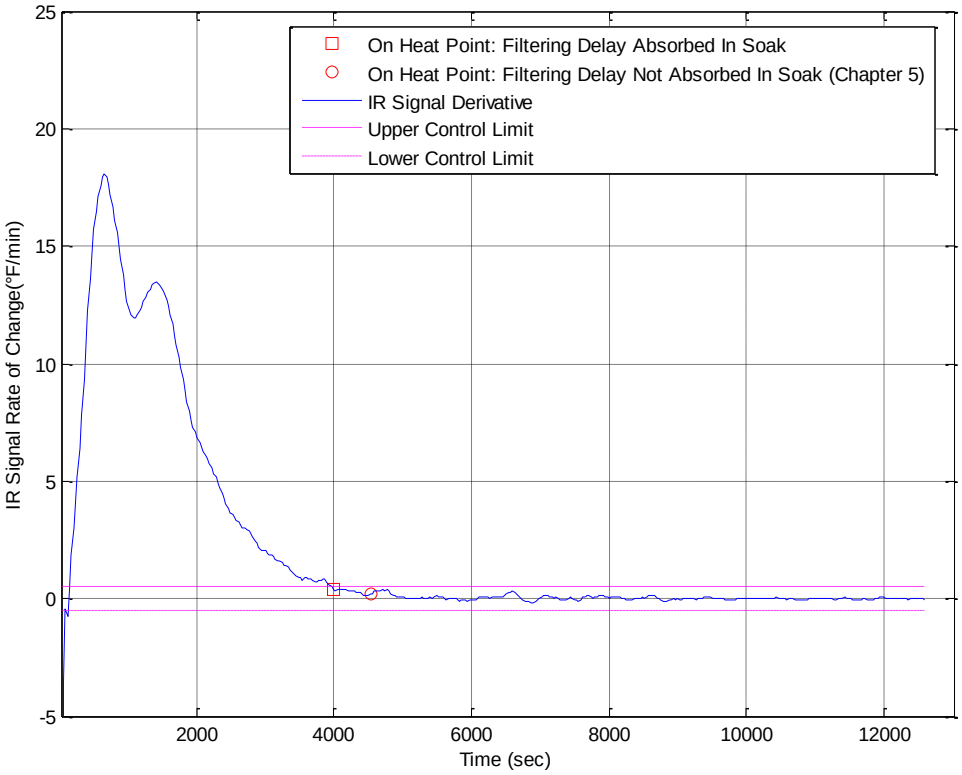

Figure 4-20: Infrared Signal Derivative Control Chart: Trial OP-AID 2

4.3.3 Trial OP-AID 3

The next type of solid geometry tested was an 8 in. diameter cylinder placed in a 2000°F furnace. Figure 4-21 displays the infrared sensor measurement and the load thermocouple measurement vs. time. As can be seen, in the later portion of the heating cycle, the infrared

sensor measurement and the surface thermocouple measurement do agree much more closely than for the rectangular geometry.

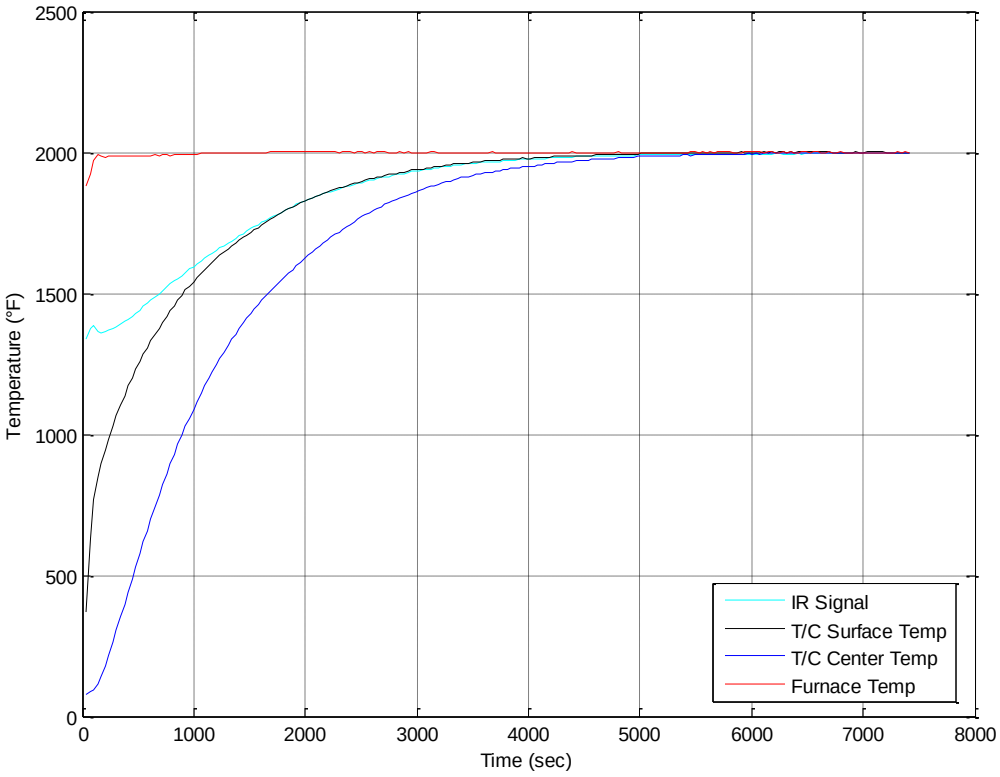

Figure 4-21: Thermocouple Data: Trial OP-AID 3

Figure 4-22 displays the results of the infrared signal derivative for the 8 in. diameter cylinder. The control limits are shown in Figure 4-22 by the dotted magenta lines. The signal shown in Figure 4-22 oscillates between these limits from 4,943 seconds into the cycle onwards. With filtering delays absorbed in the soak period, the OP-AID method would determine the load to be 'on-heat' at this point in time. The hour per inch rule would dictate that the load would take: 4 inches * 3,600 seconds/inch = 14,400 seconds to reach a uniform temperature before being declared 'on-heat'. Thus the OP-AID method represented a time savings over the hour/inch rule in this case of 9,457 seconds (157.6 minutes) which was a 65.7% improvement

over the current practice. It should also be noted that at the point in time at which the OP-AID method determines the load to be on heat, the surface thermocouple measured 1993°F which was 7°F below the target temperature (2000°F). Similarly, the center thermocouple measured 1982°F which was 18°F below the target temperature (2000°F).

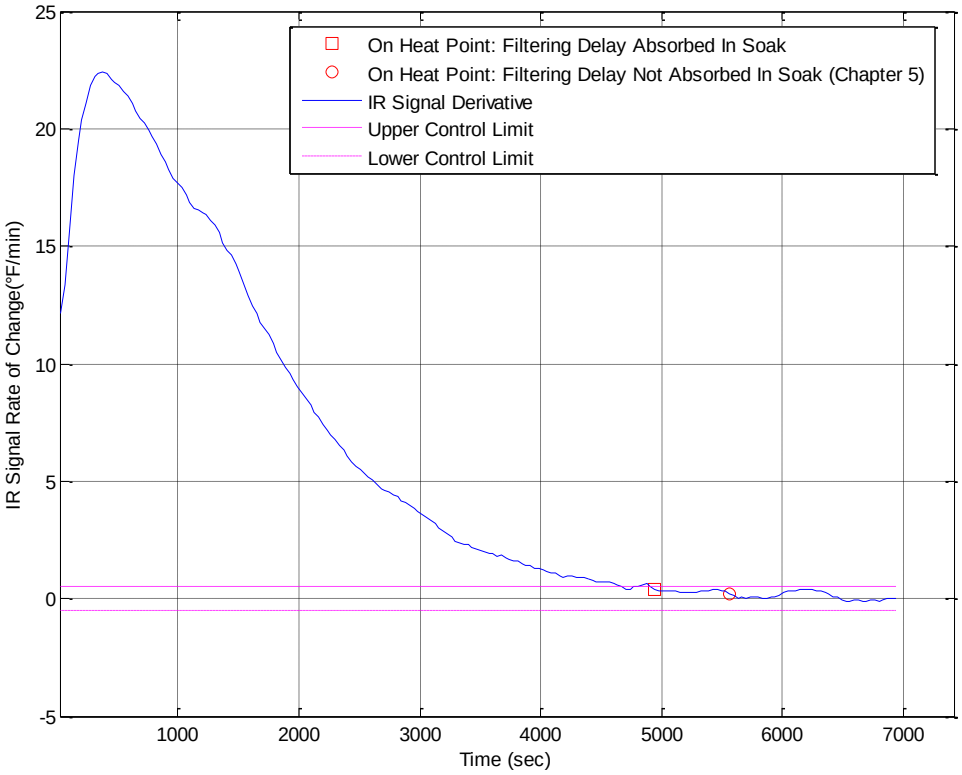

Figure 4-22: Infrared Signal Derivative Control Chart: Trial OP-AID 3

4.3.4 Trial OP-AID 4

After testing the OP-AID method on solid geometries, the next test was on a bundle of rods which are commonly encountered in practice. The bundle tested was a 3 in. diameter bundle of rods measuring 0.3125 in. in diameter. Thermocouple data is shown in Figure 4-23, along with

the infrared sensor measurement. The temperatures vs. time profiles are similar in shape to that of the solid cylinder.

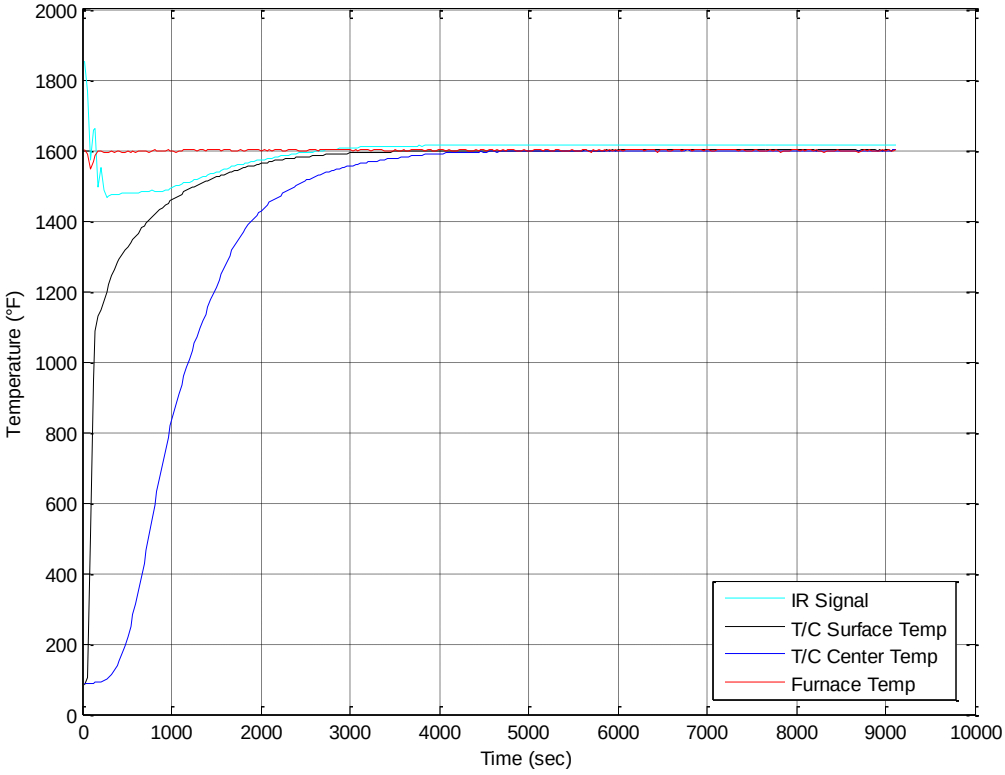

Figure 4-23: Thermocouple Data: Trial OP-AID 4

Figure 4-24 displays the derivative of the infrared signal for the rod bundle surface temperature shown Figure 4-23. As can be seen in the control chart, the signal was within the upper and lower control limits from 3,180 seconds into the cycle onwards. This point in time represents when the OP-AID method would determine the load to be 'on-heat' with filtering delays absorbed in the soak period. If the 'on-heat' time had been calculated using the hour per inch rule it would have taken: 1.5 inches * 3600 seconds/inch = 5,400 seconds. The OP-AID method then represented a time savings in this case of 2,220 seconds, or about 37 minutes. Thus the OP-AID method provided a 41.1% time improvement over the hour per inch rule. It should

also be noted that at the point in time at which the OP-AID method determines the load to be on heat, the surface thermocouple measured 1595°F which was 5°F below the surface thermocouple target temperature (1600°F). The center temperature of the load at this point in time was 1565°F which was 35°F below the target temperature (1600°F).

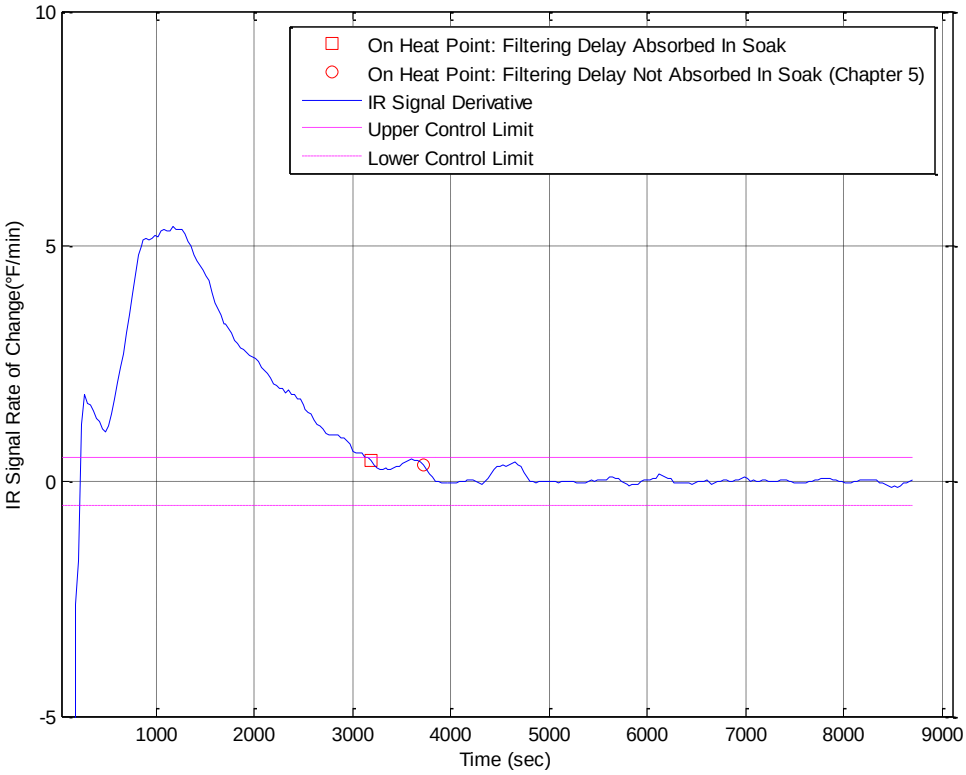

Figure 4-24: Infrared Signal Derivative Control Chart: Trial OP-AID 4

4.3.5 Summary of Trials

Table 4-5 displays a summary of the previously discussed OP-AID trials. The time savings results displayed in this table assumed that the filtering time necessary to interpret the derivative of the infrared signal is absorbed in the control soak portion of the heat treatment cycle. Additionally, it was assumed that the window of time used to verify that the signal was

within its upper and lower limits was also absorbed in the control soak period. The OP-AID method provides significant time savings under these previously mentioned assumptions as is shown in Table 4-5. Again it should be noted that the 8 in. cylinder was placed in a 2000°F furnace, while the other trials were conducted in a 1600°F furnace. It is possible that the larger time savings for this higher temperature trial is attributed to the corresponding faster rate of heating.

Also, the results show that the surface temperature in all trials was well within the maximum tolerance of 18°F. The difference between the center temperature and target was below 20°F for all trials except for the trial with the rod bundle which had a temperature difference of 35°F below the target temperature. Further trials with rod bundles should be conducted, and if the center temperatures of bundles are consistently low, then the OP-AID control limits could be made more conservative from a metallurgical standpoint. This would amount to making the control limits narrower so that a lower rate of change in the surface temperature is achieved before the load is declared ‘on-heat’. However, losses in time savings should correspondingly be considered.

Table 4-5: OP-AID Summary of Results.

Trial Description	"On-Heat" Time (sec)	Time Savings over hr/inch rule (min)	Surface Temperature (°F)	Temperature Difference Between Surface and Target (°F)	Center Temperature (°F)	Temperature Difference Between Center and Target (°F)
OP-AID 1 - Rectangle Trial 1	3960	24	1587	13	1580	20
OP-AID 2 - Rectangle Trial 2 (replicate of OP-AID 1)	3990	24	1584	16	1580	20
OP-AID 3 - 8" Cylinder	4943	150	1993	7	1982	18
OP-AID 4 - 0.3125" Rod Bundle	3180	37	1595	5	1565	35

4.4 OP-AID Multi-Criteria Analysis

4.4.1 OP-AID Control Limit Specification with a Conservative Emphasis on Time Savings

Figure 4-25 displays the weighted scores vs. the control limit values for a very conservative on-heat determination. For the conservative approach, the importance of maximizing the center temperature for each trial was given a 10, while time minimization criteria are ignored and were rated at 0. Thus, the weighted score for each alternative represented the user's preference of control limits with no emphasis given to minimizing the 'on heat' time. The weighted scores and scaled criteria values are tabulated in Table D-2. The corresponding unscaled values are tabulated in Table D-1.

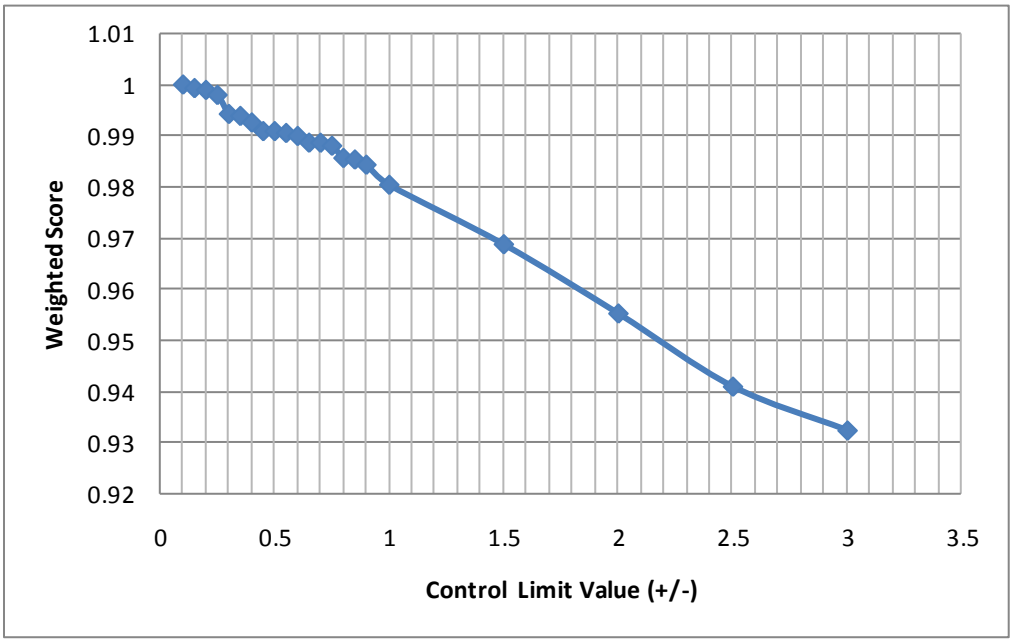

Figure 4-25: Weighted Score vs. Control Limit Value. The weighted score represents the balance of cost to quality with a conservative emphasis on cost savings.

As is demonstrated in Figure 4-25, the weighted sum which corresponds to the user's best preference decreased as the width of the control limits increased. The results are to be expected, since a conservative user would prefer to wait until a minimal rate of change in the surface temperature of the load is attained. To accomplish this, the user would specify the narrowest control limits possible, here designated at +/- 0.1°F/min. Table 4-4 displays the implications of declaring the load 'on-heat' when the rate of change in the load surface was less than 0.1°F/min. From the values shown in Table 4-4, the surface temperature at the 0.1°F/min control limit level was between 2°F to 8°F away from its target value. The center temperature was between 5°F to 13°F away from its target value. The time savings over the conventional hour/inch rule with this conservative 'on-heat' determinism was 8 to 16 minutes for the rectangular geometries, 146 minutes for the 8 in. diameter cylinder, and 26 minutes for the rod bundle.

Table 4-6: Load temperature differences from target values and time savings over inch per hour rule associated with 'on-heat' decisions corresponding to varying control limit selections.

	Rectangle Trial 1			Rectangle Trial 2			8" Cylinder			0.3125" Bundle		
Alternatives: (UCL, LCL)	Target minus Surface (°F)	Target minus Center(°F)	Time Savings Over Hour/Inch (min)	Target minus Surface (°F)	Target minus Center(°F)	Time Savings Over Hour/Inch (min)	Target minus Surface (°F)	Target minus Center(°F)	Time Savings Over Hour/Inch (min)	Target minus Surface (°F)	Target minus Center(°F)	Time Savings Over Hour/Inch (min)
0.1, -0.1	8	9	16	5	5	8	2	6	146	3	13	26
0.15, -0.15	9	11	16	5	5	8	2	6	147	3	15	27
0.2, -0.2	9	11	16	5	7	9	2	6	147	3	15	27
0.25, -0.25	9	11	16	9	11	17	2	8	147	3	15	27
0.3, -0.3	9	11	16	10	13	18	4	13	154	5	33	36
0.35,-0.35	11	13	19	12	13	20	4	13	155	5	33	36
0.4, -0.4	15	18	24	12	13	20	7	16	157	5	32	37
0.45, -0.45	13	20	24	16	20	24	7	18	158	5	35	37
0.5, -0.5	13	20	24	16	20	24	7	18	158	5	35	37
0.55,-0.55	15	20	25	16	20	24	7	18	158	8	37	38
0.6,-0.6	15	20	25	16	20	25	9	23	162	8	37	38
0.65, -0.65	18	20	26	16	20	25	9	25	163	8	43	40
0.7, -0.7	18	20	26	16	20	25	9	25	163	8	43	40
0.75, -0.75	18	20	26	16	20	25	12	30	166	8	43	40
0.8, -0.8	18	25	27	20	28	29	12	30	166	10	46	41
0.85, -0.85	20	25	28	23	28	29	14	32	167	10	46	41
0.9, -0.9	22	27	29	23	31	30	14	32	167	10	48	41
1, -1	24	33	31	29	39	33	17	39	171	10	52	42
1.5, -1.5	40	53	37	38	50	36	24	56	175	19	82	48
2, -2	51	66	40	51	67	40	33	76	180	28	121	53
2.5, -2.5	66	86	43	64	84	43	45	101	185	34	156	56
3, -3	77	101	45	72	100	45	49	113	188	36	171	57

4.4.2 OP-AID Control Limit Specification with an Aggressive Emphasis on Time Savings

Figure 4-26 displays the weighted score vs. control limit specification for aggressive 'on-heat' determinism with emphasis placed on time savings. For the aggressive approach, an importance rating of 10 was given to maximizing the center temperature and an importance rating of 2 was given to minimizing the 'on-heat' time. The weighted scores and scaled criteria values used to generate this graph are displayed in Table D-3. The corresponding unscaled values are shown in Table D-1.

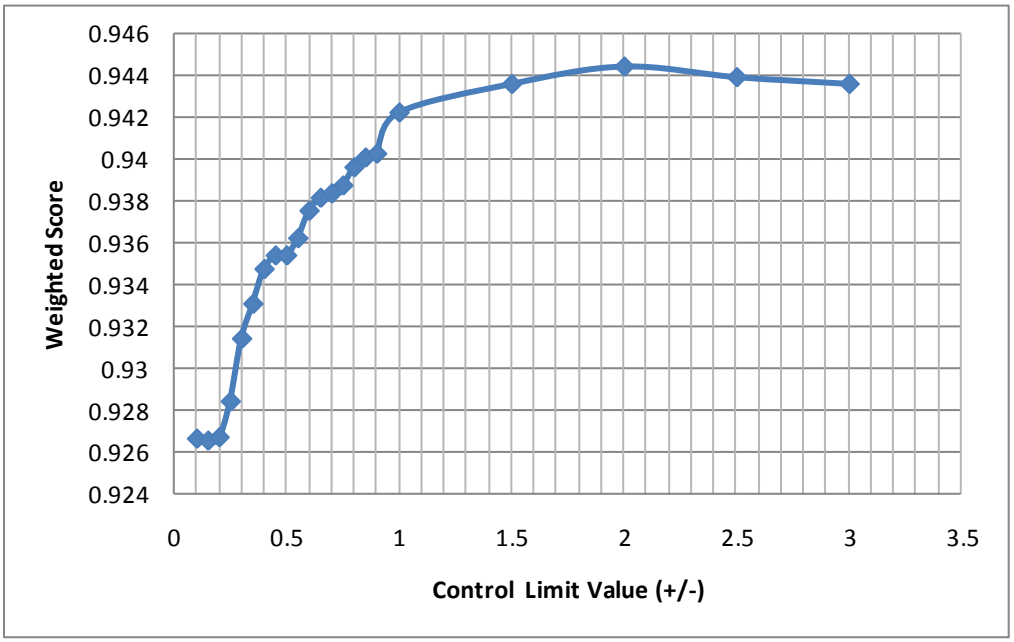

Figure 4-26: Weighted Score vs. Control Limit Value. The weighted score represents the balance of cost to quality with an aggressive emphasis placed on cost savings.

As is demonstrated in Figure 4-26, the weighted sum which corresponds to the user's best preference increased as the width of the control limits increased. The results are to be expected, since an aggressive user placed a large emphasis on time savings. In general, due to the exponential nature of the heating curve, as the load approached its target temperature, an incremental amount of load heating was lost for a large increase in time savings. Thus, when an aggressive emphasis was placed on time savings, the weighted sum was dominated by the significant time savings derived from widening the control limits. As the control limits were widened, the load was declared 'on-heat' earlier and earlier. After the control limits were widened to a certain extent, the center temperature associated with the 'on-heat' decision was low enough to outweigh the benefits of the time savings. Thus, the curve in Figure 4-26 increased at a decreasing rate.

With the increasing behavior of the weighted sum shown in Figure 4-26, an aggressive user would be satisfied with a large control limit, as long as the surface temperature of the load

was within the specified 18°F of its target value. Thus the only constraint limiting the width of the control limits in a very aggressive approach is the surface temperature restriction. Table 4-4 displays the implications of declaring the load 'on-heat' at the upper limit of the surface temperature specification. The grey regions of the table represented control limits that were outside the surface temperature requirement. Significant time savings over the conventional hour/inch rule would be possible with this aggressive 'on-heat' determinism of 25 to 27 minutes for the rectangular geometries, 171 minutes for the 8 in. diameter cylinder, and 42 minutes for the rod bundle. However, the average center temperature of the load at this point was greater than 33°F away from its target value. This may be unsatisfactory from a metallurgical perspective.

4.4.3 OP-AID Control Limit Specification with a Moderate Emphasis on Time Savings

Figure 4-27 displays the weighted scores vs. the control limit values for 'on-heat' determinism with moderate emphasis on time savings. The weighted scores represented the preference of control limits with moderate emphasis given to minimizing the 'on heat' time. For the moderate rating, the importance of maximizing the center temperature was maintained at 10, but a rating of 1 was given to the importance of minimizing the 'on-heat' time. The weighted scores and scaled criteria values used to generate this graph are displayed in Table D-4. The corresponding unscaled values are shown in Table D-1.

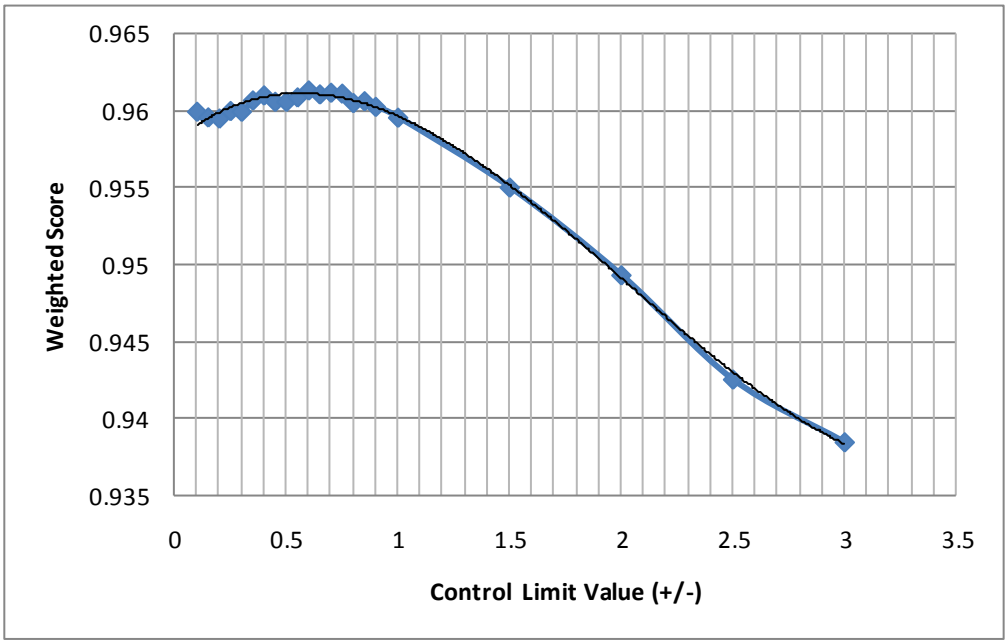

Figure 4-27: Weighted Score vs. Control Limit Value. The weighted score represents the balance of cost to quality with a moderate emphasis on cost savings.

Based on the shape of the conservative and the aggressive curves, the moderate curve shown in Figure 4-27 fitted well between the two. A small increase in the weighted sum occurred initially with the increase of the control limits from their minimum value. The moderate emphasis on time savings had a large impact on the weighted sum when the temperature increased incrementally for an exponential increase in time. When the control limits were widened to a certain point, the exponential time-temperature relationship was less pronounced (since this was at an earlier time in the heating cycle). At this point, as the control limits widened, the decrease in center temperature began to have a pronounced detrimental effect on the weighted score.

The drive to achieve cost savings increased the weighted score as the control limits were widened; however, the drive to maximize the center temperature decreased the weighted score as the control limits were widened. As is shown in Figure 4-27, with the moderate emphasis on time savings, the effects of both these criteria were reflected by the initially increasing, and then

decreasing slope of the weighted score. The inflection point represented a transition from an emphasis on cost savings to an emphasis on quality. This transition point occurred prior to the +/-0.75°F/min control limit specification, which was the upper control limit width that satisfied the surface temperature requirement for all load geometries (see Table 4-4).

To estimate this transition point in Figure 4-27, a regression analysis was conducted to first fit a curve to the data. Figure 4-27 shows the fitted curve of the control limit predictor variables. This fitted curve was a cubic polynomial (justified in detail in Section 4.4.4). Since the maximum of the fitted curve was used to estimate the aforementioned transition point, the control limit predictor variables were first centered to reduce the correlation between the estimates in the regression equation. By default, lower order terms in a polynomial regression equation are highly correlated to higher order terms. These correlations cause problems with the interpretation of results and could cause bias in the estimates (Cohen, 2003). Thus the control limit predictor variables in the model were centered by their mean, 0.84°F/min. The centered control limit values are detailed in Table D-5.

Table 4-5 shows the correlation matrix for the non centered and centered predictor variables (calculated in MINITAB). As can be seen, the correlation between the estimates was reduced in the case of the centered variables.

Table 4-7: Correlation Matrices for non centered and centered control limit variables

Correlations for non centered variables:

	Limit	Limit^2
Limit^2	0.964	
Limit^3	0.914	0.987

Correlations for centered variables:

	CLimit	CLimit^2
CLimit^2	0.835	
CLimit^3	0.863	0.974

(Cell Contents: Pearson correlation)

A new fitted curve and regression model was constructed based on these centered variables, and is displayed in Figure 4-28.

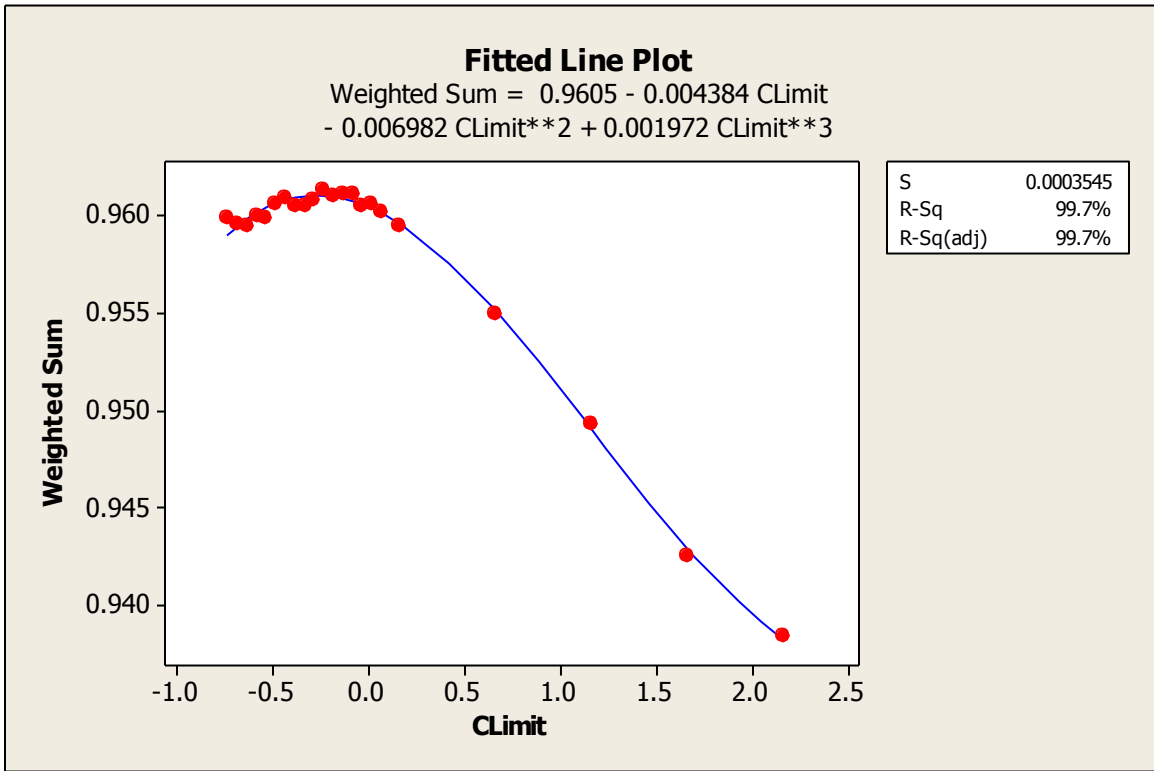

Figure 4-28: Weighted Score vs. Centered Control Limit Values. The regression equation for the fitted curve is also displayed.

Based on the regression equation shown in Figure 4-28, and accounting for the centered predictor variables, the estimated maximum weighted score occurred at a control limit specification of +/-0.56°F/min. This estimated control-limit value represented the best choice that moderately balanced time savings relative to center temperature quality concerns. Any point to the right of this maximum value would accept a lower center temperature quality than would be consistent with the original emphasis on center temperature maximization. Any point to the left of this curve would be more conservative from a cost savings perspective. Thus the original control limit chosen for the OP-AID method of +/-0.5°F/min does seem to be very suitable, given this analysis. It should be noted that the analysis was not conducted to precisely determine the control limit choice, but rather to study the cost-quality trade-offs associated with different

control limit selections, and to verify that the choice of +/-0.5°F/min was indeed a reasonable control limit choice.

For comparison to the conservative and aggressive control limit specifications, at the +/-0.5°F/min control limit width, the surface temperature across the 4 trials was well within 18°F of target temperature at the 'on-heat' detection point. Also at the 'on-heat' detection point, the difference between the center temperature and the target temperature was around 20°F for all trials except for the rod bundle which had a center temperature that was 37°F below target. The time savings over the conventional hour/inch rule with moderate 'on-heat' determinism was 24 minutes for both rectangular geometries, 158 minutes for the 8 in. diameter cylinder, and 37 minutes for the rod bundle.

4.4.3 Regression Function Justification

Figure 4-28 shows the fitted curve to be a cubic polynomial. The R^2 and R^2-adjusted metrics were used to analyze and justify the fit of the curve. The R^2 and R^2-adjusted metrics were given by (Neter, Kutner, Nachtsheim, & Wasserman, 1990):

$$R^2 = 1 - \left(\frac{SSE}{SST}\right) \tag{45}$$

$$R^2 adjusted = 1 - \left(\frac{n-1}{n-p}\right)\left(\frac{SSE}{SST}\right) \tag{46}$$

Where: n was the number of data points and p was the number of estimates in the model

$$\mathrm{SST} = \sum(\mathrm{Y_i} - \overline{\mathrm{Y}})^2 \tag{47}$$

$$SSE = \sum\left(Y_i - \widehat{Y_i}\right)^2 \tag{48}$$

Where: $\mathrm{Y_i}$ were the observed values, $\bar{Y}$ was the mean of the responses, and $\widehat{Y_i}$ were the fitted values based on the regression analysis.

As can be seen, the R^2 values do not decrease with unnecessary estimates added to the model. An unnecessary predictor would add zero to the SSE and would not be reflected in the R^2 value. On the other hand, with the R^2-adjusted, if an added estimate to the model was unnecessary and added nothing to the SSE of the model, the R^2-adjusted would be decreased since the term $\left(\frac{n-1}{n-p}\right)$ would increase. Thus, the R^2-adjusted value would be penalized if overfitting occurred through the addition of unnecessary model predictor terms. As is shown in Table 4-6, generated with MINTAB, the R^2-adjusted value increased with the addition of each additional term and the cubic polynomial displayed in Figure 4-28 gave the highest R^2-adjusted value. Thus the cubic polynomial shown in Figure 4-28 is justified as a valid regression model to predict the weighted sum based on a control limit specification for the given trials.

Table 4-8: Study of R-squared and R-squared adjusted for different terms included in regression equation.

			Terms Included in Model:		
Number of Variables	R-Sq	R-Sq (adj)	Climit	Climit^2	Climit^3
1	92.1	91.7		X	
1	85.9	85.2	X		
2	97.3	97	X	X	
2	92.4	91.6		X	X
3	99.7	99.7	X	X	X

Chapter 5

Discussion

The heat treatment control strategies developed in this project range from theoretical to practical and bridge the void between transitions from a research setting to a production setting. In this Chapter, the advantages and disadvantages of each control method will be discussed. Then, the gas flow rate analysis will quantitatively be compared to the OP-AID method, with and without the 'on-heat' detection delays due to signal filtering. Finally a control strategy recommendation will be made for control of production annealing furnaces at Carpenter Technology, Corporation.

5.1 Advantages and Disadvantages of the Differing Control Strategies

In this section the three control strategies will be discussed in terms of the advantages and disadvantages of each regarding their ease of implementation. The methods to be discussed include heat transfer modeling, gas flow rate analysis, and OP-AID. Specific advantages and disadvantages of each control strategy relative to the other strategies will be highlighted.

5.1.1 Advantages and Disadvantages of the Heat Transfer Modeling Strategy

The primary advantage of the heat transfer modeling strategy is that it quantitatively specifies the center temperature of simple load geometries within good levels of accuracy. The other two control strategies infer when the center temperature reaches its steady state target, but are not able to specify its exact temperature. This method eliminates the requirement for load thermocouples since it relies only on use of a non-contact infrared sensor to measure the surface

temperature of the load. However this modeling approach for furnace control is not easily implemented.

The heat transfer modeling approach for load temperature determinism has several significant disadvantages as a direct consequence of its very theoretical nature. The heat transfer model requires many inputs which include:

1. The furnace temperature measured by thermocouple(s)
2. The load surface temperature measured by infrared sensor (absolute measurement)
3. The thermal conductivity, the specific heat, and the thermal conductivity of the load
4. The geometry and the characteristic length of the load
5. The infrared sensor wavelength and the load emissivity (for absolute measurement correction).

As can be seen by these inputs, the modeling method is very dependent on accurate specification of the load geometry, and the material type. For a specialty alloy producer, like Carpenter Technology Corp., this is a huge drawback since they heat treat a wide variety of furnace loads in more than 60 different furnaces. The burden placed on furnace operators would become very heavy if they were required to input the load material type, the load geometry, and the load measurements for each processed part.

Another disadvantage of the heat transfer model is that it requires an absolute temperature measurement from the infrared sensor. The infrared measurement is subject to inaccuracies caused by varying load emissivity and by the reflected energy from the furnace environment. The heat transfer model algorithm does include a reflection correction factor to mitigate these sources of inaccuracies in the infrared sensor measurement. However, implementation of this reflection correction places additional burden on the annealing operator and requires definition of the load emissivity which is often difficult to accurately determine.

Due to the sheer burden placed on the operator for every heat treatment cycle, it is clear that the heat transfer modeling method is not feasible for implementation in a production setting. The acceptance of the control method by the annealing operators is crucial for implementation success. The heat transfer modeling strategy is more of a hindrance than an enabler of operator performance and this creates a barrier to implementation too great to easily overcome.

5.1.2 Advantages and Disadvantages of the Gas Flow Rate Control Strategy

The gas flow rate analysis is far more practical in approach than the heat transfer modeling control strategy. The key benefit of this method is that it is completely independent of the load type, or load placement within the furnace. The method has been demonstrated to work relatively well for loads of varying geometries, and sizes. Furthermore, this method could facilitate a completely automated strategy for load temperature determinism. It requires little more input from the furnace operator other than perhaps signaling the beginning of each heat treatment cycle. In this respect it places minimal burden on the operator, and can be considered a performance enabler.

The key disadvantages of the gas flow rate analysis are due to the challenge of measuring and differentiating the gas flow signal. The collected gas flow signal in this study is a cumulative sum of pulses generated for every 0.00625 cubic inches of gas flow. Thus, to get the gas flow rate, a derivative of the collected signal is required. Since the steady state gas flow rate is unique to the characteristics of each furnace, it is necessary to analyze the rate of change in the gas flow rate to universalize the method. Thus, two successive derivatives must be performed on the original signal. The derivative of the collected, non-smooth gas flow signal results in a very messy signal. Therefore, for both derivatives, significant filtering is necessary through the application of moving averages that together result in a total ‘on heat’ detection delay of 20

minutes. While for many annealing heat treatments this delay could effectively be absorbed in the control soak phase of the heat treatment cycle, it is clear that the gas flow rate analysis results in 'on-heat' detection delays. For example, if the gas flow rate method is used for heat treatment cycles that do not require prolonged soak phases, then the necessary filtering delays will significantly detract from the potential heat treatment time savings possible. The gas flow rate signal is dependent on both furnace dynamics and furnace load dynamics. In some cases the desired detection of furnace load dynamics could be masked by the furnace dynamics.

5.1.3 Advantages and Disadvantages of the OP-AID Strategy

The OP-AID method offers several key advantages, including some specific advantages that address the inadequacies of the aforementioned strategies. The use of the OP-AID method is independent of the load characteristics, and is applicable to most furnace types. The method can also be easily implemented since it requires minimal operator input. Furthermore, the method fulfills the basic requirement of effectively eliminating the use of contact temperature measurement while being relatively inexpensive to purchase and install.

The OP-AID control method also counters key inadequacies of the heat transfer model, and the gas flow rate control methods. In the case of the heat transfer model, one of the method's key disadvantages is that it requires an absolute temperature measurement from the infrared sensor, which is subject to inaccuracies caused by load emissivity and furnace reflections. Although the OP-AID method relies on the infrared sensor signal, it uses the rate of change in the surface temperature of the load which is not significantly influenced by temperature measurement accuracy. This relative measurement is far less subject to the inaccuracies associated with absolute temperature measurement. In the case of the gas flow rate analysis, one of the method's main disadvantages is that it requires two signal derivatives which magnify the total variation of

the interpreted signal. Since OP-AID measures the rate of change of the load surface temperature, only a single derivative of the collected infrared sensor measurement is required. This is possible since analyzing the rate of change of the surface temperature of a load to infer its center temperature is universally applicable to all furnace types and load material types. Since OP-AID requires only a single derivative of the infrared signal, the first derivative control signal is much cleaner and requires significantly less total filtering than the gas flow analysis method. Specifically, the OP-AID method requires only 7 minutes of filtering as opposed to the 20 minutes of filtering required for the gas flow rate method. It should also be noted that the infrared sensor measurement requires a shorter moving average for its derivative than is required for the first derivative of the gas flow meter signal because the original infrared sensor signal is cleaner than the original gas flow meter signal.

The OP-AID method however is not without a few disadvantages that should be mentioned. First, the method requires the operator to be mindful of load placement in the heat treatment furnace relative to the infrared sensor. The infrared sensor must be positioned in a direct line of sight to the load. In the R&D batch furnace, where testing of this method was conducted, the sensor was installed in the middle of the furnace and 3 in. above the furnace hearth. This places the infrared sensor in a natural position that maintained a line of sight for virtually all typical load placements. The infrared sensor also has a manual sighting port so the operator can verify that the sensor is targeting the load. In large furnaces it might be necessary to design a positioning device that permits the sensor to be repositioned to maintain load line-of-sight for all load placements. The sensor placement would need to be determined based on further testing and observation of the loading characteristics inherent to large scale furnaces in a production setting.

5.2 Quantitative Comparison of the Gas Flow Rate and the OP-AID Control Strategy

The following metrics for the OP-AID method and gas flow rate method will be compared:

1. The difference between the surface temperature and the target temperature at the point in time at which the method determined the load to be 'on-heat.'
2. The difference between the center temperature and the target temperature at the point in time at which the method determined the load to be 'on-heat.'
3. The time savings over the hr/inch rule at the point in time at which the method determined the load to be 'on-heat.'

Table 5-1 displays the comparison of the two methods under the assumption that the filtering delays associated with each method are absorbed in the control soak portion of the heat treatment cycle. The method that provided the most time savings for each trial has its time savings highlighted in red. As can be seen, the gas flow rate method indicated a slightly earlier 'on-heat' time for the majority of the trials. The difference between surface temperature and target temperature was within the 18°F specification for both methods across all trials. However, the center temperature of the rod bundle was quite low at the 'on-heat' point determined by the gas flow rate method.

Table 5-1: OP-AID Comparison to Gas Flow Rate Analysis with filtering times for each method assumed to be absorbed in soak period.

Geometry	49.25"x7.88"x3" Rectangle (Trial 1)		49.25"x7.88"x3" Rectangle (Trial 2)		8 Inch Cylinder		0.3125 Inch Rod Bundle	
Method	OP-AID	Gas Flow	OP-AID	Gas Flow	OP-AID	Gas Flow	OP-AID	Gas Flow
Difference between Surface Temperature and Target (°F)	13	11	16	16	7	4	5	12
Difference between Center Temperature and Target (°F)	20	13	20	20	18	16	35	61
Time Savings over hr/inch Rule (min)	24	19	24	25	150	167	37	45

While previously under the assumption that the filtering delays could be absorbed in the control soak portion of the heat treatment cycle, this may not be a valid assumption for some heat treatment applications. Table 5-2 compares the two methods where the amount of time used to filter each signal was reflected by a delay in the determination of the 'on-heat' point. As can be seen, the OP-AID method performed better in all cases than the gas flow rate method in terms of time savings. This is expected due to the large amount of time needed to filter the derivative of the gas flow rate signal. Also demonstrated here is that all surface and center temperatures corresponding to the 'on-heat' point are well within the 18°F specification that was imposed originally for the surface temperature. While the gas flow rate analysis provides no real time savings for the rectangular geometries, it still provides good time savings for the cylindrical geometries. The OP-AID method, on the other hand, still provides good time savings for the rectangular geometries, and significant time savings for the cylindrical geometries. The

consistency of the OP-AID method between the two rectangular geometry trials should also be noted.

Table 5-2: OP-AID Comparison to Gas Flow Rate Analysis with filtering times not assumed to be absorbed in soak period.

Geometry	49.25"x7.88"x3" Rectangle (Trial 1)		49.25"x7.88"x3" Rectangle (Trial 2)		8 Inch Cylinder		0.3125 Inch Rod Bundle	
Method	OP-AID	Gas Flow	OP-AID	Gas Flow	OP-AID	Gas Flow	OP-AID	Gas Flow
Difference between Surface Temperature and Target (°F)	8	3	7	3	2	0	3	1
Difference between Center Temperature and Target (°F)	9	4	9	5	8	3	15	8
Time Savings over hr/inch Rule (min)	15	-3	15	3	147	145	28	23

5.3 Control Strategy Recommendation

Based on the analysis conducted of the three different strategies for heat treatment load 'on-heat' determination, the final control recommendation is for the OP-AID method. The responsiveness of this method is superior to that of the gas flow rate method. While other types of gas meters and signal filtering techniques may improve gas flow monitoring, the OP-AID method is clearly the better and more robust option. The OP-AID method also allows for straight-forward sensitivity adjustment in control limits if quality issues are encountered related to low center temperatures. The OP-AID method directly responds to the load temperature, rather

than responding to the furnace environment temperature, as is the case in the gas flow rate method. It is thus expected that the OP-AID control method is capable of better quality assurance than could be guaranteed by the gas flow rate control method.

Chapter 6

Conclusions and Recommendations

The primary goal of this project was to develop an improved annealing heat treatment 'on heat' prediction method to quantitatively determine when a load of metal placed in a furnace had uniformly reached its target temperature. It was also a goal to eliminate the use of contact thermocouples. Three different approaches for achieving quantitative 'on-heat' determinism were evaluated: heat transfer modeling, analysis of furnace gas consumption, and analysis of load surface temperature using an infrared sensor (OP-AID method).

By comparison of the different 'on-heat' detection methods, the best solution was identified as the OP-AID method. Although the gas flow rate analysis proved to be effective, the amount of signal filtering required reduced its responsiveness compared to the OP-AID method. In addition, the OP-AID method uses direct load surface temperature measurements instead of indirect gas flow measurements to determine when the furnace load is 'on heat'. It is thus expected that the OP-AID control method would be capable of better control robustness than could be guaranteed by the gas flow rate control method.

An experimental study of the OP-AID method was conducted for four trials of varying load geometries including solid loads and rod bundles. Key results from these trials are as follows:

- At the 'on-heat' detection point determined by the OP-AID method, the surface temperature for all trials was well within the maximum tolerance of 18°F specified by Carpenter Technology Corporation.
- At the OP-AID 'on-heat' detection point, the difference between the center temperature and the target temperature was less than 20°F for all trials except for the rod bundle which had a center temperature that was 37°F below target.

- The OP-AID method achieved time savings over the conventional hour/inch rule of 24 minutes for rectangular geometries, 158 minutes for a large diameter cylinder, and 37 minutes for the rod bundle.

Additionally, an analysis was conducted to study the balance between metallurgical constraints vs. cost constraints in the design of the OP-AID on-heat detection method. The aggressiveness associated with achieving time savings opposed the maximization of metallurgical specifications (load temperature uniformity). This balance was quantified through a multi-criterion analysis. Through this analysis it was found that the chosen control limit specifications for the OP-AID method could produce heat treatment cost savings with sufficient product quality.

This project could be expanded into several areas for future work:

- Additional validation of the OP-AID method should be conducted with other varying load geometries, and both the OP-AID and gas flow analysis methods should be studied in full-size production annealing furnaces.
- Also, for implementation of the OP-AID method in production furnaces, a “traffic light signal” could be used that would warn the operator as the load approaches its target ‘on heat’ temperature. Different control limit values can be assigned that correspond to a green light for ‘continue heating load’, yellow light for ‘load approaching target’, and a red light for ‘load at temperature’. In this way, the operator could respond faster to removing the load and starting the next heat treatment cycle.
- It would also be beneficial to fully quantify the amount of gas savings that could occur in a production setting when using the OP-AID method. Realistic gas savings possible for large scale production furnaces cannot be easily estimated using the small scale batch furnace where the trials were conducted. Installation of a gas flow meter should accompany the initial implementation of the OP-AID method so that gas savings in a production setting can be directly determined.

- While this project only addresses ‘on heat’ detection during the ramp portion of the heat treatment cycle, further work can be done to study the effects of reducing the control soak portion of the cycle. To this end, it would be beneficial to quantify the extent of heat treatment that occurs during the ramp-up cycle and use this ramp-up heat treatment to shorten the soak time.
- Finally, other efficiency improvements for the heat treatment operations could be investigated involving the optimizing of load scheduling, and the batching of furnace loads.

References

Barba, A. A., & Lamberti, G. (2003). Preliminary Validation of a Numerical Code for Heat Transfer Simulations. *Heat and Mass Transfer* , 429-433.

Barron, W. R. (1992, December). Principles of Infrared Thermometry. *Sensors* , pp. 10-19.

Chandler, H. (1995). *Heat Treater's Guide - Practices and Procedures for Irons and Steels.* Materials Park, OH: ASM International.

Chapman, K. S., Ramadhyani, S., & Viskanta, R. (1989). Modeling of Heat Transfer in a Direct Fired Batch Reheating Furnace. *HTD* , 265-274.

Childs, P. R., Greenwood, J. R., & Long, C. A. (2000, August). Review of Temperature Measurement. *Review of Scientific Instruments* , pp. 2959-2978.

Cohen, J. (2003). *Applied Multiple Regression/Correlation Analysis for the Behavoiral Sciences, Third Edition.* Mahwah, NJ: Lawrence Erlbaum Associates.

Deskevich, N. (2005). *Heat Treatment Procedure Qualification - A Thesis in Industrial Engineering.* University Park, PA: Pennsylvania State University.

DeWitt, D. P., & Nutter, G. D. (1988). *Theory and Practice of Radiation Thermometry.* Hoboken, NJ: John Wiley & Sons, Inc.

Finlayson, P. C., & Schofield, J. S. (1959). Heating for Forging in Batch-Type Furnaces. *Journal of The Iron and Steel Institute* , 238-252.

Gao, M., Reid, C. N., Jahedi, M., & Li, Y. (2000). Estimating Equilibration Times and Heating/Cooling Rates in Heat Treatment of Workpieces with Arbitrary Geometry. *Journal of Materials Engineering and Performance* , 62-71.

Incopera, F. P., & DeWitt, D. P. (2002). *Fundamentals of Heat and Mass Transfer, 5th ed.* Hoboken, NJ: John Wiley & Sons, Inc.

Ingerslev, P., & Henein, H. (1997). An Integral Boundary Approach for 1- and 2-D Modeling of Ingot Reheating and Cooling. *Transactions* , 75-85.

Jaluria, Y. (1984). Numerical Study of the Thermal Processes in a Furnace. *Numerical Heat Transfer* , 211-224.

Kang, J., & Rong, Y. (2006). Modeling and Simulation of Load Heating in Heat Treatment Furnaces. *Journal of Materials Processing Technology* , 109-114.

Lankford, J. N., Samways, N. L., Craven, R. F., & McGannon, H. E. (1985). *The Making Shaping and Treating of Steel, 10th ed.* Pittsburg, PA: Herbick & Held.

Lindholm, D., & Leden, B. (1999). A Finite Element Method for Solution of the Three Dimensional Time-Dependent Heat-Conduction Equation with Application for Heating of Steels in Reheating Furnaces. *Numerical Heat Transfer* , 155-172.

Masud, A. S., & Ravindran, A. R. (2008). *Operations Research and Management Science Handbook.* Boca Raton, FL: CRC Press.

Montgomery, D. C. (2001). *Introduction to Statistical Quality Control, 4th Edition.* New York, NY: John Wiley & Sons, Inc.

Neter, J., Kutner, M., Nachtsheim, C., & Wasserman, W. (1990). *Applied Linear Statistical Models, Fourth Edition.* Chicago, IL: Richard D. Irwin, Inc.

Oosthuizen, P., & Naylor, D. (1999). A Numerical Evaluation of a Simple Procedure for Using Transient Surface Temperature Measurements to Determine Local Convective Heat Transfer Rates. *HTD* , 127-134.

Özişik, M. N. (1968). *Boundary Value Problems of Heat Conduction.* Scranton, PA: International Textbook Company.

Peacock, G. R. (1999). A Review of Non-Contact Process Temperature Measurements In Steel Manufacturing. *SPIE Conference on Thermosense XXI* (pp. 171-189). Orlando: SPIE.

Peters, F. (2007). Improving Productivity and Energy Effeciency in Heat Treatment. *Industrial and Manufacturing Systems Engineering Department* . Ames, IA: Unpublished.

Sahay, S. S., & Krishnan, K. (2007). Model Based Optimization of Continuous Heat Treatment Operation for Bundle of Packed Rods. *Ironmaking ans Steelmaking* , 89-94.

Schneider, F. (2007, May). Advances in IR Temperature Measurement. *Sensors Magazine* .

Sparkman, D., & Kearney, A. (1994). Breakthrough in Aluminum Alloy Themal Analysis Technology for Process Control. *Transactions of the American Foundrymen's Society* , 455-460.

Tagliafico, L. A., & Senarega, M. (2004). A Simulation Code for Batch Heat Treatments. *International Journal of Thermal Sciences* , 509-517.

Totten, G. E. (2007). *Steel Heat Treatment Equipment and Process Design.* Boca Raton, FL: CRC Press.

Voigt, R. C. (2004). *Heat Treatment Procedure Qualification - Final Technical Report.* USDOE Office of Energy Effeciency and Renewable Energy.

White, D. R., & Saunders, P. (2008). A Graphical Method For Calculating Reflection Errors In Radiation Thermometry. *Int J Thermophys* , 395-402.

Womack, A. (2008, July/August). Flow Meter Selection For Improved Gas Flow Measurements. *Heat Treating Progress* , pp. 25-29.

Appendix A

Heat Transfer Model Nomenclature

L = length of cylinder
r_o = cylinder radius from center to surface
r = distance from cylinder center to radial point of interest
k = thermal conductivity
T = temperature
φ = circumferential direction coordinate
z = axial direction coordinate
q = heat generation term
ρ = density
c_p = specific heat
t = time
T_i = initial temperature of the load
T_s = surface temperature of the load
T_c = center temperature of the load
h = lumped heat transfer coefficient
θ^* = dimensionless temperature
T_∞ = furnace environment temperature
θ^* = dimensionless temperature
r^* = dimensionless radial distance
Fo = Fourier number
α = thermal diffusivity of the material
L_c = characteristic length
V = volume of load
A_s = surface area of load
Bi = Biot number
ζ_1 = first positive root of Equation (14)
θ_s^* = dimensionless surface temperature
θ_c^* = dimensionless center temperature
S = spectral emissive power
T_m = load surface temperature measured via IR sensor
T_w = furnace wall temperature
ε = spectral emissivity of the load
λ = operating wavelength of infrared sensor
R = spectral response of the infrared sensor
L_b = spectral radiance of a blackbody

Appendix B

Gas Flow Analysis Signal Filtering Progression

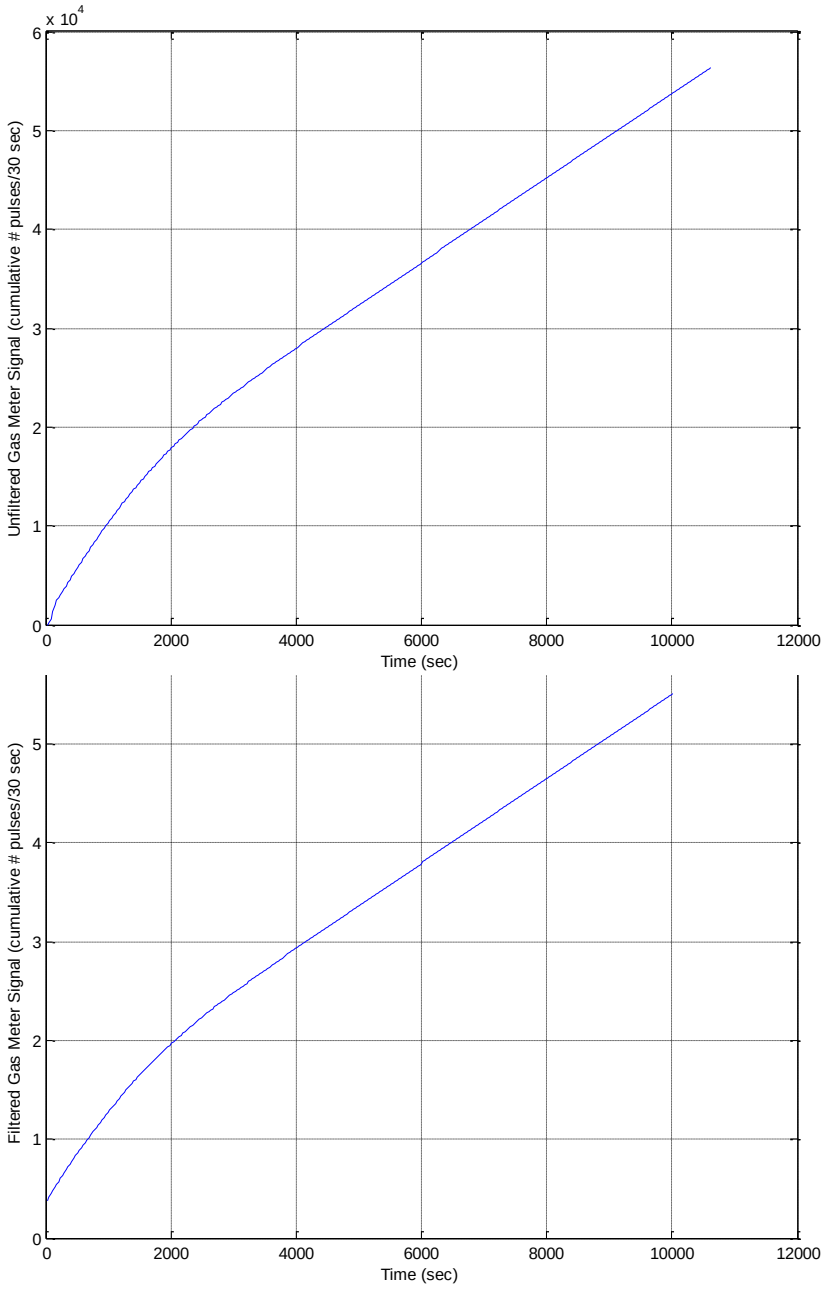

Figure B-1: Trial GF1 - The filtered gas meter pulse count (bottom) results from a 10 min moving average on the unfiltered gas meter pulse count (top).

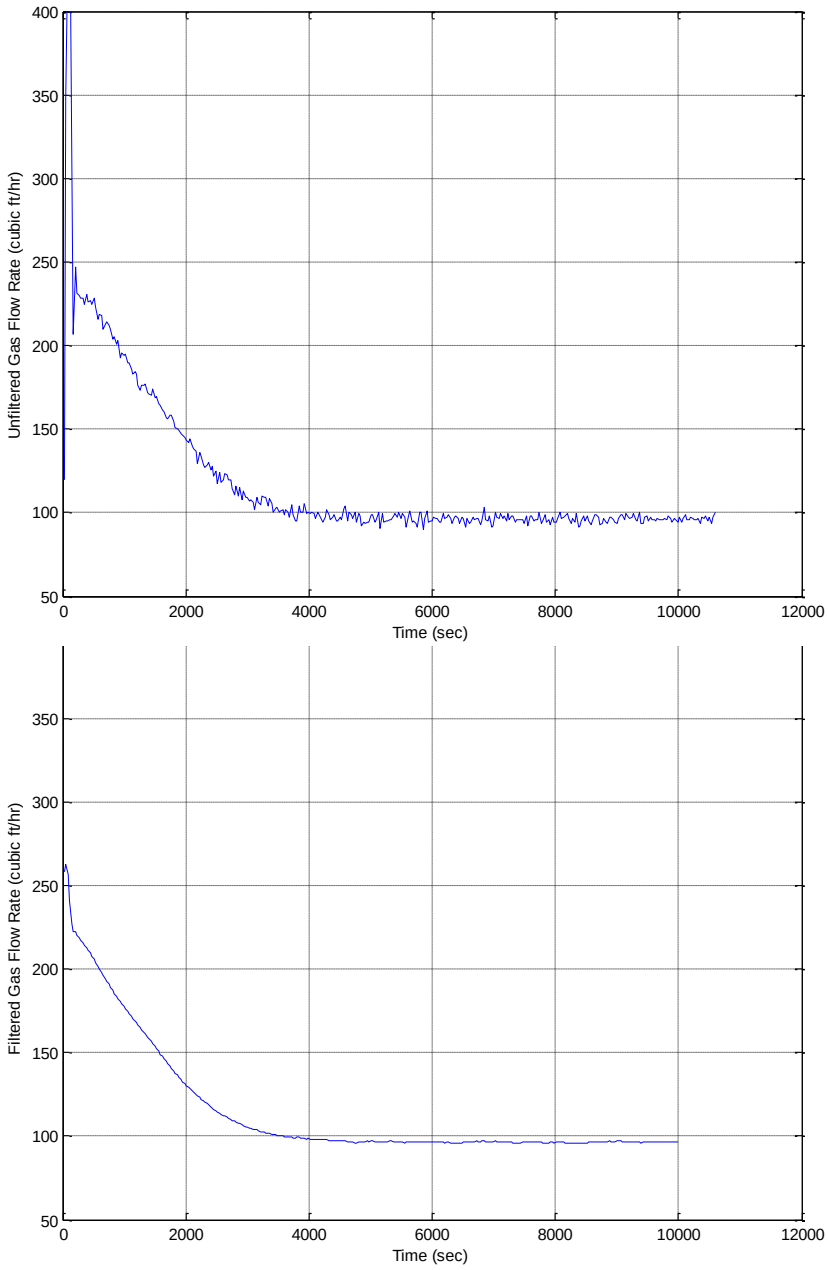

Figure B-2: Trial GF1 – The filtered gas flow rate (bottom) is the derivative of the filtered gas meter pulse count in Figure B-1. The unfiltered gas flow rate (top) is the derivative of the unfiltered gas meter pulse count in Figure B-1 (shown for comparison sake).

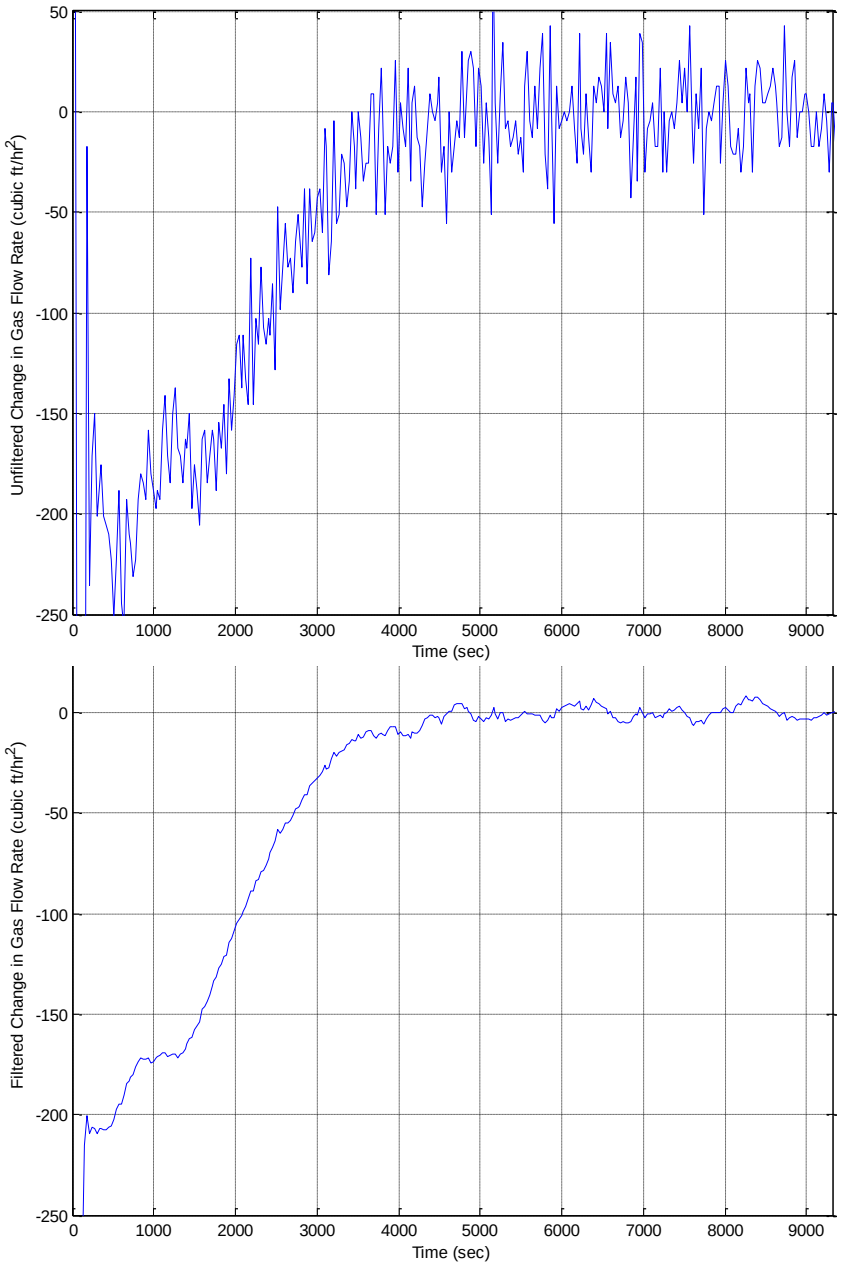

Figure B-3: Trial GF1 - A 10 min moving average on the filtered gas flow rate signal in Figure B-2 was taken prior to its derivative to yield the filtered change in gas flow rate (bottom). The unfiltered change in gas flow rate (top) is the second derivative of the unfiltered gas meter pulse count in Figure B-1 (shown for comparison sake).

Appendix C

OP-AID Signal Filtering Progression

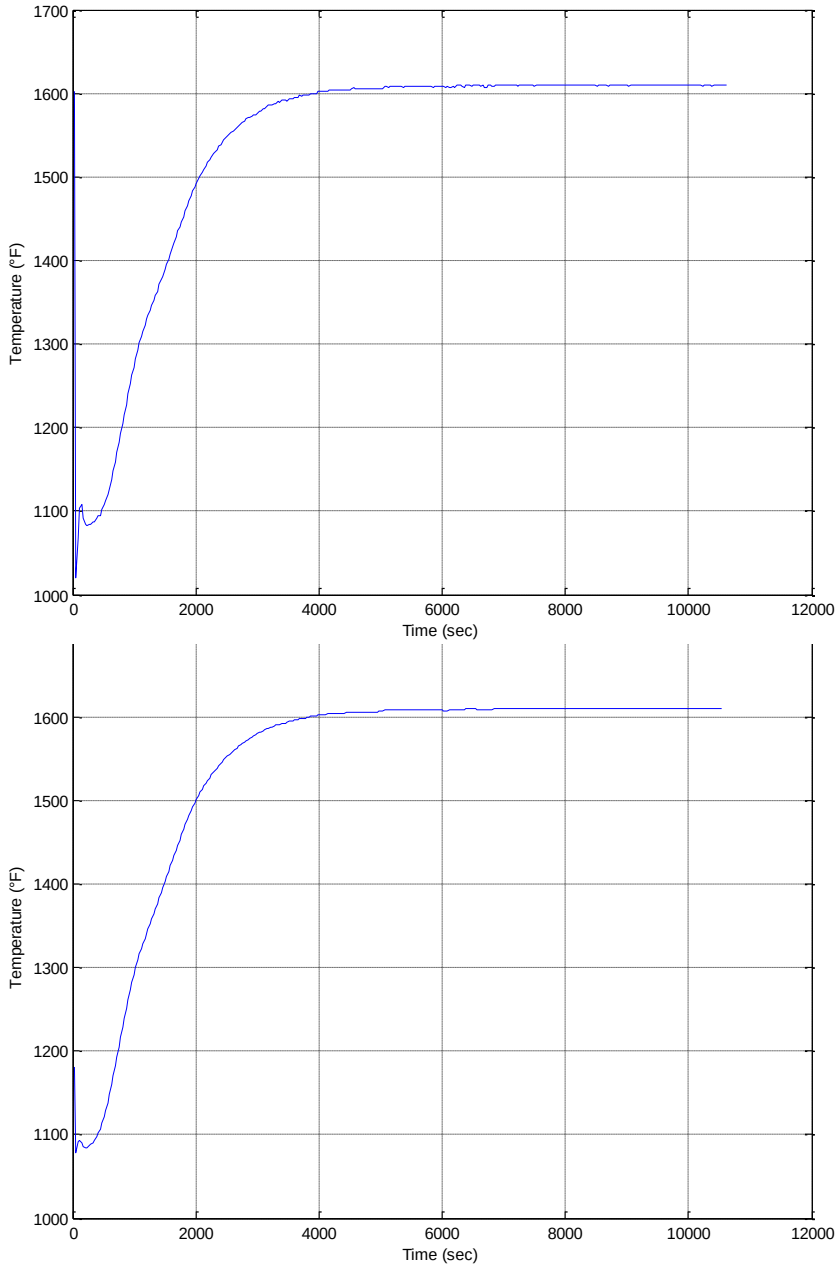

Figure C-1: Trial OP-AID1 - The filtered IR temperature signal (bottom) results from a 2 min moving average on the unfiltered IR temperature signal (top).

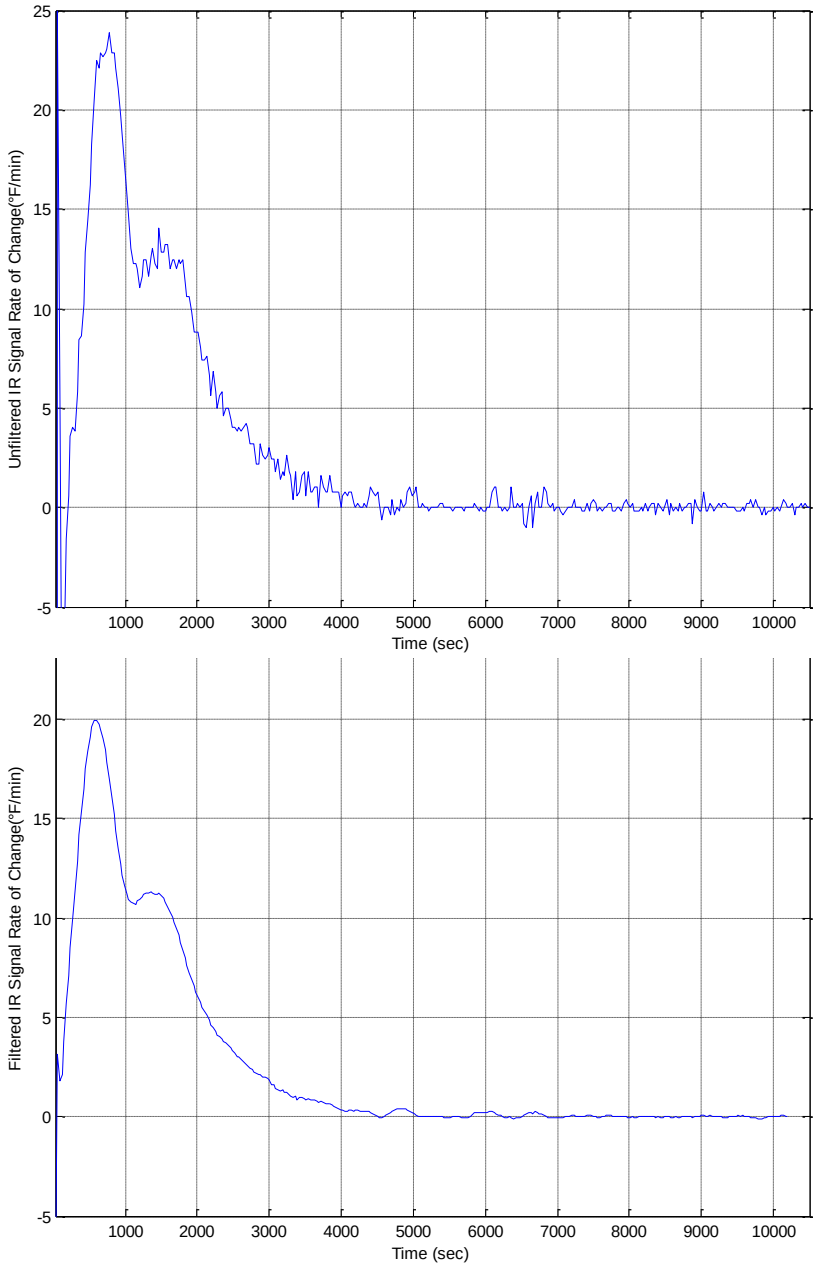

Figure C-2: Trial OP-AID 1 – The derivative of the filtered IR temperature signal from Figure C-1 yields the unfiltered IR rate of change signal (top). A 5 min moving average on the unfiltered IR rate of change signal (top) results in the filtered IR rate of change signal (bottom).

Appendix D

Multi Criteria Analysis Tables

Table D-1 Unscaled criteria values listed for each control limit alternative. Ideal Values for each criterion are also displayed.

	Rectangle Trial 1		Rectangle Trial 2		8" Cylinder		0.3125" Bundle	
	max	min	max	min	max	min	max	min
Alternatives: (UCL, LCL)	Center Temp	Time	Center Temp	Time	Center Temp	Time	Center Temp	Time
0.1, -0.1	1591.1	4470.0	1595.4	4920.0	1994.1	5629.8	1587.4	3840.0
0.15, -0.15	1588.9	4440.0	1595.4	4920.0	1994.1	5595.5	1585.2	3810.0
0.2, -0.2	1588.9	4440.0	1593.3	4860.0	1994.1	5595.5	1585.0	3780.0
0.25, -0.25	1588.9	4440.0	1588.9	4410.0	1991.8	5561.1	1585.0	3780.0
0.3, -0.3	1588.9	4440.0	1586.7	4320.0	1987.0	5149.2	1567.4	3240.0
0.35,-0.35	1586.7	4260.0	1586.6	4200.0	1986.8	5114.9	1567.4	3240.0
0.4, -0.4	1582.1	3990.0	1586.6	4200.0	1984.5	4977.6	1565.7	3210.0
0.45, -0.45	1579.9	3960.0	1580.2	3990.0	1982.1	4943.2	1565.4	3180.0
0.5, -0.5	1579.9	3960.0	1580.2	3990.0	1982.1	4943.2	1565.4	3180.0
0.55,-0.55	1580.0	3930.0	1580.1	3960.0	1982.0	4908.9	1563.2	3120.0
0.6,-0.6	1579.9	3900.0	1580.3	3930.0	1977.2	4668.6	1563.2	3120.0
0.65,-0.65	1579.9	3870.0	1580.3	3930.0	1974.9	4600.0	1556.7	3000.0
0.7, -0.7	1579.9	3870.0	1580.2	3900.0	1974.9	4600.0	1556.7	3000.0
0.75, -0.75	1579.9	3870.0	1580.2	3900.0	1970.2	4462.6	1556.7	3000.0
0.8, -0.8	1575.5	3780.0	1571.6	3690.0	1970.2	4428.3	1554.5	2970.0
0.85, -0.85	1575.4	3750.0	1571.6	3660.0	1967.9	4394.0	1554.5	2970.0
0.9, -0.9	1573.4	3690.0	1569.3	3630.0	1967.9	4394.0	1552.3	2940.0
1, -1	1566.9	3570.0	1560.8	3450.0	1960.8	4118.0	1548.0	2880.0
1.5, -1.5	1546.9	3210.0	1550.1	3270.0	1944.5	3879.1	1517.7	2550.0
2, -2	1533.7	3030.0	1532.7	3030.0	1923.7	3570.1	1478.7	2250.0
2.5, -2.5	1514.1	2820.0	1515.6	2850.0	1898.6	3295.5	1444.4	2070.0
3, -3	1498.8	2700.0	1500.5	2730.0	1887.0	3129.5	1429.4	2010.0
Ideal Values:	1591.1	2700.0	1595.4	2730.0	1994.1	3129.5	1587.4	2010.0

Table D-2: Conservative criteria ratings and corresponding weighted score for each alternative. Scaled criteria values are shown.

	Rectangle Trial 1		Rectangle Trial 2		8" Cylinder		0.3125" Bundle		Score
	max	max	max	max	max	max	max	max	
Alternatives: (UCL, LCL)	Center Temp	Time	Center Temp	Time	Center Temp	Time	Center Temp	Time	
0.1, -0.1	1.0000	0.6040	1.0000	0.5549	1.0000	0.5559	1.0000	0.5234	1.00000000
0.15, -0.15	0.9986	0.6081	1.0000	0.5549	1.0000	0.5593	0.9986	0.5276	0.99930785
0.2, -0.2	0.9986	0.6081	0.9987	0.5617	1.0000	0.5593	0.9985	0.5317	0.99894728
0.25, -0.25	0.9986	0.6081	0.9959	0.6190	0.9988	0.5627	0.9985	0.5317	0.99796945
0.3, -0.3	0.9986	0.6081	0.9945	0.6319	0.9964	0.6078	0.9874	0.6204	0.99425110
0.35,-0.35	0.9972	0.6338	0.9945	0.6500	0.9963	0.6118	0.9874	0.6204	0.99386469
0.4, -0.4	0.9943	0.6767	0.9945	0.6500	0.9952	0.6287	0.9863	0.6262	0.99258583
0.45, -0.45	0.9930	0.6818	0.9905	0.6842	0.9940	0.6331	0.9861	0.6321	0.99088914
0.5, -0.5	0.9930	0.6818	0.9905	0.6842	0.9940	0.6331	0.9861	0.6321	0.99088914
0.55,-0.55	0.9930	0.6870	0.9904	0.6894	0.9939	0.6375	0.9848	0.6442	0.99053017
0.6,-0.6	0.9930	0.6923	0.9905	0.6947	0.9915	0.6703	0.9848	0.6442	0.98994402
0.65,-0.65	0.9930	0.6977	0.9905	0.6947	0.9904	0.6803	0.9807	0.6700	0.98863198
0.7, -0.7	0.9930	0.6977	0.9905	0.7000	0.9904	0.6803	0.9807	0.6700	0.98861631
0.75, -0.75	0.9930	0.6977	0.9905	0.7000	0.9880	0.7013	0.9807	0.6700	0.98802707
0.8, -0.8	0.9902	0.7143	0.9851	0.7398	0.9880	0.7067	0.9793	0.6768	0.98564163
0.85, -0.85	0.9901	0.7200	0.9851	0.7459	0.9869	0.7122	0.9793	0.6768	0.98533756
0.9, -0.9	0.9889	0.7317	0.9836	0.7521	0.9869	0.7122	0.9779	0.6837	0.98431642
1, -1	0.9848	0.7563	0.9783	0.7913	0.9833	0.7600	0.9752	0.6979	0.98039583
1.5, -1.5	0.9722	0.8411	0.9716	0.8349	0.9751	0.8068	0.9561	0.7882	0.96876117
2, -2	0.9639	0.8911	0.9607	0.9010	0.9647	0.8766	0.9315	0.8933	0.95521073
2.5, -2.5	0.9516	0.9574	0.9500	0.9579	0.9521	0.9496	0.9099	0.9710	0.94090283
3, -3	0.9420	1.0000	0.9405	1.0000	0.9463	1.0000	0.9005	1.0000	0.93231601
Rating:	10	0	10	0	10	0	10	0	40
Weight:	0.25	0	0.25	0	0.25	0	0.25	0	

Table D-3: Aggressive criteria ratings and corresponding weighted score for each alternative. Scaled criteria values are shown.

	Rectangle Trial 1		**Rectangle Trial 2**		**8" Cylinder**		**0.3125" Bundle**		**Score**
	max	max	max	max	max	max	max	max	
Alternatives: (UCL, LCL)	Center Temp	Time	Center Temp	Time	Center Temp	Time	Center Temp	Time	
0.1, -0.1	1.0000	0.6040	1.0000	0.5549	1.0000	0.5559	1.0000	0.5234	0.92659265
0.15, -0.15	0.9986	0.6081	1.0000	0.5549	1.0000	0.5593	0.9986	0.5276	0.92649962
0.2, -0.2	0.9986	0.6081	0.9987	0.5617	1.0000	0.5593	0.9985	0.5317	0.92665904
0.25, -0.25	0.9986	0.6081	0.9959	0.6190	0.9988	0.5627	0.9985	0.5317	0.92837663
0.3, -0.3	0.9986	0.6081	0.9945	0.6319	0.9964	0.6078	0.9874	0.6204	0.93138372
0.35,-0.35	0.9972	0.6338	0.9945	0.6500	0.9963	0.6118	0.9874	0.6204	0.93305445
0.4, -0.4	0.9943	0.6767	0.9945	0.6500	0.9952	0.6287	0.9863	0.6262	0.93472055
0.45, -0.45	0.9930	0.6818	0.9905	0.6842	0.9940	0.6331	0.9861	0.6321	0.93537412
0.5, -0.5	0.9930	0.6818	0.9905	0.6842	0.9940	0.6331	0.9861	0.6321	0.93537412
0.55,-0.55	0.9930	0.6870	0.9904	0.6894	0.9939	0.6375	0.9848	0.6442	0.93619860
0.6,-0.6	0.9930	0.6923	0.9905	0.6947	0.9915	0.6703	0.9848	0.6442	0.93751687
0.65,-0.65	0.9930	0.6977	0.9905	0.6947	0.9904	0.6803	0.9807	0.6700	0.93813736
0.7, -0.7	0.9930	0.6977	0.9905	0.7000	0.9904	0.6803	0.9807	0.6700	0.93834695
0.75, -0.75	0.9930	0.6977	0.9905	0.7000	0.9880	0.7013	0.9807	0.6700	0.93872870
0.8, -0.8	0.9902	0.7143	0.9851	0.7398	0.9880	0.7067	0.9793	0.6768	0.93960116
0.85, -0.85	0.9901	0.7200	0.9851	0.7459	0.9869	0.7122	0.9793	0.6768	0.94006841
0.9, -0.9	0.9889	0.7317	0.9836	0.7521	0.9869	0.7122	0.9779	0.6837	0.94024986
1, -1	0.9848	0.7563	0.9783	0.7913	0.9833	0.7600	0.9752	0.6979	0.94222485
1.5, -1.5	0.9722	0.8411	0.9716	0.8349	0.9751	0.8068	0.9561	0.7882	0.94359175
2, -2	0.9639	0.8911	0.9607	0.9010	0.9647	0.8766	0.9315	0.8933	0.94442556
2.5, -2.5	0.9516	0.9574	0.9500	0.9579	0.9521	0.9496	0.9099	0.9710	0.94391837
3, -3	0.9420	1.0000	0.9405	1.0000	0.9463	1.0000	0.9005	1.0000	0.94359667
Rating:	10	2	10	2	10	2	10	2	48
Weight:	0.2083	0.04167	0.2083	0.04167	0.2083	0.0417	0.2083	0.0417	

Table D-4: Moderate criteria ratings and corresponding weighted score for each alternative. Scaled criteria values are shown.

	Rectangle Trial 1		Rectangle Trial 2		8" Cylinder		0.3125" Bundle		Score
	max	max	max	max	max	max	max	max	
Alternatives: (UCL, LCL)	Center Temp	Time	Center Temp	Time	Center Temp	Time	Center Temp	Time	
0.1, -0.1	1.0000	0.6040	1.0000	0.5549	1.0000	0.5559	1.0000	0.5234	0.95995963
0.15, -0.15	0.9986	0.6081	1.0000	0.5549	1.0000	0.5593	0.9986	0.5276	0.95959427
0.2, -0.2	0.9986	0.6081	0.9987	0.5617	1.0000	0.5593	0.9985	0.5317	0.95951733
0.25, -0.25	0.9986	0.6081	0.9959	0.6190	0.9988	0.5627	0.9985	0.5317	0.96000973
0.3, -0.3	0.9986	0.6081	0.9945	0.6319	0.9964	0.6078	0.9874	0.6204	0.95995980
0.35,-0.35	0.9972	0.6338	0.9945	0.6500	0.9963	0.6118	0.9874	0.6204	0.96069547
0.4, -0.4	0.9943	0.6767	0.9945	0.6500	0.9952	0.6287	0.9863	0.6262	0.96102295
0.45, -0.45	0.9930	0.6818	0.9905	0.6842	0.9940	0.6331	0.9861	0.6321	0.96060822
0.5, -0.5	0.9930	0.6818	0.9905	0.6842	0.9940	0.6331	0.9861	0.6321	0.96060822
0.55,-0.55	0.9930	0.6870	0.9904	0.6894	0.9939	0.6375	0.9848	0.6442	0.96089477
0.6,-0.6	0.9930	0.6923	0.9905	0.6947	0.9915	0.6703	0.9848	0.6442	0.96134739
0.65,-0.65	0.9930	0.6977	0.9905	0.6947	0.9904	0.6803	0.9807	0.6700	0.96108946
0.7, -0.7	0.9930	0.6977	0.9905	0.7000	0.9904	0.6803	0.9807	0.6700	0.96119666
0.75, -0.75	0.9930	0.6977	0.9905	0.7000	0.9880	0.7013	0.9807	0.6700	0.96113705
0.8, -0.8	0.9902	0.7143	0.9851	0.7398	0.9880	0.7067	0.9793	0.6768	0.96052865
0.85, -0.85	0.9901	0.7200	0.9851	0.7459	0.9869	0.7122	0.9793	0.6768	0.96064530
0.9, -0.9	0.9889	0.7317	0.9836	0.7521	0.9869	0.7122	0.9779	0.6837	0.96028012
1, -1	0.9848	0.7563	0.9783	0.7913	0.9833	0.7600	0.9752	0.6979	0.95957530
1.5, -1.5	0.9722	0.8411	0.9716	0.8349	0.9751	0.8068	0.9561	0.7882	0.95503239
2, -2	0.9639	0.8911	0.9607	0.9010	0.9647	0.8766	0.9315	0.8933	0.94932791
2.5, -2.5	0.9516	0.9574	0.9500	0.9579	0.9521	0.9496	0.9099	0.9710	0.94254767
3, -3	0.9420	1.0000	0.9405	1.0000	0.9463	1.0000	0.9005	1.0000	0.93846910
Rating:	10	1	10	1	10	1	10	1	44
Weight:	0.2273	0.02273	0.2273	0.02273	0.2273	0.0227	0.2273	0.0227	

Table D-5: Centered control limit values and corresponding weighted scores used to generate the regression equation displayed in Figure 4-28.

Control Limit Value	Centered Control Limit Value	Weighted Score
0.1	-0.74091	0.95996
0.15	-0.69091	0.959594
0.2	-0.64091	0.959517
0.25	-0.59091	0.96001
0.3	-0.54091	0.95996
0.35	-0.49091	0.960695
0.4	-0.44091	0.961023
0.45	-0.39091	0.960608
0.5	-0.34091	0.960608
0.55	-0.29091	0.960895
0.6	-0.24091	0.961347
0.65	-0.19091	0.961089
0.7	-0.14091	0.961197
0.75	-0.09091	0.961137
0.8	-0.04091	0.960529
0.85	0.00909	0.960645
0.9	0.05909	0.96028
1	0.15909	0.959575
1.5	0.65909	0.955032
2	1.15909	0.949328
2.5	1.65909	0.942548
3	2.15909	0.938469

Appendix E

MATLAB CODE

E.1 Heat Transfer Model MATLAB Code

```
function [out1,out2]=thermocalc_monster(r,load_emissivity,Tr)

%The following section is used to load the desired trial data and sets
variables to the loaded data. If one data set is selected the other two
should be commented.
%%%%%%%%%%%%%%%%%%%%%%%%%%%%%%%%%%%%%%%%%%%%%%%%%%%%%%%%%%%%%%%%%%%%%%%%

%Loads Williamson Test 3 data when uncommented (1.65um sensor with 8in
diameter cylinder of metal at furnace temperature of 2000F):

% load Williamson_Trial_3

% Sets variables to Williamson Test 3 data (when uncommented):

% Q=Williamson_Trial_3;
% x=1:1:length(Q(:,1));
% y=Q(:,5);
% z=Q(:,2);
% Tcenter=Q(:,3);
% Tir=Q(:,5);
% TStc=Q(:,4);

% Loads Williamson Test 2 data when (1.65um sensor with 8in diameter
cylinder of metal at furnace temperature of 1600F):

load Trial2_Tir
load Trial2_Tsurface
load Trial2_Tcenter
load Trial2_Tfurnace
load TSnew
load Trial_2_with_initial_noise

%sets variables to Williamson Test 2 data:

x=1:1:length(Trial2_Tir);
y=Trial2_Tir;
z=Trial2_Tfurnace;
Tcenter=Trial2_Tcenter;
TStc=Trial2_Tsurface;
Tir=Trial2_Tir;
```

```
% Loads Williamson Test 1 data when uncommented (1.65um sensor with 8in
diameter cylinder of metal at furnace temperature of 1200F):

% load monster_IRsurface
% load monster_TCsurface
% load monster_Tinf_1200
% load monster_TCcenter
% load monster_scaled

% Sets variables to Williamson Test 1 data when uncommented:

% x=1:1:length(monster_IRsurface);
% y=monster_TCsurface;
% z=monster_Tinf_1200;
% Tcenter=monster_TCcenter;
% Tir=monster_IRsurface;
%%%%%%%%%%%%%%%%%%%%%%%%%%%%%%%%%%%%%%%%%%%%%%%%%%%%%%%%%%%%%%%%%%%%%%%%%%%


%The following section is used to correct the IR sensor measurement for
furnace reflections.  This is accomplished by converting the IR sensor
temperature measurement to energy, applying a correction to this energy
and converting back to a corrected temperature.
%%%%%%%%%%%%%%%%%%%%%%%%%%%%%%%%%%%%%%%%%%%%%%%%%%%%%%%%%%%%%%%%%%%%%%%%%%%

%Sensor wavelength:
lambda=1.6; %[um]
%Blackbody Radiation Constants:
C1=3.742E8; %[W*um^4/m^2]
C2=1.4388E4; %[um*K]
%Emissivity:
em=load_emissivity;

%Fahrenheit to Kelvin conversion:
yK=5/9.*(y+459.67);
zK=5/9.*(z+459.67);
%Temp to Energy conversion:
yE=C1./((lambda^5).*(exp(C2./(lambda.*yK))-1));
zE=C1./((lambda^5).*(exp(C2./(lambda.*zK))-1));
%Energy Scaling:
yE=(yE-(1-em).*zE)./em;

%Energy to Temp conversion:
yK=C2./(lambda.*log(C1./(yE.*lambda^5)+1));
yK=real(yK);
%Kelvin to fahrenheit conversion:
y=9/5.*(yK)-459.67;
%%%%%%%%%%%%%%%%%%%%%%%%%%%%%%%%%%%%%%%%%%%%%%%%%%%%%%%%%%%%%%%%%%%%%%%%%%%

%Pyromet 718 properties:
k=0.000285491;
rho=0.2970;
c=0.04124678;
```

```
% Defines the time step such that Fo>0.2 so the first term
approximation can be used for the infinite series. Fo=alpha*dt/(r/2)^2:
alpha=k/(rho*c);
dt=(0.2*(r^2))/(4.*alpha);

%Interpolates data into time steps of 'dt' that satisfy the condition
of Fo>0.2:
xi=(1:dt:length(x))';
Ts=interp1(x,y,xi,'pchip');
Tinf=interp1(x,z,xi,'pchip');
ctr=interp1(x,Tcenter,xi,'pchip');
Tir=interp1(x,Tir,xi,'pchip');
TStc=interp1(x,TStc,xi,'pchip');

%Initializes values of Ti and thetastar from which the first z-value is
calculated.  The z-value is then used to determine center temperature,
Tc, at the end of the first time step:
Tc(1,1)=Tr;
Ti(1,1)=Tr;
thetastar(1,1)=abs((Ts(1,1)-Tinf(1,1))./(Ti(1,1)-Tinf(1,1)));
z(1,1)=fminbnd(@(zz)fun1(zz,thetastar(1,1)),0,5);

%Calculates values of Ti and thetastar for each timestep from which the
respective z-values are calculated.  The z-value is then used to
determine center temperature, Tc, at the end of each time step:
for c1=2:length(xi)
Ti(c1,1)=(Ts(c1,1)+Tc(c1-1,1))./2;
thetastar(c1,1)=abs((Ts(c1,1)-Tinf(c1,1))./(Ti(c1,1)-Tinf(c1,1)));
z(c1,1)=fminbnd(@(zz)fun1(zz,thetastar(c1,1)),0,5);
Tc(c1,1)=(Ts(c1,1)-Tinf(c1,1))./besselj(0,z(c1,1))+Tinf(c1,1);
end

%Calculates the heat transfer coefficient based on the z-values
determined above:
h=(2*k./r.*z.*(besselj(1,z)./besselj(0,z)));
h=h(1:length(xi));

%Conversions to SI units (when uncommented):
% Tc=(5/9).*(Tc-32);
% Ts=(5/9).*(Ts-32);
% Tinf=(5/9).*(Tinf-32);
% ctr=(5/9).*(ctr-32);
% h=h.*(2.944E6);

%The following calculates the descriptive measures of the model
accuracy
RMSE=sqrt(mean((Tc-ctr).^2));
avg=(sum(Tc)*dt)/max(xi);
out2=RMSE/avg;

%The following interpolation is for graphing display purposes, so that
the number of points displayed is reduced.
```

```
xj=(1:250:max(x))';
Tc=interp1(xi,Tc,xj,'pchip');
Ts=interp1(xi,Ts,xj,'pchip');
Tinf=interp1(xi,Tinf,xj,'linear');
ctr=interp1(xi,ctr,xj,'pchip');
h=interp1(xi,h,xj,'pchip');
TStc=interp1(xi,TStc,xj,'pchip');
Tir=interp1(xi,Tir,xj,'pchip');

out1=[xj,Tinf,Ts,Tc,h,ctr,TStc,Tir]; %Specifies the output

%The following plots the results of the modeling algorithm
subplot(2,1,1)
plot(out1(:,1),out1(:,2),'-*k');hold      on;plot(out1(:,1),out1(:,3),'-
k');plot(out1(:,1),out1(:,6),'ok');plot(out1(:,1),out1(:,4),'--
k');plot(out1(:,1),out1(:,7),'-r');plot(out1(:,1),out1(:,8),'-b')
axis([0,xi(end,1),0,max(Tinf)+25])
grid on
subplot(2,1,2)
plot(out1(:,3),out1(:,5),'.k');

%The following sub functions are used for calculations involving Bessel
functions:
function out=fun1(z,thetastar)
J0=besselj(0,z);
J1=besselj(1,z);
J=(J0*J1)./(J0.^2+J1.^2);
out=thetastar-(2./z.*J);
out=sqrt(out.^2);

function out=fun2(z,Bi)
J0=besselj(0,z);
J1=besselj(1,z);
J=z.*(J1/J0);
out=Bi-J;
out=sqrt(out.^2);

function out=fun3(z)
J0=besselj(0,z);
J1=besselj(1,z);
J=(J1)./(J0.^2+J1.^2);
out=(2./z.*J);
```

E.2 Gas Flow Analysis MATLAB Code

```
function out=gas_flow_derivative2
close all
```

```
%The following data sets assign variables to experimentally collected
gas flow and temperature data for each trial which is stored as
Microsoft Excel files.  To analyze a trial data set, one should
uncomment the desired data set for the gas flow, and the corresponding
set for temperature. All other data sets should remain commented. The
data is sampled every thirty seconds for the duration of the heat
treatment cycle.

%Gas Flow Data:
%rawgaslong=xlsread('C:\MATLAB701\work\Carpenter\GasFlowDerivative\8_5_
08_Rectangle_1600_2.2_0.925em_gas.xls');
%rawgaslong=xlsread('C:\MATLAB701\work\Carpenter\GasFlowDerivative\8_6_
08_0.3125inch_bundle_1600_1.65_0.9em_gas.xls');
rawgaslong1=xlsread('C:\MATLAB701\work\Carpenter\GasFlowDerivative\7_25
_08_8inchcylinder_2000_22_0.95em_gas.xls');rawgaslong=rawgaslong1(1:end
-76,:); %this cuts out end noise on the 8incylinder trial
%rawgaslong=xlsread('C:\MATLAB701\work\Carpenter\GasFlowDerivative\8_4_
08_0.75inch_bundle_1600_2.2_0.925em_gas.xls');
%rawgaslong=xlsread('C:\MATLAB701\work\Carpenter\GasFlowDerivative\8_6_
08_Rectangle_1600_1.65_0.875_gas.xls');
rawgas=rawgaslong((1:30:length(rawgaslong)),:);

%Temperature Data:
%templong=xlsread('C:\MATLAB701\work\Carpenter\GasFlowDerivative\8_5_08
_Rectangle_1600_2.2_0.925em.xls');
%templong=xlsread('C:\MATLAB701\work\Carpenter\GasFlowDerivative\8_6_08
_0.3125inch_bundle_1600_1.65_0.9em.xls');
%templong=xlsread('C:\MATLAB701\work\Carpenter\GasFlowDerivative\8_6_08
_Rectangle_1600_1.65_0.875.xls');

%temp=templong((1:30:length(templong)),:);   %this   line   should   be
uncommented with any of the above temperature data sets, to sample them
every 30 seconds (ie. the above data sets were originally run at one
data point per second)

temp=xlsread('C:\MATLAB701\work\Carpenter\GasFlowDerivative\7_25_08_8in
chcylinder_2000_22_0.95em.xls'); %originally run at one data point
every 30 secs.

%The following for-loop is necessary to convert the time stamp into a
cumulative measurement of time in seconds for the heat treatment trial.
for n=1:length(temp)-1
     x(n,1)=temp(n+1,1)-temp(n,1);
end
Ttime=(cumsum(x)/1000);

%Here the temperature data is plotted:
figure
plot(Ttime,temp(1:end-1,3),'k');hold     on;     plot(Ttime,temp(1:end-
1,4),'b');plot(Ttime, temp(1:end-1,5),'r');
legend('T/C      Surface      Temp','T/C      Center      Temp','Furnace
Temp','location','southeast');
ylabel('Temperature (°F)');xlabel('Time (sec)');
grid on
```

```
%The following for-loop performs a moving average on the original gas
meter signal (cumulative # pulses every 30sec) prior to taking the 1st
derivative to get the gas flow rate.  'q' denotes the window size of
the moving average in terms of number of indices.  Since each data
point occurs at 30sec intervals, the total filtering time here is
q*30sec = 20*30sec = 10 minutes.
q=20;
for n=1:length(rawgas(:,3))-q
    gas(n)=mean(rawgas(n:n+q,3));
end

%The derivative of the gas meter signal is now taken to get the gas
flow rate.  The derivative has unit conversions as follows
d/dt[(cumulative # pulses in 30 sec)/30sec] =
(pulses/sec)*(3600sec/hr)=(pulses/hr) * (.00625 cu ft/pulse) = (cu
ft/hr).
dgas=(diff(gas))./30.*0.00625.*3600;

%The following for-loop performs a moving average on the gas flow rate
prior to taking its derivative.  The moving average window is again
q*30sec = 20*30sec = 10 minutes.
for n=1:length(dgas)-q
    dgasavg(n)=mean(dgas(n:n+q));
end

%The derivative of the gas flow rate is taken here to get the change in
gas flow rate/time.  The result is divided by 30sec/(3600 sec/hr) since
the derivative is taken over a 30 second window and the prior
derivative is in units of (cu ft/hr).  Thus, the result is expressed as
(cu ft/hr^2)
dgas2=diff(dgasavg)./(30/3600);

%This is where the upper and lower bounds are set for the three-sigma
control chart.  The mean and standard deviation is calculated from
steady state behavior is given in Figure 3-3.
for n=1:length(dgas2)
    upper(n,1)=7.7242;
    lower(n,1)=-7.2698;
end

%The following for-loop checks to make sure the gas flow rate is within
the upper and lower control limits for a period of 2 minutes (w*30sec =
4*30 = 2minutes).  This check only occurs at times greater than 2000sec
into the cycle, to avoid false 'on heat' alarms associated with initial
signal noise.
w=4;
for n=1:length(dgas2)-w
    dgas2max(n,1)=max(dgas2(n:n+w));
    dgas2min(n,1)=min(dgas2(n:n+w));
    if  dgas2max(n,1)<upper(n,1)  &&  dgas2min(n,1)>lower(n,1)  &&
rawgas(n,1)>2000
       indx(n)=n;
       break
```

```
    end
end

onheat=max(indx)+20+20+4;%This correction adjusts the designated 'on-
heat' time to account for the delay in filtering. This corresponds to
relaxing the assumption that the filtering time is absorbed in the
control soak portion of the heat treatment cycle.

%Calculates load temperatures that correspond to the 'on-heat' point
IRss=dgas2(onheat:end);
onheattime=rawgas(onheat,1)
surface=temp(onheat,3)
center=temp(onheat,4)
difference=surface-center
%plots the derivative of the IR signal:
figure
plot(rawgas(1:end-(q+1),1),dgas);ylabel('Gas    Flow    Rate    (cubic
ft/hr)');xlabel('Time (sec)');
grid on
figure
plot(rawgas(onheat,1), dgas2(onheat), 'pentr');hold on;
plot(rawgas(1:end-2*(q+1),1),dgas2);ylabel('Change  in  Gas  Flow  Rate
(cubic ft/hr^2)');xlabel('Time (sec)');
plot(rawgas(1:end-2*(q+1),1),    upper,    '--m');    plot(rawgas(1:end-
2*(q+1),1), lower, '-.m');
legend('On  Heat  Point','Change  in  Gas  Flow  Rate',  'Upper  Control
Limit', 'Lower Control Limit', 'location', 'southeast');
grid on
```

E.3 OP-AID MATLAB Code

```
function out=ir_derivative3
close all

%The following data sets assigns a variable to the experimentally
collected load temperatures that are stored as Microsoft Excel files.
The data set to be analyzed is uncommented, while all other data sets
remain commented. One data point is sampled every thirty seconds for
the duration of the heat treatment cycle.

%templong=xlsread('C:\MATLAB701\work\Carpenter\IRderivative\8_5_08_Rect
angle_1600_2.2_0.925em.xls');
%templong=xlsread('C:\MATLAB701\work\Carpenter\IRderivative\8_6_08_0.31
25inch_bundle_1600_1.65_0.9em.xls');
```

```
%templong=xlsread('C:\MATLAB701\work\Carpenter\IRderivative\8_6_08_Rect
angle_1600_1.65_0.875.xls');

%temp=templong((1:30:length(templong)),:);   %this   line   should   be
uncommented with any of the above temperature data sets, to sample them
every 30 seconds (ie. the above data sets were originally run at one
data point per second)

temp=xlsread('C:\MATLAB701\work\Carpenter\IR
derivative\7_25_08_8inchcylinder_2000_22_0.95em.xls');  %originally  run
at one data point every 30 secs.

%The following for-loop is necessary to convert the time stamp into a
cumulative measurement of time in seconds for the heat treatment trial.
for n=1:length(temp)-1
     x(n,1)=temp(n+1,1)-temp(n,1);
end
time=(cumsum(x)/1000);

IRinit=temp(:,2); %This is the original unfiltered IR signal.

%The following for-loop performs a moving average on the IR signal
prior to taking the derivative.  'q' denotes the window size of the
moving average in terms of number of indices.  Since each data point
occurs at 30sec intervals, the total filtering time here is q*30sec =
4*30sec = 2 minutes.
q=4;
for n=1:length(IRinit)-q
    IR(n)=mean(IRinit(n:n+q));
end

%The derivative of the filtered IR signal is now taken.  Since the
derivative is taken over a time delta of 30 seconds, the resulting
derivative is divided by thirty and multiplied by 60sec/min so that
dIRinit can be expressed in units of F/min.
dIRinit=(diff(IR)./30).*60;

%The following for loop takes a moving average of the derivative
signal. 'p' denotes the window size of the moving average in terms of
number of indices.  Even though the derivative is expressed in F/min,
each data point still occurs at 30sec intervals, so the total filtering
time here is p*30sec = 10*30sec = 5 minutes.
p=10;
for n=1:length(dIRinit)-p
    dIR(n)=mean(dIRinit(n:n+p));
end

%The result is rounded to a number of significant figures consistent
with the measuring accuracy of the IR sensor.
dIR=round((dIR)*100)/100;

%The upper and lower bounds of the OP-AID control limits are set here
at +/-0.5 F/min
```

```
for n=1:length(dIR)
    upper(n,1)=0.5;
    lower(n,1)=-0.5;
end

%The following for-loop checks to make sure the infrared derivative is
within the upper and lower control limits for a period of 2 minutes
(w*30sec = 4*30 = 2minutes).  This check only occurs at times greater
than 2000sec into the cycle, to avoid false 'on heat' alarms associated
with placing the load in front of the sensor at the beginning of the
heat treatment cycle.
w=4;
for n=1:length(dIR)-w
    dIRmax(n,1)=max(dIR(n:n+w));
    dIRmin(n,1)=min(dIR(n:n+w));
    if dIRmax(n,1)<upper(n,1) && dIRmin(n,1)>lower(n,1) && time(n)>2000
       indx(n)=n;
       break
    end
end

onheat=max(indx)+10+4+4; %This correction adjusts the designated 'on-
heat' time to account for the delay in filtering and the delay needed
to determine the signal is within the limits. This corresponds to
relaxing the assumption that the filtering time is absorbed in the
control soak portion of the heat treatment cycle.

%The following calculates load temperatures that correspond to the 'on-
heat' point
onheattime=time(onheat)
surface=temp(onheat,3)
center=temp(onheat,4)
difference=surface-center

%plots the derivative of the IR signal:
plot(time(onheat), dIR(onheat), 'pentr'); hold on;
plot(time(1:end-p-q), dIR,'b');
plot(time(1:end-p-q), upper, '--m'); plot(time(1:end-p-q), lower, '-
.m');
legend('On Heat Point','IR Signal Derivative', 'Upper Control Limit',
'Lower Control Limit', 'location', 'northeast');
axis([min(time), max(time), -5, 25]);
ylabel('IR Signal Rate of Change(°F/min)');xlabel('Time (sec)');
grid on

%plots the original temperature curves of the load thermocouples and
%infrared sensor:
figure
plot(time,temp(1:end-1,2),'c');hold on; plot(time,temp(1:end-
1,3),'k');plot(time, temp(1:end-1,4),'b');
plot(time, temp(1:end-1,5),'r');
legend('IR Signal','T/C Surface Temp','T/C Center Temp','Furnace
Temp','location','southeast');
ylabel('Temperature (°F)');xlabel('Time (sec)');grid on
```